Energy Aware Radio and neTwork tecHnologies

SEVENTH FRAMEWORK PROGRAMME

INFSO-ICT-247733 EARTH

Deliverable D3.2

Green Network Technologies

Contractual Date of Delivery: December 31th, 2011

Actual Date of Delivery: January 30th, 2012

Editor(s): Main editor: Fabien Héliot (UNIS) / Chapter editors: Oliver Blume (ALUD), Péter Fazekas (BME), Dario Sabella (TI), Changsoon Choi (DOCOMO), Albrecht Fehske (TUD), István Gódor (ETH), Emilio Calvanese-Strinati (CEA), António Serrador (IST-TUL), and Pål Frenger (EAB)

Author(s): Fabien Héliot, Yinan Qi, Oluwakayode Onireti, Muhammad Ali Imran (UNIS), Oliver Blume, Anton Ambrosy (ALUD), Péter Fazekas, Márton Bérces, Attila Vidács (BME), Dario Sabella, Giorgio Calochira, Marco Caretti, Mauro Boldi, Roberto Fantini, Sergio Barberis (TI), Hauke Holtkamp, Changsoon Choi, Luca Scalia (DOCOMO), Fred Richter, Albrecht Fehske (TUD), István Gódor, László Hévizi (ETH), Rohit Gupta, Emilio Calvanese-Strinati, Mohamed Kamoun, Mireille Sarkiss (CEA), António Serrador, Luís M. Correia (IST-TUL), Pål Frenger (EAB), Keeth Jayasinghe, Pekka Pirinen, Nandana Rajatheva (UOULU), and Alberto Pellón (TTI)

Participant(s): UNIS, ALUD, BME, TI, DOCOMO, TUD, ETH, CEA, IST-TUL, EAB, UOULU, TTI

Work package: WP3 – Green Networks

Security: Public

Version: 1.0

Keyword list: Mobile communications, green networks, energy efficiency, deployment, network management, radio resource management, future architectures.

Abstract: The main goal of EARTH project is to reduce the power consumption of cellular networks by 50%. This document is an intermediate report on energy efficiency improvements expected from green network technologies studied by WP3. These technologies include deployment strategies, network management concepts, radio resource management techniques and some proposal future architectures that are inherently designed to be energy efficient. These results can contribute a lot to achieve the ultimate goal of 50% energy consumption reduction on system level and will be exploited in WP6 to build an “Integrated Solution”.

EXECUTIVE SUMMARY

This document contains the intermediate results on energy efficiency (EE) improvements provided by different green network technologies, which has been selected amongst the "Most Promising Tracks" of [EARTH-D3.1]. This includes: a) deployment strategies tracking the long-term evolution of traffic, b) network management techniques adapting the system to daily traffic variation, c) radio resource management (RRM) solutions defining when and how to send out user data over the air interface and d) novel energy efficient concepts for designing future architectures.

In traditional network planning the inter-site distance (ISD) between base stations (BSs) is optimally adjusted for providing the desired performance. The most energy efficient ISD greatly depends on the type of BS and its power consumption. We have found that HetNets can provide 10% energy saving in high-traffic scenarios compared to a macro only deployment with extra sectors or carriers, and even 20% energy can be saved in hotspot scenarios.

Naturally operators rely on existing legacy (GSM and 3G) deployments, where legacy systems provide the coverage and low-traffic demanding services in a multi-radio access technology (RAT) scenario, while LTE serves the increased capacity needs. We have found that site co-location may provide 5% energy saving due to better cooling efficiency and daily network reconfiguration actions can provide up to 30% energy saving (see related results below, as well).

Relays are candidates to extend coverage and increase capacity; however, their gains strongly depend on their offset power. In case of low offset power, relays need 5-10% less energy per bit than macro only deployments and two-hop scheme is better than multicast cooperative scheme. We have found that hybrid relaying based on decode/compress and forward outperforms traditional solutions in large macro cells, to which solutions network coding (NC) can be an alternative. Moreover, relaying needs less energy than direct communication in an in-building scenario.

The evolution of radio access networks (RANs) involve multiple antennas, which provides further possibilities, e.g., for BS cooperation. Multiple antennas have a great EE potential in theory, but a system with two transmit antennas is not necessarily more energy efficient than a single antenna system when considering a realistic power model.

Beyond these techniques, coordination or cooperation between BSs are alternative solutions to cope with increased traffic demand by better utilising the available bandwidth. We have found that cooperation is mainly useful for cell edge users and should be limited to 3 BSs. It can save 15 to 25% of energy per bit especially in heavily loaded systems. The analysis of cooperative system has revealed the importance of having a realistic backhaul power model and, thus, a comprehensive comparison between today's most relevant backhaul technologies is here provided for future use.

Adaptively reducing the number of active network elements by following the daily traffic variation is a simple way to save energy. The maximum number of resource blocks can be adaptively set by dynamic bandwidth management, which yields 25% in energy saving. In low-traffic hours of interference limited urban networks, macro BSs can switch to fewer but larger sectors by dynamic sectorisation or can be put in sleep mode by cell on/off techniques providing 13 to 30% energy saving. Such on/off techniques can be applied on the capacity layer of HetNets providing 25 to 40% energy saving and up to 7% saving by using macros with remote radio head (RRH) in the coverage layer.

The goal of RRM techniques is to ensure minimal energy consumption especially in low-traffic situations. The dynamics of scheduling allows short sleep periods that can be utilized by Multicast Broadcast Single Frequency Network (MBSFN) frames providing 20-30% energy saving per bit. Cell discontinuous transmission (DTX) is an alternative approach to exploit sleep modes providing 45% energy saving when combined with power control. Furthermore, delay constraints allow biding packets' "best" time to be scheduled providing up to 20% energy savings per bit. Finally, users can be dynamically allocated to the best available RAT by means of vertical handovers for an energy saving of up to 10%.

Looking beyond today's existing system standards and typical deployments, a promising conceptual idea is to logically separate the transmission of data and control information providing more space to utilize sleep modes and, thereby, further reducing the energy consumption. Another idea is to create a distributed cloud RAN infrastructure where geographically separated central controllers are shared among the nodes. Furthermore, mobile multihop relaying can be used to increase coverage or fill up coverage holes providing up to 30% energy savings. We have also found that NC can be an alternative to the classical automatic repeat request (ARQ) without any forward error correction (FEC).

Note that nearly all of the above techniques combine well with most of the radio hardware improvements in [EARTH-D4.2] forming a solid basis for the upcoming deliverables [EARTH-D6.2b] and EARTH-D6.3 on integrated solutions.

Authors

Partner	Name	Email and Phone
UNIS University of Surrey	Fabien Héliot Yinan Qi Kayode Onireti Muhammad Ali Imran	f.heliot@surrey.ac.uk yinan.qi@surrey.ac.uk o.onireti@surrey.ac.uk m.imran@surrey.ac.uk
ALUD *Alcatel-Lucent Deutschland AG*	Oliver Blume Anton Ambrosy	oliver.blume@alcatel-lucent.com anton.ambrosy@alcatel-lucent.com
BME *Budapest University of Technology and Economics*	Péter Fazekas Márton Bérces Attila Vidács	fazekasp@hit.bme.hu berces@hit.bme.hu vidacs@tmit.bme.hu
TI *Telecom Italia S.p.A.*	Dario Sabella Giorgio Calochira Marco Caretti Mauro Boldi Roberto Fantini Sergio Barberis	dario.sabella@telecomitalia.it giorgio.calochira@telecomitalia.it marco.caretti@telecomitalia.it mauro.boldi@telecomitalia.it roberto.fantini@telecomitalia.it sergio.barberis@telecomitalia.it
DOCOMO *DOCOMO Communications Laboratories Europe GmbH*	Hauke Holtkamp Changsoon Choi Luca Scalia	holtkamp@docomolab-euro.com choi@docomolab-euro.com scalia@docomolab-euro.com
TUD Technische Universität Dresden	Fred Richter Albrecht Fehske	fred.richter@ifn.et.tu-dresden.de albrecht.fehske@ifn.et.tu-dresden.de
ETH *Ericsson Hungary Ltd.*	István Gódor László Hévizi	istvan.godor@ericsson.com laszlo.hevizi@ericsson.com
CEA *Commissariat à l'Energie Atomique*	Rohit Gupta Emilio Calvanese Strinati Mohamed Kamoun Mireille Sarkiss	rohit.gupta@cea.fr emilio.calvanese-strinati@cea.fr mohamed.kamoun@cea.fr mireille.sarkiss@cea.fr
IST-TUL *Instituto Superior Tecnico*	António Serrador Luís M. Correia	aserrador@deetc.isel.ipl.pt luis.correia@lx.it.pt
EAB *Ericsson AB*	Pål Frenger	pal.frenger@ericsson.com
UOULU *University of Oulu*	Keeth Jayasinghe Pekka Pirinen Nandana Rajatheva	kladdu@ee.oulu.fi pekkap@ee.oulu.fi rrajathe@ee.oulu.fi

Partner	Name	Email and Phone
TTI *TTI Norte, SL*	Alberto Pellón	apellon@ttinorte.es

Table of Contents

EXECUTIVE SUMMARY 2
1. INTRODUCTION 12
2. OPTIMAL MIX OF CELL SIZES 14
2.1. Optimum Interside distance of macro cell deployment 14
2.1.1. ISD with cells of fixed transmit power 15
2.1.2. ISD with cells of adapted transmit power 15
2.1.3. Optimum Inter-Site Distance when using EARTH transceiver hardware 16
2.2. HetNets with Small cells at cell edges 18
2.3. Small Cell DEPLOYMENTS in traffoc hotspots 18
2.3.1. System Model Aspects 19
2.3.2. Results and Discussion 19
2.4. non-hexagonal DEPLOYMENTS by moving BSs in forcefields 21
3. MULTI-RAT NETWORK EVOLUTION 23
3.1. multi-RAT network deployment Methods 23
3.1.1. Basic algorithm 23
3.1.2. Management extension 24
3.1.3. Multi-RAT extension 25
3.1.4. Implementation and use potential 25
3.2. Multi-RAT Roll-out Plans 26
3.2.1. Roll-out strategy considerations 28
4. RELAY NODES 29
4.1. Two hop vs. cooperative relaying in homogeneous traffic conditions 29
4.2. Hybrid relaying techniques 31
4.3. Energy Efficient MIMO Two-Way Relay System with Physical Layer Network Coding 34
4.3.1. Background 34
4.3.2. System Model 35
4.3.3. Error Performance 36
4.3.4. Background Optimum Power Allocation 36
4.4. In-building communication 37
4.5. relay nodes performances in hotspots of traffic 39
5. MIMO AND ADAPTIVE ANTENNAS 42
5.1. MIMO vs. SISO: An Energy Efficiency analysis 42
5.1.1. MIMO vs. SISO EE gain : Idealistic PCM 42
5.1.2. MIMO vs. SISO EE gain : Realistic PCM 43
5.2. Adaptive MIMO 44
5.2.1. Introduction of MIMO muting 44
5.2.2. Energy saving operation by advanced CoMP 45
6. BASE STATION COOPERATION 47

6.1. ENERGY EFFICIENCY IN THE UPLINK OF COMP: AN ANALYTICAL STUDY 47
6.2. BASE STATION COOPERATION UNDER LIMITED BACKHAUL CAPACITY 49
6.2.1. System Model 49
6.2.2. Information Theoretical Energy Efficiency Analysis 50
6.2.3. Numerical Results 51
6.3. FRACTIONAL FREQUENCY REUSE 52
6.4. MULTI-CELL SCHEDULING 54
6.5. IMPACT OF BACKHAULING TECHNIQUES 56
7. ADAPTIVE NETWORK RECONFIGURATION 59
7.1. DYNAMIC BANDWIDTH MANAGEMENT 60
7.2. DYNAMIC SECTORIZIATON 62
7.2.1. Adaptive, prediction-based sectorisation 62
7.2.2. A fast algorithm for dynamic sectorisation of base stations 64
7.3. CELL ON/OFF SWITCH SCHEMES IN SINGLE-LAYER NETWORKS 66
7.4. CELL ON/OFF SCHEMES IN HETNET AND MULTI-RAT NETWORKS 69
7.4.1. Efficiency Analysis of HetNets 69
7.4.2. Operational proposal and implementation aspects 71
8. ADAPTIVE SCHEDULING 73
8.1. EE SCHEDULING FRAMEWORK BASED ON MBSFN SUBFRAME SWITCHING 73
8.1.1. MBSFN provisioner 75
8.1.2. QoS aware scheduler 75
8.1.3. Current Results 76
8.2. DTX & POWER CONTROL 77
8.3. PRIORITIZED SCHEDULING 79
8.3.1. Algorithm Description 79
8.3.2. Implementation Aspects and Operation Proposal 79
8.3.3. Simulation results 80
8.4. VERTICAL HANDOVERS 81
8.4.1. Algorithm Description 81
8.4.2. Implementation Aspects and Operation Proposal 82
8.4.3. Scenarios and Simulation Results 82
9. ARCHITECTURES IN THE FUTURE 85
9.1. LOGICAL DECOUPLING OF BASIC SYSTEM FUNCTIONALITY AND DATA TRANSMISSION 85
9.1.1. Distributing access information 87
9.1.2. Random Access and Paging 87
9.1.3. Mobility 88
9.2. MULTIHOP EXTENSION 89
9.2.1. Coverage extension in single-cell macro system 90
9.2.2. Keeping coverage in multicell network 90
9.3. ACTIVE ANTENNAS IN COOPERATIVE SYSTEMS 91
9.4. ENERGY-EFFICIENCY COMPARISON BETWEEN NETWORK CODING AND RETRANSMISSIONS 93
10. CONCLUSIONS 95
11. REFERENCES 97

List of Figures

FIGURE 1. POWER CONSUMPTION OF MACRO BSS OVER ISD WITH A MINIMUM SYSTEM THROUGHPUT OF 20 MBPS/KM^2. (A) LEFT: FIXED TRANSMIT POWER. (B) RIGHT: TRANSMIT POWER SCALED TO THE CELL AREA. 15
FIGURE 2. (A) LEFT: AREA POWER CONSUMPTION OF MACRO BS DEPLOYMENTS OVER THE ISD. (B) RIGHT: SYSTEM THROUGHPUTS OVER ISD, THE RED LINE IS MARKING 120 MBPS/KM^2. 17
FIGURE 3. SMALL CELL DEPLOYMENT AT EDGE OF MACRO CELLS WITH ONE, TWO, 3, OR 5 SMALL CELLS PER MACRO SITE. 18
FIGURE 4. AREA POWER OF DIFFERENT DEPLOYMENT SCHEMES AS A FUNCTION OF SERVED TRAFFIC. 20
FIGURE 5. AREA POWER OF DIFFERENT DEPLOYMENT SCHEMES AS A FUNCTION OF SERVED TRAFFIC. 20
FIGURE 6. (A) DEPLOYMENT IN BALANCED COVERAGE STATE, (B) ENERGY EFFICIENCY PROGRESS. 22
FIGURE 7. EXAMPLE OF NETWORK LAYOUT ADAPTATION FOR 3 DIFFERENT TRAFFIC MAPS. 24
FIGURE 8. EE RESULTS. 25
FIGURE 9. THEORETICAL MAPPING BETWEEN COOLING CAPACITY (W) AND COP VALUES. 27
FIGURE 10. RESULTS OF URBAN EVOLUTION STUDY STARTING FROM A 50:50 2G, 3G RATIO. 27
FIGURE 11. RESULTS OF RURAL EVOLUTION STUDY STARTING FROM A 50:50 2G, 3G RATIO. 27
FIGURE 12. TWO HOP AND MULTICAST COOPERATIVE RELAY SCHEMES 30
FIGURE 13. OVERALL ECI WITH DIFFERENT POWER MODELS AND DEPLOYMENTS (HIGH TRAFFIC PROFILE). 31
FIGURE 14. TWO WAY RELAY CHANNEL. 32
FIGURE 15. (A) SHORT RANGE ENERGY PER BIT, AND (B) LONG RANGE ENERGY PER BIT. 33
FIGURE 16. (A) SHORT RANGE ENERGY EFFICIENCY (R=100M), AND (B) LONG RANGE ENERGY EFFICIENCY (R=1000M). 33
FIGURE 17. EE IN CELLULAR SYSTEM. 34
FIGURE 18. MULTIPLE ACCESS STAGE. 35
FIGURE 19. BROADCASTING STAGE. 35
FIGURE 20. COMPARISON OF SIMULATION TO UPPER AND LOWER BOUNDS OF END-TO-END BER. 36
FIGURE 21. (A) SUM RATE WITH TOTAL POWER, AND (B) SUM RATE WITH VARIED RELAY LOCATION. 37
FIGURE 22. EE, SE AND TOTAL CONSUMED POWER OF MIMO P2P AS WELL AS MIMO AF VS. THE BS TRANSMIT POWER PER ANTENNA IN DBM FOR VARIOUS NUMBERS OF ANTENNAS AND Σ VALUES. 38
FIGURE 23. TRAFFIC DISTRIBUTION WITH TWO HOTSPOTS COVERED BY THE RELAY NODES. 39
FIGURE 24. OVERALL ECI IN THE HOTSPOT SCENARIO, WITH DIFFERENT DEPLOYMENTS (HIGH TRAFFIC PROFILE). 40
FIGURE 25. IDEALISTIC MIMO VS. SISO EE GAIN DUE TO POWER SAVING VS. SE IMPROVEMENT AS A FUNCTION OF THE SE AND NUMBER OF ANTENNA ELEMENTS WHEN N_{ANT}= T = R. 43
FIGURE 26. 2X2MIMO VS. SISO EE GAINS AND THEIR RESPECTIVE SE AND TOTAL CONSUMED POWER WHEN CONSIDERING A REALISTIC PCM. 44
FIGURE 27. ENERGY CONSUMPTION OF COMPONENTS IN BS. 45
FIGURE 28. (A) NORMAL OPERATION AND (B) PROPOSED ENERGY SAVING OPERATION BY ADVANCED COMP. 46
FIGURE 29. VARIOUS EE GAINS OF COMP AGAINST NON-COOPERATIVE SYSTEM AS A FUNCTION OF (A) USER RELATIVE DISTANCE AND (B) THE ISD FOR VARIOUS NUMBER OF COOPERATING BSS (M) AND ANTENNA CONFIGURATIONS. 48
FIGURE 30. REALISTIC EE GAIN OF COMP AGAINST NON-COOPERATIVE SYSTEM DUE TO SE IMPROVEMENT AS A FUNCTION OF THE USER RELATIVE DISTANCE AND ISD FOR M = 3 AND T = R = 2. 49
FIGURE 31. DOWNLINK BS COOPERATION. 50
FIGURE 32. EE NUMERICAL RESULTS. 52
FIGURE 33. ADAPTIVE FFR SCENARIO WITH TWO BSS. 53
FIGURE 34. ENERGY SAVING GAINS WITH ADAPTIVE FFR (RATIO BETWEEN ENERGY CONSUMPTION USING ADAPTIVE FFR AND ENERGY CONSUMPTION USING STATIC APPROACH). 54
FIGURE 35. ADJACENT SECTORS OF THREE BSS COORDINATION MODEL. 55
FIGURE 36. ENERGY EFFORT, SUM-RATE AND TOTAL CONSUMED POWER PER SECTOR FOR THREE TYPES OF SCHEDULING METHODS 55
FIGURE 37. BACKHAUL NETWORKS (A) PASSIVE OPTICAL NETWORK (PON) (B) ACTIVE OPTICAL NETWORK (AON), ALSO REFERRED TO POINT-TO-POINT (P2P) (C) FIBRE-TO-THE-NODE (FTTN) (D) MICROWAVE LINKS. 56
FIGURE 38. (A) PER BS POWER CONSUMPTION VS. ACCESS RATE; (B) OVERALL BACKHAUL POWER CONSUMPTION VS. NUMBER OF BSS. 58
FIGURE 39. DENSE URBAN SCENARIO: POWER CONSUMPTION PER AREA UNIT ALONG A DAY FOR PEAK SYSTEM THROUGHPUT OF 120 MBPS/KM^2 (LEFT) AND DAILY ENERGY SAVINGS VS. PEAK SYSTEM THROUGHPUT (RIGHT). 60
FIGURE 40. RURAL SCENARIO: POWER CONSUMPTION PER AREA UNIT ALONG A DAY FOR PEAK SYSTEM THROUGHPUT OF 4 MBPS/KM^2 (LEFT) AND DAILY ENERGY SAVINGS VS. PEAK SYSTEM THROUGHPUT (RIGHT) 60

FIGURE 41. DAILY ENERGY SAVINGS OF BANDWIDTH ADAPTATION APPROACHES IN COMBINATION WITH DIFFERENT REUSE SCHEMES FOR DENSE URBAN (LEFT) AND RURAL SCENARIOS (RIGHT) BASED ON IMPROVEMENTS BY THE PA ONLY. 61
FIGURE 42. SINR MAP....63
FIGURE 43. TRAFFIC DEMAND, BLOCKING PROBABILITY, COVERAGE AND M_{SAV}. 64
FIGURE 44. CELL LEVEL ANALYSIS OF SWITCHING PATTERN....65
FIGURE 45. ANALYSIS OF PERFORMANCE AND ENERGY CONSUMPTION WITH DYNAMIC SECTORISATION. 66
FIGURE 46. OBSERVED NUMBER OF VEHICLES ON HIGHWAY DURING A DAY © [NRC_US2010]. 67
FIGURE 47. DIFFERENT CELL CLASSIFICATION ON THE SIMULATED SCENARIO AND THEIR CORRESPONDING CURVES. 68
FIGURE 48. CONFIGURATION AND ACTIVATION PROCEDURES 71
FIGURE 49. OVERALL ARCHITECTURE OF THE EE SCHEDULING FRAMEWORK. 74
FIGURE 50. EXAMPLES OF MBSFN PROVISIONING IN A PERIOD OF 4 RADIO FRAMES (T = 40 MS). 75
FIGURE 51. ECI OF THE PROPOSED MBFSN SCHEDULING FRAMEWORK (LOW AND HIGH RESOLUTION VIDEO STREAMING USERS). 76
FIGURE 52. EE GAINS (EXPRESSED IN [JOULE/BIT]) WITH RESPECT TO MAX C/I SCHEDULER....77
FIGURE 53. EE GAINS (EXPRESSED IN [WATT/USER]) WITH RESPECT TO MAX C/I SCHEDULER 77
FIGURE 54. SIMULATION RESULTS. (BANDWIDTH ADAPTATION REPRESENTS A TRADITIONAL BS.)....78
FIGURE 55. GREEN SCHEDULING ARCHITECTURE. 80
FIGURE 56. GREEN METRIC PERFORMANCE. 80
FIGURE 57. FF BS/RAT SELECTION ALGORITHMS....82
FIGURE 58. EE GAINS FOR WCDMA AND HSDPA. 83
FIGURE 59. EE GAINS FOR WCDMA AND LTE. 84
FIGURE 60. EXAMPLE OF SYSTEM OPERATION ENABLED BY A LOGICAL SEPARATION OF SYSTEM BROADCAST CHANNELS AND PACKED DATA TRANSMISSIONS. 86
FIGURE 61. ONLY THE SMALL PART OF THE SYSTEM INFORMATION RELATED TO INITIAL ACCESS (DENOTED ACCESS INFORMATION) NEED TO BE BROADCASTED. 87
FIGURE 62. EXAMPLE OF HOW A PAGING MESSAGE AND A RANDOM ACCESS RESPONSE MESSAGE CAN BE TRANSMITTED IN AN AREA SMALLER THAN THE WHOLE BCH AREA. 88
FIGURE 63. (LEFT) FIRST MOBILITY MECHANISM HAS NOT YET TRIGGERED THE SECOND MOBILITY MECHANISM; (RIGHT) SECOND MOBILITY MECHANISM IS TRIGGERED. 89
FIGURE 64. COVERAGE EXTENSION IN SINGLE CELL SYSTEM....90
FIGURE 65. COVERAGE PROBABILITY IN MULTICELL SCENARIO. 91
FIGURE 66. LAYOUT FOR CLOUD RAN INCLUDING AAS. 92
FIGURE 67. SCENARIO OF THE SYSTEM MODEL USED FOR EVALUATION OF HETNET. 92
FIGURE 68. SYSTEM MODEL WHERE A SINGLE SOURCE MULTICASTS S_K PACKETS TO D DESTINATIONS....93
FIGURE 69. ENERGY CONSUMPTION COMPARISON OF RLNC AND ARQ (A) WITHOUT FEC AND (B) WITH FEC....94

List of Tables

TABLE 1. SIMULATION PARAMETERS....16
TABLE 2. EARTH PARAMETERS FOR DIFFERENT BASE AND RELAY STATIONS (2010-SOTA). 30
TABLE 3. UPDATED PARAMETERS FOR DIFFERENT BASE AND RELAY STATIONS (2014 –ESTIMATION). 40
TABLE 4. BACKHAUL NETWORK CHARACTERSTICS. 58
TABLE 5. HETNETS COVERAGE AND CAPACITY LAYERS' SYSTEM PARAMETERS. 69
TABLE 6. UTILIZATION OF SMALL CELLS AND ENERGY SAVING POTENTIAL BY SWITCHING OFF EMPTY SMALL CELLS. 70
TABLE 7. SIMULATION PARAMETERS....76
TABLE 8. MODEL PARAMETERS FOR MICRO-CELLS. 82
TABLE 9. SERVICES AND TRAFFIC (REFERENCE). 83
TABLE 10. RESULTS OF HETNET SCENARIO CASE. 93

Acronyms and Abbreviations

3G	3rd Generation
3GPP	3rd Generation Partnership Project
AAS	Active Antenna System
AC	Alternating Current
AF	Amplify-and-Forward
AON	Active Optical Network
ARQ	Automatic Repeat reQuest
AWGN	Additive White Gaussian Noise
BA	BCH Area
BBU	BaseBand Unit
BCCH	Broadcast Control Channel
BCH	Broadcast CHannel
BER	Bit-Error-Rate
BLS	BaseLine System
BPSK	Binary Phase Shift Keying
BS	Base Station
BW	BandWidth
BwA	Bandwidth Allocation
C/I	Carrier-to-Interference ratio
CAC	Call Admission Control
CAPEX	CAPital Expenditure
CF	Compress-and-Forward
CN	CoNnection switch
CoF	Cost Function
CoMP	Coordinated Multi-Point
COP	Coefficient Of Performance
C-RAN	Cloud-Radio Access Network
CRS	Cell specific Reference Symbol
DC	Direct Current
DeNB	Donor E-UTRAN NodeB
DF	Decoded-and-Forward
DL-SCH	Downlink Shared Channel
DP	Demand Position
DRX	Discontinuous Reception
DTX	Discontinuous Transmission
E^3F	EARTH Energy Efficiency Evaluation Framework
EARTH	Energy Aware Radio and neTwork tecHnologies
ECI	Energy Consumption Index
EDF	Earliest Deadline First
EE	Energy Efficiency
eNB	E-UTRAN NodeB
E-UTRAN	Evolved UTRAN
FF	Fittingness Factor
FFR	Fractional Frequency Reuse
FTP	File Transfer Protocol
FTTN	Fibre-To-The-Node

GAS	Green Adaptive Scheduler
GSM	Global System for Mobile Communications
HetNet	Heterogeneous Network
HSDPA	High Speed Downlink Packet Access
HSPA	High Speed Packet Access
ICT	Information and Communication Technology
ISD	Inter-Site Distance
KKT	Karush-Kuhn-Tucker
KPI	Key Performance Indicator
LTE	Long-Term Evolution
LTE-A	LTE-Advanced
M2M	Machine-to-Machine
MAC	Medium Access Control
MBB	Mobile BroadBand
MBSFN	Multicast Broadcast Single Frequency Network
MIMO	Multiple-Input Multiple-Output
MISO	Multiple-Input Single-Output
MMPP/M/1/D-PS queue	single-server Processor Sharing queue, with Markov-Modulated Poisson arrival Process, Markovian service times and finite capacity
MS	Mobile Station
MW	MicroWave
NC	Network Coding
NMT	Nordic Mobile Telephone
NT	Network Terminal
OFDM	Orthogonal Frequency Division Multiplexing
OFDMA	Orthogonal Frequency Division Multiple Access
OLT	Optical Line Terminal
ONU	Optical Network Unit
P2P	Point-to-Point
PA	Power Amplifier
PC	Power Control
PCM	Power Consumption Model
PNC	Physical Layer Network Coding
PON	Passive Optical Network
PRB	Physical Resource Block
PSK	Phase Shift Keying
PwA	Power Allocation
QAM	Quadrature Amplitude Modulation
QoS	Quality of Service
QPSK	Quadrature Phase Shift Keying
RAN	Radio Access Network
RAT	Radio Access Technology
RBS	Radio Base Station
RF	Radio Frequency
RLNC	Random Linear Network Coding
RN	Remote Node
RN	Relay Node
RNTP	Relative Narrowband Transmit Power
RRC	Radio Resource Control
RRH	Remote Radio Head

RRM	Radio Resource Management
RSRP	Reference Signal Received Power
RSRQ	Reference Signal Received Quality
RX	Receiver
S-D	Source-to-Destination
SE	Spectral Efficiency
SFBC	Space-Frequency Block Coding
SFN	Single Frequency Network
SI	System Information
SINR	Signal-to-Interference-plus-Noise-Ratio
SISO	Single-Input Single-Output
SNR	Signal-to-Noise Ratio
SOTA	State-Of-The-Art
TCP	Transmission Control Protocol
TDD	Time-Division Duplex
TTL	Time To Live
TX	Transmitter
UE	User Equipment
UMTS	Universal Mobile Telecommunications System
UTRAN	UMTS Terrestrial RAN
VHO	Vertical HandOver
WCDMA	Wideband Code Division Multiple Access
WWW	World Wide Web
XOR	eXclusive OR

1. INTRODUCTION

Preface

The Energy Aware Radio and neTwork tecHnologies (EARTH) project aims to address the global environmental challenge by investigating and proposing effective mechanisms to drastically reduce energy wastage and improve energy efficiency of mobile broadband (MBB) communication systems with 50% without compromising users' perceived quality of service (QoS) and system capacity [EARTH_Leaflet]. The ultimate results of the EARTH project will be an integrated solution, which will be built on the building blocks from network technologies solution presented here and radio technologies (see the related results in [EARTH-D4.2]).

This document contains the intermediate results on energy efficiency improvements provided by the different green network technologies selected as "Most Promising Tracks" in the EARTH project [EARTH-D3.1]. These technologies comprise deployment strategies following the long-term evolution of traffic, network management techniques adapting the system to the daily variation of the traffic, radio resource management (RRM) solutions defining when and how to send out user data over the air interface and basic concepts of future architectures inherently providing energy efficient systems.

The analysis presented in the document is based on the network level energy consumption analysis of wireless communication systems according to the EARTH energy efficiency evaluation framework (E^3F) defined by the project in [EARTH-D2.3]. The analysis identified large potentials for savings, especially in situations of low load periods. Each single technique can provide savings of up to 30%, depending of the use case. Further improvements (just partially considered in this document) are possible for the underlaying hardware components. However, these savings cannot simply be added. It has to be analyzed whether two or more techniques can cooperate or even provide synergy (see [EARTH-D6.2b] for preliminary studies). On the other hand, different techniques can be applied in different areas of the network (dense urban vs. rural areas) or at different times of the day (e.g. by network reconfiguration between busy hour and night times). Thereby, these network technologies associated with their operating conditions will be exploited in WP6 to build an "Integrated Solution".

Network Technology Areas of Investigation

In traditional network planning the distance between base stations (BSs) is adjusted to the maximum inter-site distance (ISD) that provides the requested system performance. A lower ISD implies more sites, thus increases network capacity, but also increases capital expenditure (CAPEX) costs for site acquisition and equipment. The issue of lowering network energy consumption adds another dimension to the optimization problem. Among many other questions, Section 2 discusses the impact of ISD on the energy cost and how to deploy additional cells (e.g., an underlay of micro cells) to save energy.

Practical considerations call for investigating how to utilize operators' existing legacy (global system for mobile communications (GSM) and 3rd generation (3G)) deployments. Legacy systems will mainly provide the coverage and low-traffic demanding services in a multi-radio access technology (RAT) scenario, while long-term evolution (LTE) will serve the increased capacity needs. Among many other questions, Section 3 discusses when and where it is beneficial to deploy new BSs to serve the increased user demands; and what are the limitations of co-siting and sharing components (like cooling).

In addition to small cells, relays are also candidates to extend coverage and increase capacity. Relay deployment options provides flexible and cost-effective alternatives. Among many other questions, Section 4 compares the energy efficiency of type 1 (two hop relays) and type 2 (multicast cooperative) relays, and compares the performance of relaying techniques (amplify-and-forward (AF), compress-and-forward (CF), decode-and-forward (DF) or hybrid solutions based on these three basic techniques). This chapter also discusses when network coding (NC) can be a good alternative compared to traditional relaying techniques and how to serve hotspots with relays.

The evolution of radio access networks (RANs) introduced multiple antennas like multiple-input multiple-output (MIMO), which provides further possibilities, e.g., for BS cooperation. E.g., antenna systems can be partially "shared" between neighbouring BSs. Among many other questions, Section 5 discusses when the antennas can be shared and how many antennas should be used to serve a given traffic level.

Beyond the above described techniques focusing on densifying the network, coordination of BSs or cooperation between BSs are alternative solutions to cope with increased traffic by utilizing more the available bandwidth of the system. Among many other questions, Section 6 discusses how many BSs are worth to cooperating, what the trade-off are between the increased cell throughput and the increased coordinated multi-point (CoMP) processing & backhaul needs, and which backhauling technique is the best to serve a given traffic level.

In today's networks, the full system capacity is only used during a "small" portion of time [Auer+2011]-[Sandvine2010]. Thereby, considerable amount of energy can be saved by dynamically reducing the number of active network elements to follow adaptively the daily variation of the traffic. Among many other questions, Section 7 discusses how many resource blocks should be used or how many sectors or BSs should be activated to serve a given traffic level. This chapter also discusses the impacts of application of macro BSs with remote radio head (RRH) and how much capacity should be allocated to the coverage layer of heterogeneous networks (HetNets).

Going further below the above timescales during the analysis of mobile systems, the goal of traditional RRM techniques should be rephrased to secure the minimal energy consumption when serving a given traffic demand with special focus on low traffic situations. Among many other questions, Section 8 discusses how to utilize cell sleep modes like cell discontinuous transmission (DTX), how to combine DTX with power control and how to allocate enough "space" for sleep modes by introducing multicast broadcast single frequency network (MBSFN) subframes. This chapter also discusses how to utilize the characteristics of applications like the delay tolerance or which RAT should serve a given application.

Looking further ahead in time and beyond today's existing system standards and typical deployments, there are several promising design options and technology solutions that may enable enhanced energy efficiency in future mobile radio systems. Such enablers are discussed in Section 9, which includes, e.g., a discussion of the benefits with the conceptual idea of logically decoupling the transmissions of data and control information and how mobile multihop relaying may be used to increase coverage and reduce energy consumption. Section 9 further describes a cloud-RAN (C-RAN) architecture that suits HetNet deployments and provides insight into the energy efficiency of NC in relation to commonly used retransmission techniques.

2. OPTIMAL MIX OF CELL SIZES

In traditional network planning the distance between BSs is adjusted to the maximum ISD that provides the requested system performance. A lower ISD implies more sites, thus increases network capacity, but also increases CAPEX costs for site acquisition and equipment. The issue of lowering network energy consumption adds another dimension to the optimization problem. How does the ISD impact the energy cost? Can the deployment of additional cells (e.g. of an underlay of micro cells) save power?

Broadband transmission requires a strong signal even at the cell edge. However, due to the high path loss coefficient (α >3) of radio frequency (RF) propagation smaller transmission ranges offer high savings in transmit power: The necessary transmission power at the antenna grows faster with the ISD than the covered area, i.e., larger cells use excessive transmission power per area. This is often interpreted in a way that small cells lower the system power consumption. However, each BS consumes power for basic operation and for signalling purposes. The selection of the most energy efficient ISD therefore is non-trivial and depends on the type of BS (e.g., power class, antenna height), on the traffic demand, and on the detailed behaviour of power consumption over traffic load. In the previous deliverable [EARTH-D3.1] we have shown that the parameters of the power model, that maps the RF transmission power to the total power taken from the supply grid, strongly influence the result. The most important parameter is the amount of power amplifier (PA) offset power. The EARTH project has therefore created a detailed power model based on a study of actual hardware [EARTH-D2.3], [EARTH-D4.1]. Section 2.1 provides results for two different traffic scenarios, showing that in dense urban scenarios an ISD of 500m is optimum, while in urban scenarios 1400m is the best ISD. A bad choice of the ISD can increase the power consumption by a factor of three.

Next to the optimization of the ISD, a densification of the macro cell network can be achieved by adding small cells. Such heterogeneous deployments beneficially place the small cells at the cell edge where the macro cell signal is most impacted by path loss and neighbour cell interference. The possible gain of this scenario is briefly summarized in Section 2.2. However, for a homogeneous traffic distribution a significant gain is only achieved for rather high traffic scenarios of more than 150Mbps/km^2. In real-world scenarios traffic is often distributed inhomogeneously with hotspots of higher user density. Heterogeneous deployment allows offloading a large part of the hotspot traffic to small cells. When the traffic load is rather low, the added small cells increase the power consumption of the network. But Section 2.3 shows that the offload reduces the power consumption of the macro cells and saves power already at traffic scenarios of below 100Mbps/km^2 in the average. Further, the small cells are the most efficient deployment of extra capacity when the traffic surpasses the capacity of a macro cell of around 160Mbps/km^2. Increasing the number of sectors or adding a second carrier (i.e. doubling the BS power model) would need more power than the heterogeneous deployment.

Finally, Section 2.4 develops a mathematical tool for finding the optimum BS positions for deployment with inhomogeneous traffic over larger areas. This will allow studying cases where not only hotspots occur within a macro cell, but also the macro BS are no longer arranged in a hexagonal grid. The method uses force fields that move the BS sites into the equilibrium positions with minimum energy consumption.

2.1. OPTIMUM INTERSIDE DISTANCE OF MACRO CELL DEPLOYMENT

In two preliminary studies [EARTH-D3.1] the fundamental behaviour of area power consumption has been analysed. The studies were using different assumptions for the scaling rules of ISDs: The first study assumed a fixed transmit power of 40 W per sector, as typically assumed for macro cell scenarios in 3rd Generation Partnership Project (3GPP) standard. The second study was assuming that the BS transmit power is adapted to the ISD to just provide (nearly) full coverage. We summarize the results here to compare them in Section 2.1.3 to the simulations using the now available full-blown EARTH power model.

2.1.1. ISD with cells of fixed transmit power

In a system level simulation the cell capacity, the cell edge rate, and the power consumption have to be computed. A typical 3GPP scenario is applied with a hexagon arrangement of 3-sectorized macro cells with 2x2 MIMO antennas in the 2.6 GHz band. The ISD is varied, subject to a minimum capacity of 20 Mbps/km² system throughput and of 2 Mbps cell edge bit-rate. A simplified linear power model has been applied with 700 W offset power for the empty BS and a load dependent power component of up to 600 W: P_{in} = 700 W + L·600 W. The traffic load is modelled in the following way: For the sake of simplicity it is assumed that at any timeslot (i.e. at any LTE subframe) an LTE cell is either transmitting with 40 W per sector or not transmitting at all. The probability of transmitting during a timeslot is calculated from the average traffic load per cell, neglecting the power needed to transmit reference symbols and the broadcast channel.

The power consumption per area has been shown to be a decreasing function of the ISD (see FIGURE 1 left), dominated by the fixed part of the power model. The optimum deployment is the one with the minimum number of nodes satisfying the coverage/capacity conditions. Thus, there are two complimentary ways of reducing the total system power: decreasing the offset power of the BSs or decreasing the number of BSs in the system.

2.1.2. ISD with cells of adapted transmit power

At smaller ISD the required coverage can be achieved already at lower transmit power than 40 W, which also reduces the interference from neighbour cells. Therefore, the second study analysed the optimum BS ISD when the transmit power of the macro BSs is adapted to provide coverage in 95 % of the area. In the range of ISDs of 500 m to 1500 m this yields macro cell transmit powers P_{TRX} of about 0.7 W to 87.3 W [ArRiFe+2010]. A further increase in transmit power would allow to cover the area with ISD even larger than 1500 m, however, the cell capacity is spread over the larger area and no longer achieves the required area throughput of 20 Mbps. The total input power is computed from the detailed EARTH power model, which basically is scaling the same offset power and slope given in Section 2.1.1 above: P_{in} = 700 W + L·600 W/40 W*P_{TRX} . Here we assume a full buffer traffic model, i.e. L=1 for a cell with at least one active user and L=0 is used for an empty cell).

The simulation compares deployments of different ISD by means of area power consumption, area throughput, and coverage. The throughput is calculated for indoor users with full buffer, considering the interference from all BSs. For homogeneous macro deployment the optimum ISD is between 500 m and 1500 m, which are the typical ISDs for dense urban and urban environments (see FIGURE 1 right).

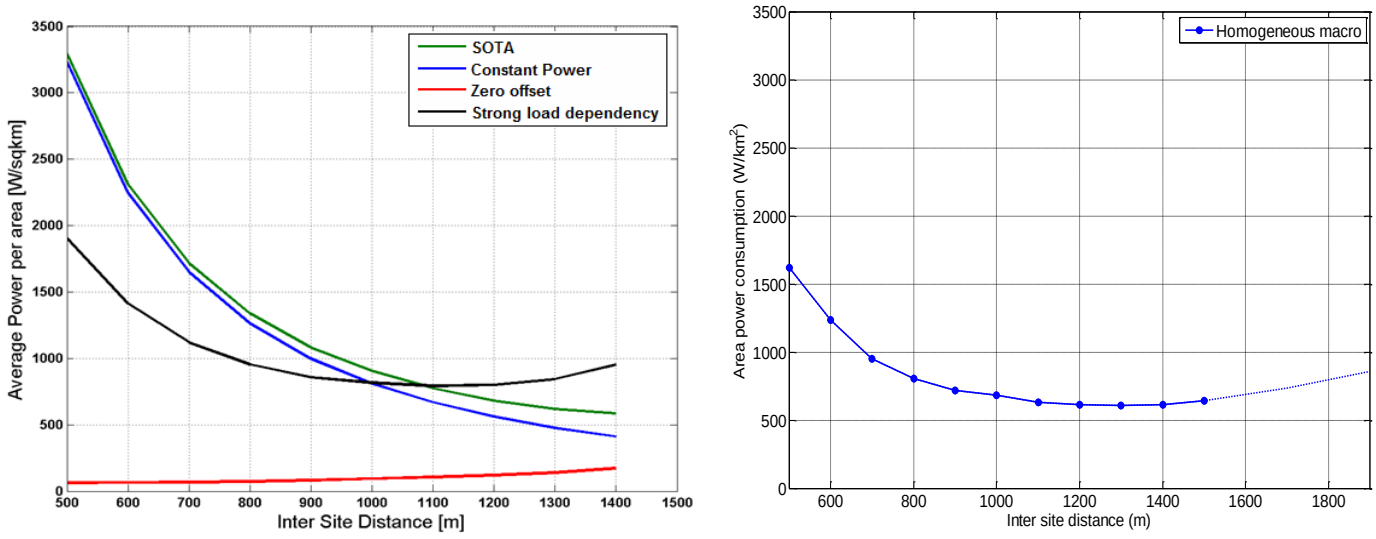

(a) (b)

FIGURE 1. Power consumption of macro BSs over ISD with a minimum system throughput of 20 Mbps/km^2. (a) Left: Fixed transmit power. (b) Right: Transmit power scaled to the cell area.

Compared to the result in the previous section, for small ISD the area power consumption is only half as high. This is due to the excessive transmit power of the fixed power assumption. On the other hand, for larger ISD than 1400 m the adaptation of transmit power leads to a significant increase in total area power – without being able to provide the area throughput of 20 Mbps as required for urban areas. For 1200 m to 1400 m the two models largely agree, so both provide 1400 m as the optimum deployment for the studied QoS requirements.

2.1.3. Optimum Inter-Site Distance when using EARTH transceiver hardware

We now study the ISD using the full E^3F evaluation framework. The framework defines dedicated BS hardware models. For macro deployments these provide up to 40 W of transmit power. For deployments with smaller ISD less power may be sufficient, but operators usually equip all BSs with off-the-shelf hardware. However, in these cases the operation point of PA is configured for lower output power, leading to power saving. State-of-the-art (SOTA) equipment allows for tuning the output power by a few dBs [Section 6.2 of TS 36.104]. Advanced hardware as developed in D4.2 of EARTH [EARTH-D4.2], will allow up to 10 dB of tuning range. Obviously, with smaller PA output the cell can no longer use the full amount of spectral resources. Only a reduced bandwidth can be scheduled. We use this feature to adapt the cell throughput statically to a target value of 120 Mbps, as required in E^3F for the high traffic in busy hour of dense urban areas. The tuning may also be applied dynamically for network management of busy hour; this is studied in Section 7.1.

Furthermore, the down-tilt angle of the antennas is also optimized for each ISD. For smaller cells larger tilt angles allow to confine the transmit power closer to the antenna, providing higher receive power and at the same time reducing inter-cell interference. Both effects improve the cell throughput at a given RF output power.

System level simulations have been performed to evaluate the optimum ISD for lowest area power consumption of macro BSs. For these simulations a hexagonal cell layout has been used that contains 19 macro BSs each serving 3 cells. The simulation parameters are summarized in TABLE 1.

TABLE 1. Simulation parameters.

Parameter	Value
Playground	57 hexagonal cell deployment with wrap around
Bandwidth @ Carrier frequency	10MHz @ 2 GHz
Inter-site distance	250 m, 354 m, 500 m, 707 m
Antenna model	3D model (1Tx, 1 Rx), optimised downtilt for each ISD
Shadowing	Correlation distance of 50 m Shadowing correlation of 0.5 between sites
Application	Video streaming with constant bit rate of 2 Mbps per user
User mobility	3 km/h
Power model	EARTH E^3F 2012 for macro BS, including adaptation

The power consumption per area is depicted in FIGURE 2 (a) for a SOTA macro BSs running with 10 MHz bandwidth at the specified 40 W. The power consumptions have been calculated for high system throughputs of 120 Mbps/km^2 in dense urban environments (see [EARTH-D2.3]). The resulting area power consumption

compares well to the values in FIGURE 1. However, due to the higher traffic demand assumed here, an ISD of 1400 m cannot serve the QoS level (see FIGURE 2 (b)). The area throughput drops below 120 Mbps/km^2 at ISD of larger than 700 m. Regarding a traffic mix with not just pure video streaming and with handover margins for moving user equipments (UEs), a stable operation of the network typically is only possible at an average cell load level of 60 %. This is achieved for ISD of up to 500 m. This value is therefore considered the optimum ISD for dense urban deployments in E^{3}F. The area power consumption is 1.94 kW/km².

This can be compared to macro BSs equipped with adaptive PAs and applying a static bandwidth adaptation (see Section 7.1 for more details). Due to the throughput requirements the optimum ISD is still 500 m, but the area power is reduced by 14.3 % to 1.67 kW/km². The third curve in FIGURE 2 (a) is assuming a modified power model as provided in an integrated solution of all EARTH hardware approaches [EARTH-D4.1], [EARTH-D6.2b]. This also considers improvements of the baseband processing, RF part, efficiency of direct current (DC)-DC conversion, alternating current (AC)-DC power supply, and cooling. In this case a RRH without active cooling has been considered. This allows for further savings of 26 %, cutting the area power consumption to 1.16 kW/km².

For an ISD of 250 m the site density grows fourfold and the maximum system capacity per area improves roughly by a factor of 4 (see simulation results including interference effects in FIGURE 2 (b). At the fixed traffic demand of 120 Mbps/km² this leads to a very low load of only approx. 10 %. SOTA area power consumption increases by a factor of 3.1 in comparison to an ISD of 500 m. The increase is slightly lower than the 4-fold increase in offset power due to the reduced interference at 10 % load. The low load also implies that bandwidth (BW) adaptation has a higher saving potential than at 500 m ISD: For the bandwidth adaptation approach the area power consumption increases only by a factor of 2.6 (or 1.7 including improvements of all other components next to the adaptation of the PA), respectively. This yields a saving potential of 66 % for the application of static BW adaptation at 250 m ISD. However, the absolute value is still slightly higher than for 500 m ISD.

To conclude, an optimum ISD according to area power consumption can be achieved for deployments with ISD of 500 m. BW adaptation combined with other EARTH hardware improvements does not lead to a change in the optimum ISD, but provides 50 % of savings in area power consumption. However, these saving strategies can also be used for a more flexible deployment: They can turn a deployment of 250 m ISD into basically the same power consumption as a 500 m SOTA deployment. But such a deployment provides large capacity reserves that can gradually adapt the capacity to a traffic growth of nearly a factor of 4 over the years, without having to deploy additional hardware. This can be advantageous because requiring new sites and rolling out additional BSs takes long planning times and therefore operator have to design the network capacity already to future needs.

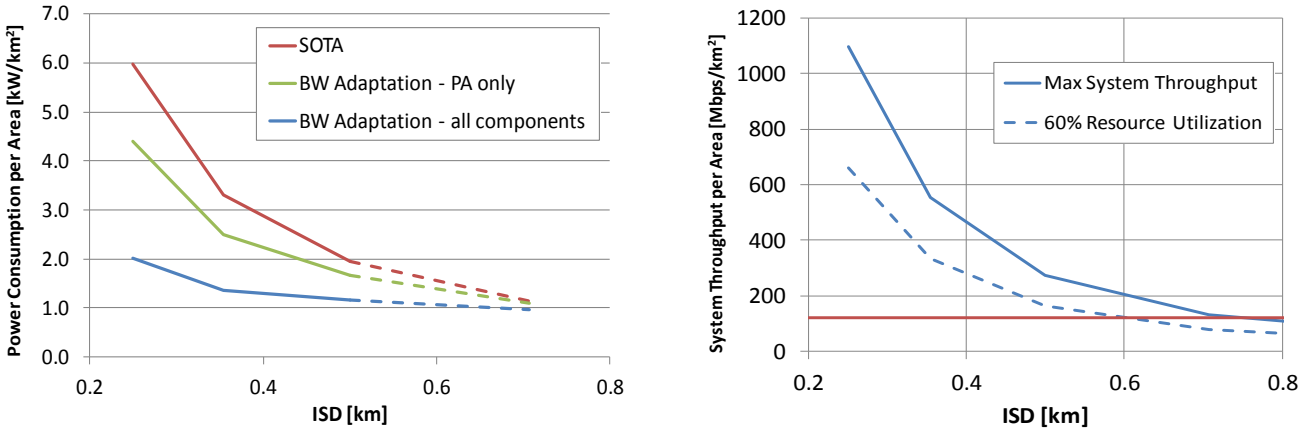

FIGURE 2. (a) Left: Area power consumption of macro BS deployments over the ISD. (b) Right: System throughputs over ISD, the red line is marking 120 Mbps/km^2.

2.2. HETNETS WITH SMALL CELLS AT CELL EDGES

At the vertices of the hexagonal macro cells the signal quality from the macro BSs is comparably low and, thus, the data rates in these areas are low. Remote users require more transmission resources for a given data rate than users close to the antenna. Therefore, potentially much power can be saved by offloading cell edge users into micro cells dedicatedly serving the cell edge (see FIGURE 3). We briefly recapture the prior results of [EARTH-D3.1] here in order to compare to the study of deployment of small cells in traffic hotspots in Section 2.3.

The micro cells at cell edge are considered as an additional under-layer, i.e., they add capacity but the macro cell overlay is designed to provide the 95 % coverage target. Micro BSs are designed for comparably short distances, hence their transmit power is typically 1 W or below. Also the amount of power consumed by signal processing and cooling is lower, thus, they consume much less power than macro cells.

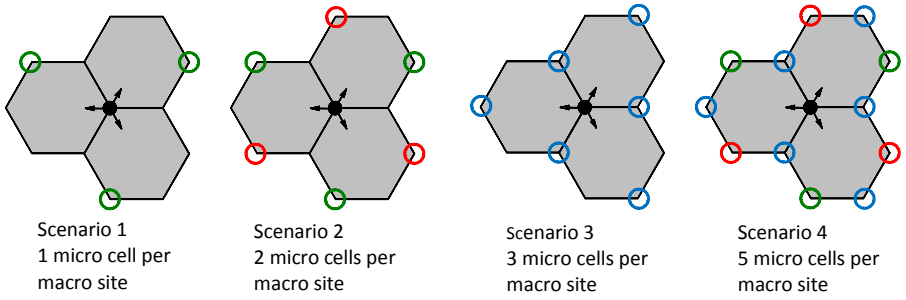

FIGURE 3. Small cell deployment at edge of macro cells with one, two, 3, or 5 small cells per macro site.

The addition of micro cells shifts the optimum ISD to larger ISDs (for more details, see delivery [EARTH-D3.1]), but always increases the total power consumption, i.e., the lower transmission power of micro BSs is overcompensated by the additional offset power of the added cells. For a network consisting of micro cells only, the optimum ISD is around 100 m for the full load case. However, it has been shown that the area power consumption is much higher than for a macro deployment.

Thus, the addition of small BS is not saving power *per se*. Rather; the higher area power consumption of deployments with micro cells has to be related to its superior throughput. It can be seen that the energy saving effect of the small cell deployment strongly depends on the traffic demand. For up to 70 Mbps/km² the conventional macro cell scenario is best. For higher throughput requirements, micro cells can reduce the optimum area power consumption. For traffic density of up to 100 Mbps/km² one micro cell per macro site is the optimum deployment. At very high densities above 150 Mbps/km², which can be expected due to quickly rising data rates in the near future, deployments with five or more micro cells are becoming interesting with a saving potential of more than 10 %.

Another promising case for micro cells occurs in situations with inhomogeneous traffic density. In this case micro cells would not only be placed at the cell edge but also at hotspots inside the macro cell. However, we lack reliable traffic data as input to an evaluation of the optimum deployment. In the following section we will model special traffic rates under the assumption that micro sites are only deployed where required by the traffic demand.

2.3. SMALL CELL DEPLOYMENTS IN TRAFFOC HOTSPOTS

The previous investigations of Section 2.2 focused on small cell deployments under the full buffer assumption, i.e., in all simulated scenarios there is an arbitrarily high traffic demand and all deployed BSs are under full load conditions. The following discussion considers situations where the amount of offered traffic to the overall system

is limited. Further we assume that the traffic density is inhomogeneous and small cells are deployed in the traffic hotspots, instead of locating them at the cell edge. We investigate the effect of micro site deployment alongside existing macro sites on the energy consumption (W/km²) as well as the energy effort (J/Mbit) of the network.

2.3.1. System Model Aspects

The system model follows all specifications laid out in [EARTH-D2.2]. In particular, we consider the downlink of an LTE 10 MHz system with 3-fold sectorised macro sites set up in a regular grid with ISD of 500 m. Micro sites are placed randomly in the area of interest. All access points are using two transmit and two receive antennas. In order to mitigate edge effects with respect to the micro site deployment, we evaluate an area corresponding to 7 macro sites with two additional tiers of interference instead of the usual single central site. The coverage requirement is 95% with an 80% fraction of uniformly distributed indoor users.

The traffic model assumes Poisson arrivals of users requesting files of exponentially distributed size using a mean of 2 MB. The user arrival intensity is adjusted to produce different demand intensities (Mbit/s/km² or equivalently Mbit/s/site). *The overall traffic demand is distributed equally among all micro and macro sites, independent of their respective cell sizes*, i.e., a micro site attracts as many users as a larger macro site. Through this assumption we capture a certain localization of traffic which is required to render micro deployment feasible.

A BS utilizes all available time and frequency resources whenever there is data to transmit, i.e., there is at least one active user in the cell. According to this assumption and depending on the load conditions, BSs spend these active periods of time under full resource utilization, i.e., maximum output power. During the remaining time (periods without user data transmission), we assume 26% of the time to be dedicated to signalling with a resource utilization of 29% (e.g. for reference symbols). In other words, the BSs operate at 29% of its maximum output power. The remaining fraction of the idle time the BSs spend in micro sleep mode consuming only the corresponding sleep mode power. In all cases we employ the power model as presented in [EARTH-D2.3] to determine the power consumption value in each state.

2.3.2. Results and Discussion

FIGURE 4 and FIGURE 5 display the relations between the served traffic per area and the required area power (kW/km²) and the system's energy effort (J/Mbit), respectively, assuming different numbers of micro sites deployed. The points on the curves were obtained by exposing each deployment to increasing amount of traffic demand (offered traffic). We observe the accumulation points for deployments with few micro sites where those networks become overloaded, i.e., in spite of an increase in offered traffic the served traffic and the power consumption stagnate. Comparing different curves yields the following findings

- In the range of <10 micro sites per macro site, depending on the demand different numbers of micro sites appeared to provide minimal total energy consumption. Starting at demand of about 100 Mbit/s/km², the utilization of 3 micros decreased the energy consumption compared to the case of macros only. The main effect here is that enough load is shifted to the small cells to yield a significant reduction in resource utilization at the larger cells. Similar observation is made at around 275 Mbit/s/km² where the case of 10 micro sites per macro site becomes the best.
- A large amount of micro sites (> 10) per macro site results in dramatically increased energy consumption and did not appear meaningful. This conclusion holds even under the assumption of equal demand distribution, which resulted in rather low load conditions for all small cells. The flat power characteristic of the micro sites, however, eventually resulted in a large amount of accumulated offset power in those scenarios. Note in this regard that we considered the small cells to utilize micro sleeps!
- Below the accumulation point of the macro-only scenario the BS can handle the traffic without micro cells, so the additional micro BS can be sent to a deep sleep mode in which no cell specific signalling is provided and the cell dwells at close to zero power. The potential energy savings resulting from utilizing such a deep sleep mode are estimated as the difference between any pair of curves in FIGURE 4 at low

load conditions. In particular, in case of 3 and 10 micros deployed per macro the peak savings (by sending all to sleep) are approximately of 14% and 40%, respectively. The envelope of the blue, green and red curve provides the area power consumption when dynamically the minimum required number of micro cells is activated.

- The slope of the area power with increasing traffic is rather small. Due to its definition, the energy effort (J/Mbit) is a strongly decreasing function of the actual traffic transported by the system in FIGURE 5. Since, according to the simulation setup, deployments with larger number of micro sites on average have a larger fraction of traffic offloaded to them, they also exhibit a lower energy effort (J/Mbit). Since the served traffic is equal for all deployments in FIGURE 5, we observe the same ratios for the energy efforts (J/Mbit) of the different deployments as we observe for the area powers (kW/km²) in FIGURE 4.

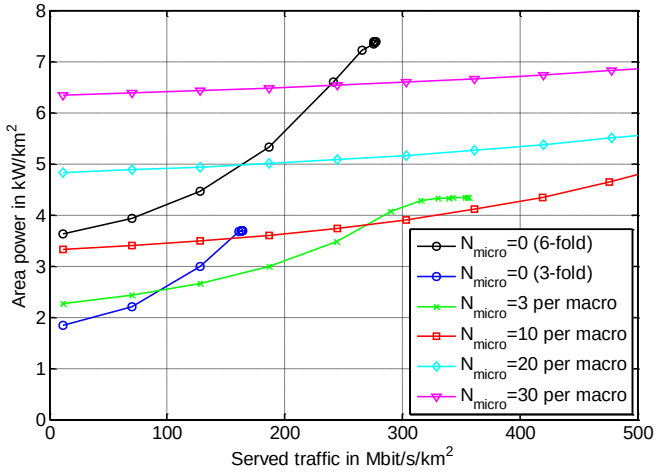

FIGURE 4. Area power of different deployment schemes as a function of served traffic.

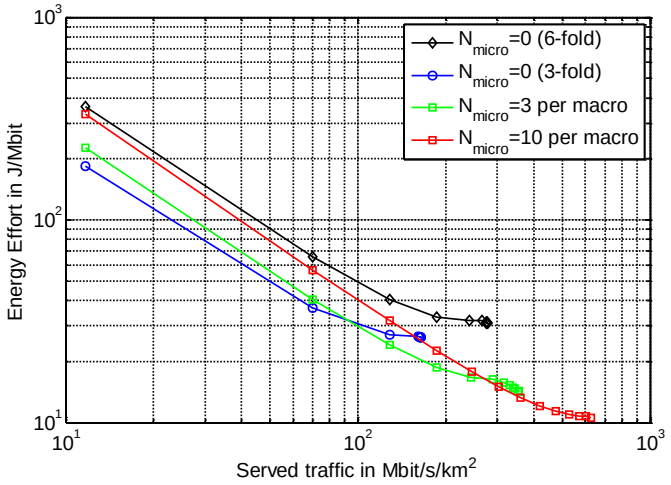

FIGURE 5. Area power of different deployment schemes as a function of served traffic.

In comparison to the case of small cells at the cell edge (section2.2) small cells show benefit already at much lower traffic density. For edge deployment a deployment with 3 small cells per macro is only efficient above 160Mbps/km^2 and only saves 8% compared to the macro only deployment (see [EARTH-D3.1]). For the hotspot scenario 3 small cells already pay off at 100Mbps/km^2 and at 160Mbps/km^2 save as much as 22%. The difference is that in hotspots much more traffic can be offloaded: the 3 small cells at the edge of the macro cover only around 10% of the overall traffic, while in the hotspot scenario 50% of the traffic is offloaded. Therefore, the saving effect in the macro BS is more pronounced.

Following the general tendencies observed from the simulations, it can be further inferred that even more pronounced energy reduction can be achieved if the same amount of traffic is offloaded to even smaller cells, e.g. indoor femto cells.

Summing up, we state that the deployment of additional small cells alongside macro cells, even though more energy consumers are present in the network, can lead to a reduction in the overall energy consumption and an improvement in the overall energy efficiency. Prerequisite to obtaining these gains is, however, that traffic is sufficiently localized, i.e., that enough traffic can be offloaded from large to small cells such that the reduction in dynamic power at the macro BSs over-compensates the additional power required by the micro BSs.

2.4. NON-HEXAGONAL DEPLOYMENTS BY MOVING BSS IN FORCEFIELDS

In Sections 2.1 and 2.2, the ISD in hexagonal macro deployments has been optimized for area power consumption. It was found those ISDs between 500 m and 1500 m, typical urban/dense urban ISDs, yield lowest network power consumption. In order to further increase energy efficiency of the networks, additional small cells at cell edges have been considered. The power saving potential by deploying small cells strongly depends on the traffic conditions. While for low traffic demands up to 70 Mbit/s/km^2 a conventional macro cell deployment is optimal, small cells should be deployed for higher traffic demands, e.g., 5 micro cells per macro site for 150 Mbit/s/km^2.

These results were obtained based on a symmetrical setup, i.e., flat plane, homogeneous spatial user distribution, and uniformly distributed traffic demand. In real world, such symmetries do not necessarily occur. On the contrary, traffic demand is concentrated in certain areas, where such areas also change during the course of a day. Thus, it is obvious that an optimal deployment will inherit those irregularities in some way, e.g., by adjusted BS locations and appropriate selection of BS types.

Current network planning and optimization tools are designed for optimization with regard to different key performance indicators (KPIs) such as coverage, throughput, blocking rates, and handover failure rates, neglecting the power consumption aspect completely. Hence, there is need for an algorithm that provides optimal BS locations and, optionally, optimal BS parameters, for inhomogeneous scenarios reflecting real world conditions. The problem of optimal BS placement is typically approached by site selection where the domain of BS locations is discretised and a binary/discrete program is solved by integer programming. Such an approach requires objective and constraints to be formulated as linear functions for being tractable numerically. In order to reduce the problem's dimension, BS locations are treated as continuous variables. Problems that do not make use of this so called candidate site concept usually optimize BS locations by means of stochastic methods, e.g., genetic algorithms and simulated annealing.

In the new approach, which is still a heuristic but does not contain stochastic elements such as random search, BS locations are considered as continuous variables. This avoids the problem of increased complexity of a discrete approach since some relations cannot be formulated as linear functions. The problem of BS placement is formulated by means of forces acting between BSs and between BSs and environment (e.g., users), which translate to BS displacements. The target is to track these displacements in search for a balanced state, where the acting forces compensate each other. The crucial part is the definition of the forces and their combined evaluation.

A basic KPI to be considered is the interference. An interference force field can be modelled as repulsive force between BSs, where the magnitude of the force is determined by the accumulated interference in the corresponding cell. An example for an external force is the coverage force field, where the force directions and magnitudes are determined by the non-covered areas and the amount of non-covered traffic, respectively.

The different forces acting on BSs can be combined sequentially or contemporaneously. The total force at each BS is then translated to a displacement. This is done by following Newton's Laws of motion, which yields an acceleration for each BS. By introducing a mass for each BS, this acceleration eventually provides a displacement.

Those masses could be equal for each BS, leading to displacements which are proportional to the acting forces. On the other hand, a mass can be used to express the quality of a BS in the network. Different masses finally introduce a kind of inertia to the system, i.e., BSs with good properties are less likely forced to change location. A balanced state could finally be reached by following those trajectories. More details on the model and some exemplary forces can be found in [RicFet2012] .

The advantage of this novel approach is, amongst others, that only one deployment is considered. In comparison, genetic algorithms and particle swarm optimization are based on evaluating and manipulating populations of deployments, where the size of the populations has to ensure a certain diversity. Another advantage compared to stochastic optimization models is based on the fact that identical initial conditions lead to identical results.

In order to exemplarily show the behaviour of the system using the force field approach, the coverage force is considered to act within a deployment consisting of 5 macro BSs, each with three sectors. In the initial deployment the BSs are clustered in the lower left corner of a rectangular area of 2 km by 2 km. An LTE system operating at 2.0 GHz and 10 MHz bandwidth is considered. The traffic demand is non-homogeneously distributed with a density of 120 Mbit/s/km^2. The urban macro path loss model from [WINNER II] for flat plane is considered, where all users are considered indoor with an additional penetration loss of 20 dB.

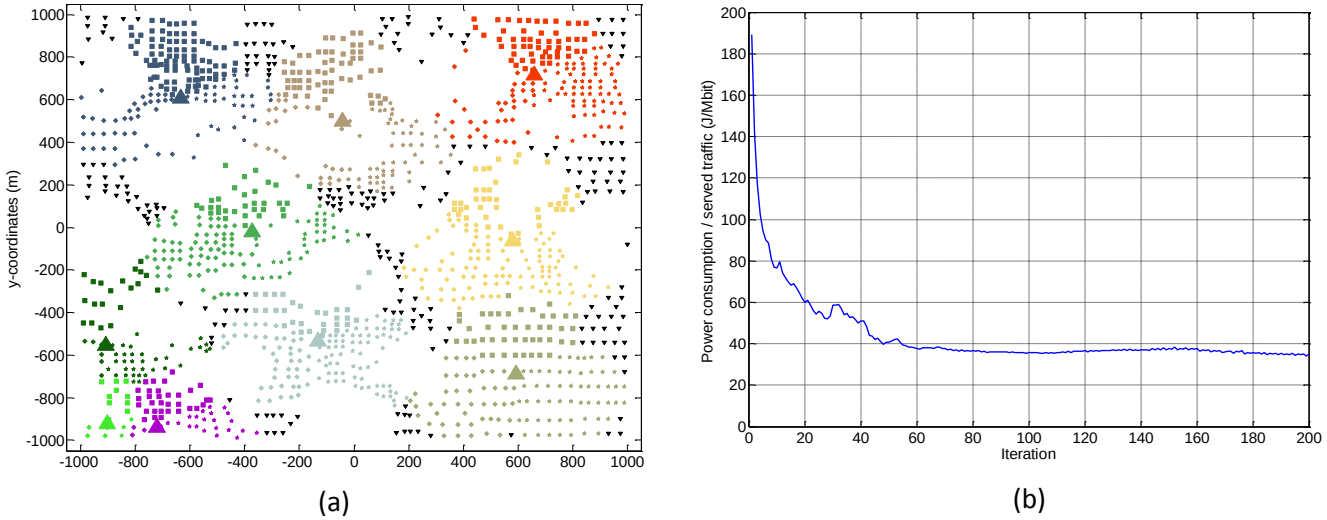

FIGURE 6. (a) Deployment in balanced coverage state, (b) Energy efficiency progress.

In FIGURE 6 (a) the deployment after 200 iterations is shown. The colours and markers of the user positions indicate site and sector association, respectively. The black triangles identify users which are not covered. It can be observed that the coverage force field leads to a distribution of the BSs over the given area. Further, it can be seen that not all BSs are displaced (refer to the two (light green and pink) BSs located in the lower left corner) which is due to the convergence to a balanced state. The energy efficiency progress of the system is plotted in FIGURE 6 (b). After the first 80 iterations, there is no further gain. This results from fully loaded cells, meaning the served traffic is not increased while coverage is improved. Note that in this example only the coverage force field is considered, where the load in the different cells is completely neglected.

The main goal of this approach is to provide a complexity reduced method for optimizing deployments. Combining all different force fields (e.g., interference, coverage), considering different deployment relevant parameters (e.g., power per transmit antenna, antenna down tilt), and integrating the different important KPIs in the mass concept (e.g., served traffic, energy consumption) will yield a dynamic deployment model which eventually provides optimal figures with regard to the number, the types, and the location of BSs (as well as some of its parameters) with respect to energy efficiency.

3. MULTI-RAT NETWORK EVOLUTION

The previous section discovered the energy efficiency consequences of network deployments, based on dual layer macro-micro coverage. The underlying assumption of the studies considered single RAT system (LTE), sharing the same band for both coverage layers. However, several practical considerations raise the need to examine deployment solutions that take several different co-existing networking technologies into account. Namely operators' existing legacy (GSM and 3G High Speed Packet Access (HSPA)) deployments are in place and, thus, future LTE roll-outs should be planned considering this. The penetration of LTE capable UEs is foreseen to grow steadily, however, realistic scenarios should consider that non-LTE capable UEs will be used on for significant time periods, hence pure LTE deployment would not be able to serve them; this is again a motivation towards deployment optimization with multiple RATs. To tackle these issues, this chapter first introduces a self-deployment (and network management) method developed to take EE into account besides coverage and capacity requirements. Later LTE roll-out strategies and scenarios are analysed in terms of EE, based on assumptions of existing legacy networks.

The first main contribution of this section is an effective automatic deployment method that minimizes total power consumption. This method is applicable mainly in rural and suburban scenarios, where shadowing is not very prevalent. It is shown that based on this method, network management reconfiguration actions can be pursued in case of changing traffic environment, resulting in up to 30% saving in consumed power. Furthermore, it is shown that if the deployment targets the planning of a second RAT, some savings are available by re-using sites of previous deployment, but this gain is very limited. Analysis of an example network evolution carried out in this section shows how network power consumption scales with this evolution. The drive in adopting more energy efficient RATs should be, nonetheless, carefully balanced with the constraints coming from the forecast increase of capacity demand, terminal capabilities, electro-magnetic coverage, interference management, electro-magnetic emission limits, legacy networks.

3.1. MULTI-RAT NETWORK DEPLOYMENT METHODS

This section reveals the efforts being carried out towards the development and implementation of a self deployment method that results in RAN topologies that are optimized taking energy consumption into account as well. The method and its subsequent improvements are described in detail in [TorFaz2010], [TorFaz2011a] and [TorFaz2011b].

3.1.1. Basic algorithm

The algorithm supposes that an area is described by means of the traffic demands, given at discrete points in kbps (DP denotes the *demand position*; the set of these DPs is called the *traffic map*). As these points can be defined by arbitrary resolution, this approach, depending on the number of demands, includes a "pixel wise" traffic demand as well as having just a few isolated traffic spots. These might either represent individual users as well as smaller areas described by the traffic originated there. As such this traffic definition might describe the actual demand by arbitrary precision and details.

The area to be covered is also described by the possible locations enabled for BSs to be deployed there. Again, this is of arbitrary precision, hence allowing the algorithm to work in a scenario where BSs might be placed anywhere, as well as in scenarios where stations might only be placed to restricted locations (e.g. rooftops, or existing sites, etc.)

The algorithm is based on the well-known K-means clustering method and tries to cluster DPs. In a first phase, the clusters correspond to the set of demands served by a particular BS. The objective function of this clustering is to minimise the sum of traffic demands multiplied by their distances from serving BSs. The motivation behind is to put BSs closer to higher demands – this ensures minimum resources for their service, including power. This might

not be true in case of shadowing; when more distant, but not shadowed demands might get higher received power, than closer, but shadowed ones. However, the algorithm still reflects a general goal of having BSs in the vicinity of high traffic demands, which is a widely followed approach. During this phase, the BS is "moved" by the algorithm, until the objective is minimized or maximum number of iterations reached. The second phase of the algorithm is again based on K-means clustering and sets the main lobe direction of sectorised antennas (three of which is basically supposed on a station, their main lobes closing 120 degrees). The objective function of this step is to minimise the traffic demands multiplied by the angles they are away from the main lobe. This has the goal of having the higher demands in the centre of the antenna pattern.

After placing a single station the algorithm evaluates if the traffic demands assigned to cells can be served. For this, a simplified LTE RRM model is applied. If the service is not satisfactory (namely more than a maximum δ – which might be 0 as well – percentage of total traffic is not served), the algorithm finds the most overloaded cell, places a new BS near it and the above clustering procedure starts again with phase 1, at the end having the system with this extra BS. The whole procedure runs until less than δ percent of traffic remains not served.

3.1.2. Management extension

The algorithm is further improved, in order to allow slow reconfiguration management of the network layout. The motivation of this is to allow a deployment that is optimised for a changing traffic environment. For this, it is supposed that the area is described by several traffic maps, representing several traffic situations (e.g. representing several periods over the day); the volume and spatial distribution of demands might be different over these. The main algorithm is used for determination of BS positions optimal for the union of the traffic maps. This gives the ultimate positions of BSs; each traffic map will be later base of individual run of the algorithm, with the possible sites that were resulted for the union of the maps.

It is recognised that reconfiguration of a network can be interpreted as a new deployment, for the new traffic map, with restricted BS positions (coming from the first phase of the algorithm). The deployment method is then applied to each individual traffic map. The difference in this case is that the cells are also added one by one, so it is possible that a station will have less than three sectors. The resultant deployment typically contains less stations and cells than resulted in the initial phase: the rest is supposed to be turned off for energy efficiency reasons. Also main lobe directions and output power levels are set by the algorithm: it is supposed that the network management is able to change these parameters accordingly. FIGURE 7 contains an example how the algorithm adapts network layout for 3 different traffic maps; first the most traffic is concentrated top left, then in the middle, finally in bottom right of the area.

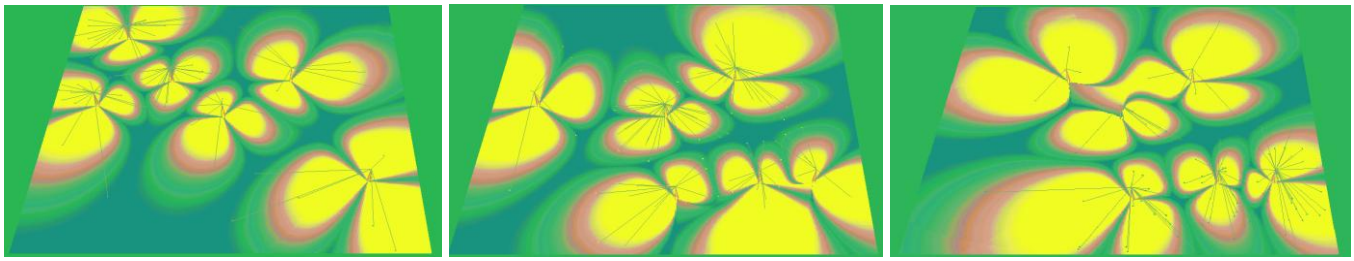

FIGURE 7. Example of network layout adaptation for 3 different traffic maps.

Applying this reconfiguration management gives room for energy saving compared to the case when this adaptation is not applied. The left graph of FIGURE 8 shows the gain in energy consumption for a given scenario (three traffic maps), when different numbers of DPs were considered (60, 40, 30) for the maps, spatially migrating or not changing their positions. The power consumption gain compared to no adaptation can reach 30% for high traffic scenarios considering spatial variation of the demands as well.

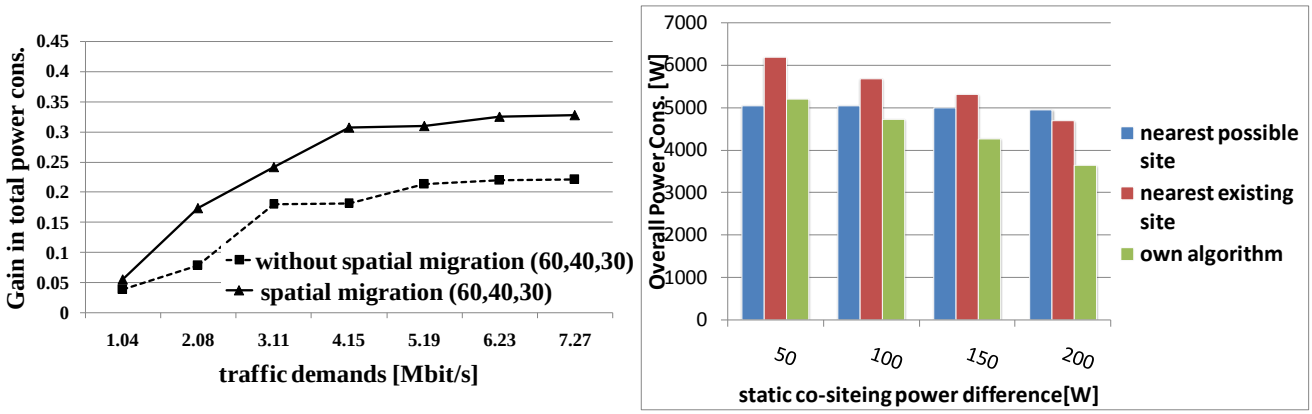

FIGURE 8. EE results.

3.1.3. Multi-RAT extension

The algorithm is extended to support deployment when there is an already deployed network, e.g. Universal Mobile Telecommunications System (UMTS) and traffic demand increase forces a deployment extension, with a novel RAT system (LTE). Basically the algorithm has to be run simply considering the extra traffic and placing the new stations to the resultant places. However, rational deployment strategies would prefer sites where there is already a station from the original deployment. To catch this from EE point of view, we assign a certain static co-siting power difference. It is assumed that two co-located stations consume less power than two stations at different sites; this difference is identified as a factor that influences multi-RAT deployment strategies. The examined strategies are the following: (1) placing the new BS to the nearest possible site position (regardless of whether it contains already a former station or not) the algorithm suggested; (2) placing the new station to the nearest position where there's already a BS. The latter apparently tries to exploit the co-siting power difference (at the price of not putting the station to the optimal place returned by the algorithm).

An own algorithm was also defined. This is again based on substituting the position of the nearest former BS with a virtual user, having a demand that would require as much power for the service, as much the power difference is. Then the K-means clustering is run again, if the resultant place for the new station is closer to the old station, finally the placement would be there. The idea behind is to implicitly calculate if the power difference would be more then what is lost when we place the new station away from its "optimal" position. As an example scenario, the total power consumption is shown for different co-siting power difference values in the right side of FIGURE 8. It is apparent that for low gain constants it is not worth choosing co-siting from energy point of view, because more power is needed to serve the network with the suboptimal position of new sites, then what gain is coming from the co-siting power difference. It has to be noted however, that the main incentive of co-siting is not energy consumption, but other cost parameters. The algorithm can be extended to these other types of optimization criterion (e.g. site rental cost) as well.

3.1.4. Implementation and use potential

The methods described can be used for either deployment over non-covered areas, or deployment predictions for changing traffic volume/patterns. This requires estimate or forecast of traffic over spatial and time domain. As deployment this does not require any specific operational solution from the network. The resultant deployment can be viewed as a starting point for any later management or RRM actions. It also has to be noted that due to the radio interface of LTE the RRM affects the amount of traffic that can be served by the cell, as such this could influence the deployment algorithm. However, RRM can be viewed as an input to our algorithm.

As management it can be viewed that slow timescale (several hours) configurations can be planned, or predicted by the method. As such, more detailed management operations can be operated base on the actual deployment configuration resulted by the algorithm for a given traffic map.

The multi-RAT extension of the algorithm enables the planning of new LTE deployments, based on existing 3G networks. To obtain realistic (re)planning of the whole dual system network, the algorithm should be fed by the penetration of LTE capable UEs (directly translated into amount of traffic that could be served by the new RAT).

3.2. MULTI-RAT ROLL-OUT PLANS

Since new LTE BSs will be gradually deployed in an environment where legacy mobile communication systems (GSM and UMTS) will be operational for a significant time period, multi-RAT deployment evolution should be considered within the framework of energy efficiency, and, in this context, energy efficient multi-RAT deployment guidelines are investigated here.

The aim is to exploit the roll-out process and evolution over time of a legacy network which expands to cope with traffic increase to get some gain in the energy efficiency of the overall HetNet.

In this section, in line with previous results presented in [EARTH-D3.1], an analysis to consider not only the insertion of new technologies but also the legacy through simple modelling of power consumption (linear power model correlated with traffic load), is presented: the idea is to focus on a capacity distribution among RATs that takes into account traffic demand increase, the different types of UEs available, the energy efficiency aspects and a possible reuse of legacy sites.

In accordance with [EARTH-D3.1], since the aim was to understand the key aspects that should be taken into account while tackling the increasing capacity demand, an annual traffic increase of 108% over three years was considered. Furthermore, EARTH power models of LTE and legacy RATs in relation with the data throughput were used. A linear relation identified by two points is considered: one representing the maximum throughput capacity of the network node while the other occurs when no UE is served but only pilot or common control channels are transmitted. More specifically, for LTE RAT 31% of the resource elements are used for the transmission of control information [EARTH-D2.3], for the GSM RAT, the broadcast control channel (BCCH) carrier should be considered always active while in the UMTS RAT 10% of the power of each carrier is devoted to common control channels [Laiho+2002]. In this case, the power consumption becomes proportional to the data throughput of the cell of a considered RAT.

To adapt our previous analysis to the E^3F [EARTH-D2.3], a new EE KPI was adopted (kW/km^2) and it was assumed that the E^3F ISD values were applicable to the LTE final deployment at year 3. Since the analysis was extended to the rural scenario, LTE ISD urban and rural target values and the number of sites achieved at Year 3 were the reference upon which area extensions were derived for insuring consistency with the E^3F model. For the other RATs layers, as RATs served areas were supposed to be the same, ISDs were calculated from LTE area extension values and from the number of sites of the considered RAT deployed in the three steps of the evolution analysis.

To simplify the analysis, the impact of the cell size on the consumed power was not taken into account and the traffic distribution was uniform for macro sites with the exception of micro cells urban deployment. In reality, the deployed micro cells (LTE micro cells are assumed to be 23% of new sites) were supposed to cover hotspots in the scenario, therefore in those areas the traffic was assumed not to be uniformly distributed.

In the presented analysis a refinement of site co-location analysis in terms of cooling cost savings was performed. Since dissipated heat could be calculated as the difference between total site power consumption and total RF power output, for each site configuration (single or multi-RAT) the maximum dissipated heat was determined. It was then assumed that a cooling unit should have a cooling capacity at least equal to the maximum dissipated heat related to the site. To evaluate the efficiency of a cooling device, the coefficient of performance (COP), defined as the cooling capacity against the rated power consumption has been used. An analysis was performed, to investigate typical COP values for Telco cooling systems in relation with the cooling power and trends of COP values in newer devices [AeaDai-Webs]. Relying on this survey, a theoretical mapping between cooling capacity and COP values was devised to capture the trend that larger cooling units are generally more efficient than smaller ones and newer devices increase COP values substantially, starting from a COP value of 2.5 up to 5.0, with

200 W steps (see FIGURE 9). The cooling power consumption of the power model described in [EARTH-D3.1] was then accordingly revised.

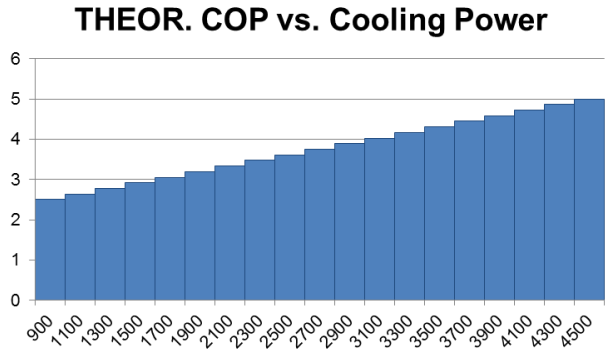

FIGURE 9. Theoretical mapping between cooling capacity (W) and COP values.

In FIGURE 10 and FIGURE 11, results of the urban and rural scenarios are shown. P/A_{max} indicates the power over area ratio of the entire network at peak capacity, while $P/A_{offpeak}$ specifies the power over area ratio of the entire network at off-peak capacity in the hypothesis of a daily off-peak evaluated 20 % [EARTH-D3.1] of traffic peak values. As in [EARTH-D3.1], the penetration of multimode UEs over time was considered. The ratio of legacy 2G and 3G sites was 50:50 (e.g. City of York, Ofcom website [OFCOM-web]). For each scenario, the resulting area derived from the LTE site number and ISD at year 3 are shown, as well as the ISDs of all the RATs at each step of the evolution. In our examples, under the considered assumptions, site co-location could result in a decrease in power consumption up to around 5% due to better cooling efficiency, depending on the balance between the different RAT types (when possible, up to 60% of shared sites for each RAT was considered).

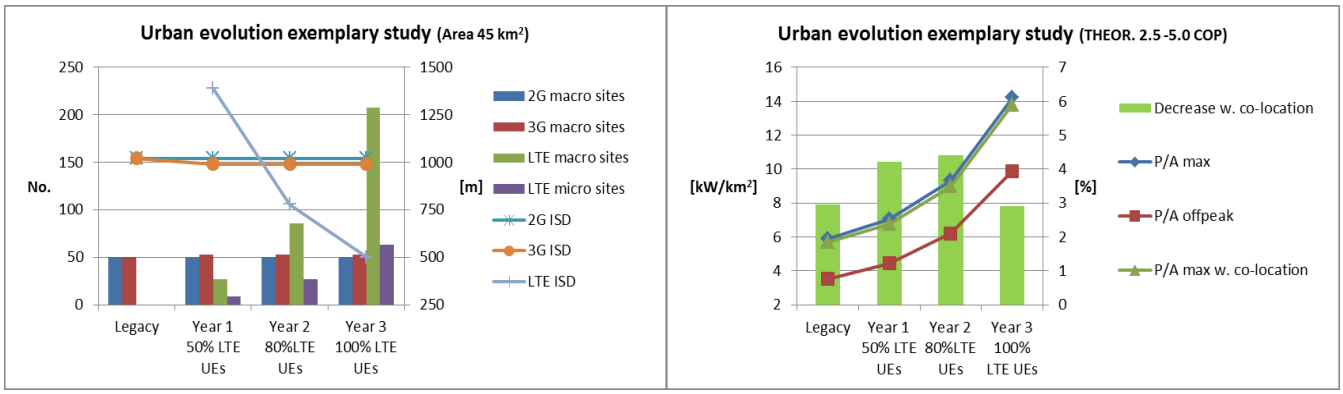

FIGURE 10. Results of urban evolution study starting from a 50:50 2G, 3G ratio.

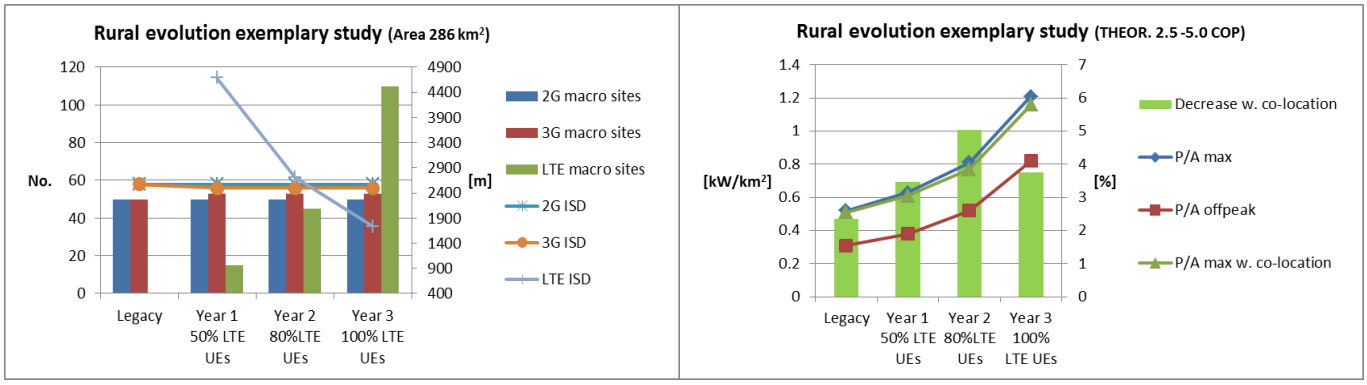

FIGURE 11. Results of rural evolution study starting from a 50:50 2G, 3G ratio.

Please note that, due to the technology evolution, while the kW/km^2 values increase 141% in urban and 133% in rural scenarios, the total carried traffic of the network from legacy to year 3 is multiplied by 9 with a 800% increase. It should be noted that, the tables aim is to describe methodology and trends: specific values should be computed with more comprehensive models taking into account the actual data from the network under investigation.

3.2.1. Roll-out strategy considerations

The study shows that an annual increase of capacity demand should be estimated and a precise knowledge of the distribution and trends of UE types is central as terminal availabilities lead to constraints on capacity distribution. However, the most relevant aspect to be considered is the importance of a good and precise knowledge of the energy consumption parameters of all the different nodes and RATs in terms of their power models. In a detailed roll-out plan that takes into account energy efficiency, the importance of the above mentioned inputs is key and to analyze and quantify, even if approximately, the energy consumption of each network node deployed should be seen as a fundamental baseline for the operator. The drive in adopting more energy efficient RATs should be, nonetheless, carefully balanced with the constraints coming from the forecast increase of capacity demand, terminal capabilities, electro-magnetic coverage, interference management, electro-magnetic emission limits, legacy networks. Setting aside the technological constraints, the actual roll-out priorities should also be harmonized with the network policies, marketing requirements and strategies as well as possible regulatory constraints. It should be noted that additional constraints that may lead to non-optimal LTE roll-out can derive from the limitation on voice service in its early years and from the licensed band(s) used by the new system, with respect to the interworking with the legacy RATs (e. g. in terms of inter-system handovers and coverage).

Another aspect of the analysis to be taken into account is the co-location of different RATs within the same site. It should be noted that, in sharing a location, fixed power consumptions components can be shared among the different RATs while the energy efficiency of other components (for example cooling systems) can benefit by the economy of scale and technological advancement of newer and bigger systems.

Generally speaking this concept can be extended to newer and therefore more efficient multi-RAT radio base station (RBS) replacements. Newer RBS will be beneficial also during the management phase of a network, granting more flexibility in the day to day energy efficient management described in the following chapters. The roll-out phase will have to take into account the different load scenarios in the network adopting the right technology solutions in the areas where certain dynamicity in the traffic can be met by more dynamic network nodes (e. g. in terms of variable radio resources and different levels of sleep-modes).

4. RELAY NODES

Relaying is part of LTE-Advanced (LTE-A) as a technology that offers the possibility to extend coverage and increase capacity, allowing more flexible and cost-effective deployment options [3GPPTR36.814]. In this section relay nodes deployment options are analyzed from an energy efficiency perspective, first considering a comparison between Type 1 (two hop relays) and Multicast Cooperative (possible Type 2) in uniform traffic distributions, then evaluating the performances of several relaying techniques (AF, CF, DF, or hybrid solutions); moreover, also the possibility to use NC is evaluated and compared to other relaying techniques in terms of energy efficiency, and finally the possibility to deploy relay nodes in order to serve hotspots of traffic is analyzed.

By analyzing the obtained results, in general it can be observed that energy efficiency of a macro-only system can be improved by a correct relay nodes deployment for serving additional capacity needs. Nevertheless gains strongly depend on several factors, and the following considerations should be made when evaluating the relay nodes deployment:

- Relay Nodes performance evaluations showed a strong impact of the power model of both Donor E-UTRAN NodeB (DeNB) and relay node (RN), and two-hop scheme provides a gain w.r.t. the direct transmission, especially in high traffic situations when considering advanced power model. This suggests an indication about the timeline for a possible introduction of Relay Nodes in a LTE-A network, where efficient radio nodes and huge capacity demand will motivate the introduction of this particular kind of small nodes.
- From the transmission point of view several relaying techniques have been compared. Results showed that hybrid relaying DF/CF scheme can flexibly switch between two different forwarding schemes and adapt to the current channel status as well as the decoding status at the relay. This scheme demonstrated considerable improvement in terms of EE in comparison with conventional non-hybrid solutions.
- However, the energy efficiency enhancement can only be achieved when the distance between the source and the destination is long enough. When deployed in a cellular system, not only the position but also the number of deployed relay nodes has significant impacts on the system's energy efficiency performance.
- When analysing the possibility to use NC, numerical results showed that when the transmission is divided into three phases and the direct link is considered in a two way relay channel, NC is not necessarily better than other forwarding schemes including AF, DF and CF.
- In an in-building scenario, performance analysis revealed that relaying can increase the EE in comparison with point-to-point (P2P) communication by either power saving or spectral efficiency (SE) improvement, especially at low SE, when the number of receive antennas at the UE is lower than the number of antennas at the DeNB and RN, or when the quality of the donor link is higher than the quality of the direct link. Results also indicated that even though transmitting with maximum power implies maximum SE, it does not necessarily imply maximum EE.
- Additional benefits can be achieved if relay nodes deployment is conceived for serving hotspots of traffic (non-homogeneous distribution) and the variability of the daily traffic profile suggest the potential usage of some on-board sleep mode functionalities in the hardware of the relays, e.g. triggered by a proper MBSFN switching mechanism in the packet scheduler of the RN and/or in the link scheduler of the DeNB.

4.1. TWO HOP VS. COOPERATIVE RELAYING IN HOMOGENEOUS TRAFFIC CONDITIONS

Results summarized in deliverable [EARTH-D3.1] provided a first positive indication for the possibility to use relays as a tool to increase the energy efficiency in a communication network. The study considered both a two hop half-duplex scenario, which can be seen as a Type 1 relay node in 3GPP nomenclature, or advanced schemes like the Multicast cooperative scheme, which can be a possible implementation of a Type 2 relay node (see FIGURE 12).

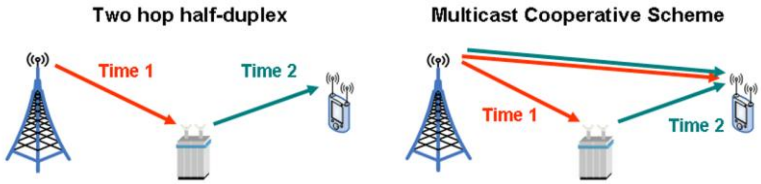

FIGURE 12. Two hop and multicast cooperative relay schemes.

However the results presented in the past suffered for two limitations: they were obtained considering only the consumption due to the radiated RF power of the transmitting nodes, and they were relative to the specific case of full load.

As highlighted in [EARTH-D2.3], in order to assess correctly the energy efficiency it is necessary to include in the simulation framework a power model that captures the whole power consumed by the transmitting nodes: for this study the linear approximation of the power model presented in [EARTH-D2.3] was used. One of the main impacts from the introduction of a realistic power model is that in that case relays will still have a certain amount of consumed power, even when they are not actually transmitting. Moreover, the power model scales the consumed power with the actual amount of resources used in the transmission, which varies when we drop the full load assumption. The static simulator introduced in [EARTH-D3.1] has been therefore improved with the possibility to evaluate capacity and energy efficiency for variable traffic load.

The simulator has been then aligned to the various propagation scenarios (urban, suburban, rural) presented in 3GPP [3GPPTR36.814] and in the EARTH project [EARTH-D2.2], and it has been used to calculate in each point of the cell, given a certain amount of traffic to serve, the amount of RF resources necessary to reach the desired rate, and consequently, using a defined power model, the correspondent energy consumption index (ECI). The map of ECI so obtained for each point of the cell has been averaged to provide the average ECI necessary to satisfy a certain traffic request in the cell.

At present, realistic power models for relay nodes cannot be provided, since no commercial solution is available. For this study network performance from an energy consumption point of view has been evaluated deriving two different power models for this kind of node (see TABLE 2). These models should be considered just as first theoretical references for the evaluation of relay nodes performances, in order to underline the importance of the power consumption model PCM to the overall energy efficiency. Section 4.5 will contain further power models for both macro and relays, seen as reasonable assumptions under the hypothesis of a smooth evolution from current equipments.

TABLE 2. EARTH parameters for different base and relay stations (2010-SOTA).

LTE node type	P_{max} [W]	P_0 [W]	Δ_P
Relay SOTA	5 or 1	84.13	6.35
Macro Advanced	40	156.38	28.4
Relay Advanced	5 or 1	13.91	20.4

The SOTA model “Relay SOTA” has been derived scaling a micro BS model (see [EARTH-D2.3]) proportionally considering the different peak RF powers. The “Relay Advanced” model, and a similar model for the macro BS (“Macro Advanced”) has been also introduced, starting from a model presented in [ArRiFe+2010] for an advanced node that strongly scales the consumed power with the actual traffic load.

The simulator has been used to provide evaluations for all scenarios (urban, suburban and rural) and for a representative set of traffic loads, which captures the range between the minimum and the maximum load observed for a certain deployment. These small scale short-term evaluations have been used as inputs to the E³F framework [EARTH-D2.3], in order to evaluate the overall ECI for the network. In particular, long-term traffic variations for the high traffic profile defined in [EARTH-D2.3] have been considered at the beginning. Results for this kind of evaluation are collected in FIGURE 13 considering different solutions: a network without relay nodes and E-UTRAN NodeBs (eNBs) with SOTA power models, a network with SOTA eNB enhanced with SOTA relay nodes, a network with SOTA eNB enhanced with advanced power model relay nodes, a network with only eNBs having advanced power models and finally a network with advanced eNBs and advanced Relay Nodes.

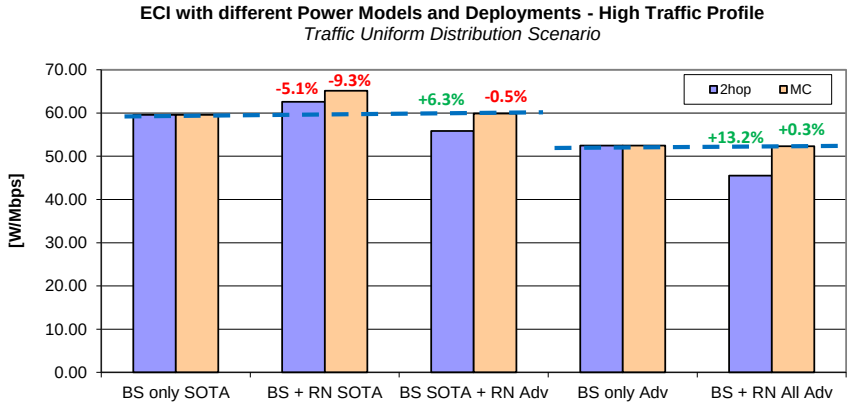

FIGURE 13. Overall ECI with different power models and deployments (High Traffic Profile).

From FIGURE 13 it is clear how the power models play a very important role in the overall energy consumption of the system. In general results also show that the 2 hop scheme is more energy efficient than the multicast scheme, and that a gain up to 13.2% can be reached with the high traffic profile and assuming advanced power models for both relays and eNBs. It should be noted however that this value is the result of a gain up to 68% in energy consumption in the area covered by relays. For the multicast scheme on the other hand no gain is visible, and in general from an energy consumption point of view this solution is less efficient, even if from a capacity point of view is the one that provides the greater gains.

From small scale simulations, it appears that higher gains are observed in high load condition, when relay nodes are actually needed. In low traffic condition the additional constant power consumed by relay nodes makes the advantages of their presence less significant. For this reason, power savings techniques (e.g. sleep mode, DTX) will be probably needed to improve the energy efficiency at low load.

Results previously shown are averaged in the whole cell, while if only the area covered by relay nodes is considered, power savings increase considerably (up to 68% as previously reported). The potential gain of hot spot scenarios has been therefore investigated in section 4.5.

4.2. HYBRID RELAYING TECHNIQUES

In this work, the energy efficiency of relaying techniques in two scenarios is studied: firstly, hybrid relaying schemes, which allow the relay to dynamically switch between DF and CF schemes according to its decoding status. The analysis is conducted in two perspectives: link level and system level. In the link level analysis, the consumed energy per bit is main evaluation metric and the circuitry energy consumption of all involved nodes is taken into consideration. In the system level analysis, we study the EE performance when the relay is located in

different places. Secondly, the link level analysis is extended to two way relay channel as shown in FIGURE 14, where node 1 and 2 communicate through the relay node.

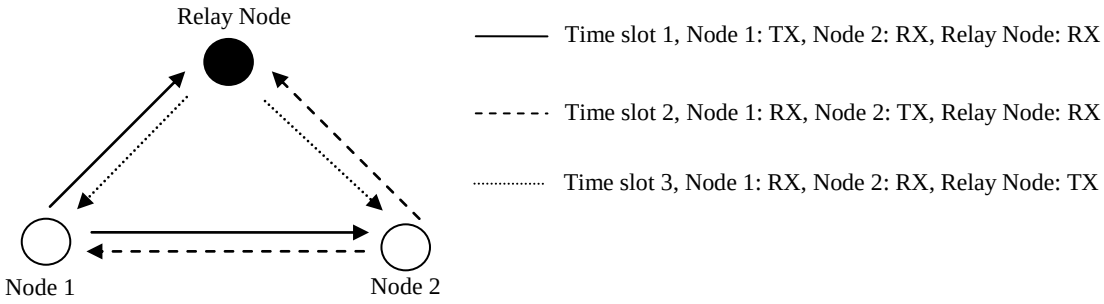

FIGURE 14. Two Way Relay Channel.

Link level analysis for hybrid one way relay scheme is a starting point of this work. A complete transmission lasts for T_{on} seconds, where $T_{on} \le T_{max}$ and is optimized as a design parameter. A half-duplex model is assumed, where a complete frame consists of a relay-receive phase with duration αT and a relay-transmit phase with duration $(1-\alpha)T_{on}$. The source transmits message w to the destination. In phase 1, the source broadcasts and the relay and the destination receive. The selection of different relaying modes during phase 2 is purely based on the decoding results of the relay and the decision can be made once the decoding procedure at the relay is finished at the end of the first phase. If the decoding is successful, DF mode is activated; otherwise, CF mode is activated (or AF mode is activated if hybrid AF/DF relaying strategy is used). In CF mode, the relay quantizes and compresses its received signal. In contrast to DF mode, the relay now forwards its compressed observation [HuLi2006]. At the destination, the estimation of the relay's observation is reconstructed [LiChLi+2006]. The destination then tries to decode w. AF mode is nothing different but replacing CF with AF.

For two way relay channel, the entire transmission is separated into three time slots. Each time slot lasts for $T_{on}/3$ seconds. We assume that the message from node 1 to 2 is L_1 bit message m_1 and L_2 bit message m_2 is in the reverse direction. The transmission power of node 1 and 2 are P_1 and P_2, respectively. During the first time slot, node 1 transmits X_1 to the relay node and node 2. Node 2 transmits X_2 during time slot 2 and the relay node broadcasts in the last time slot such that node 1 and 2 receive it.

Define the transmission energy per bit at the source and the relay as E_s and E_r, respectively. Taking circuitry power into account, the overall energy consumption per bit can be expressed as a function of E_s, E_r and T_{on} [StSiBa+2009] for both cases. The optimization of $E_b(E_s,E_r,T_{on})$ must be subject to some QoS constraints. Here outage probability is used and the optimization problem can be formulated as

$$\textit{min}\ \mathrm{E_b}(\mathrm{E_{s,1}},\mathrm{E_r},\mathrm{T_{on}})\ \textit{or}\ \mathrm{E_b}(\mathrm{E_{s,1}},\ \mathrm{E_{s,2}},\mathrm{E_r},\mathrm{T_{on}})\ ,\ \textit{subject to}\ \mathrm{p_{out}} \le \mathrm{p_T},\ \textit{and}\ \mathrm{T_{on}} \le \mathrm{T_{max}}, \qquad (4\text{-}1)$$

where p_{out} is the outage probability and p_T is the target outage probability.

The energy per bit is optimized for both the source and the relay in hybrid one way relay case and comparison the energy efficiency performance of various strategies is presented in FIGURE 15. FIGURE 15 (a) shows the situation where the source-to-destination (S-D) distance is short (r<100m). The direct transmission is more efficient than any of the cooperative strategies until the S-D distance r is around 90m. The reason is that in small distance the circuitry energy consumption is the major part of the overall energy consumption. If the relay is activated, although the transmission energy per bit can be reduced, the overall circuitry consumption is almost doubled. When the S-D distance is increased (r>100m) as in FIGURE 15 (b), circuitry energy consumption becomes minor and the relay is able to help to reduce the overall energy per bit more efficiently. Among all the relaying strategies, the CF/DF based strategy has the best energy efficiency performance. For each cooperative strategy, the point where it shows better energy efficiency performance than direct transmission can be named as the switching point. As shown in the figure, the switching point of the hybrid CF/DF strategy is much smaller than the one corresponding to other strategies.

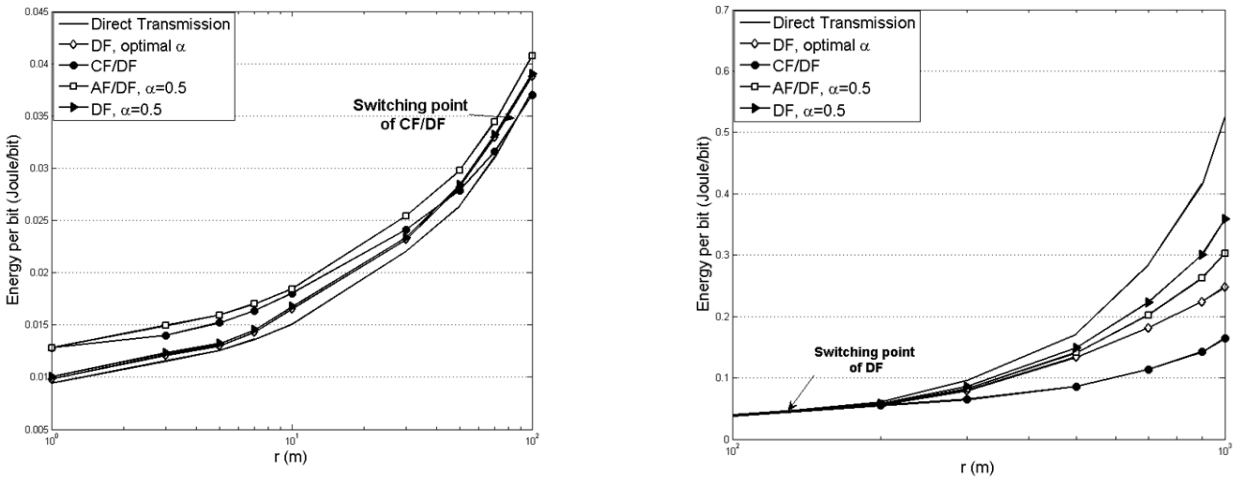

(a) (b)

FIGURE 15. (a) Short range Energy per bit, and (b) Long range Energy per bit.

Now we compare the energy efficiency performance of different strategies including AF, DF, CF and NC [HuSuSh2010] for two-way relay channel. The distance between node 1 and the relay node is denoted as *d*. The two source nodes and the relay node are assumed to be in a straight line and the relay is moving along this line.

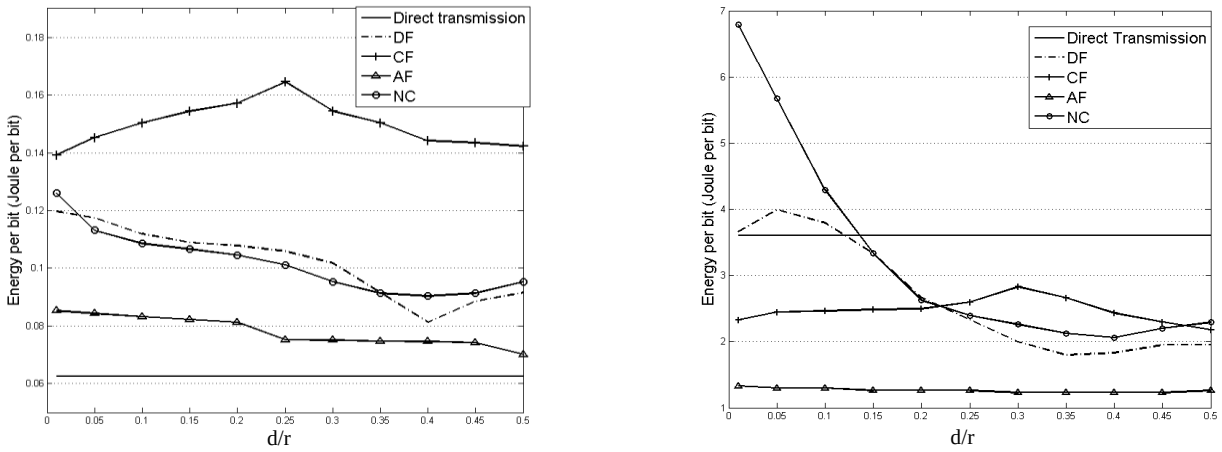

(a) (b)

FIGURE 16. (a) Short range energy efficiency (*r*=100m), and (b) long range energy efficiency (*r*=1000m).

In short distance case, the direction transmission without the relay node has the best energy performance for the same reason as in one way relay case. When the transmission range is increased to 1000m, as shown in FIGURE 16 (b), most of the relaying strategies outperform direct transmission because the transmission energy is the main part of the total energy consumption. AF has the best performance. When the relay node is in the proximity of either node 1 or 2, CF is better than DF and NC, whose energy efficiency performance are even worse than direct transmission. When the relay is somewhere in the middle, DF and NC outperforms CF.

The EE performance of hybrid one way relaying in a cellular system is also investigated. In FIGURE 17, the EE performance of DF and hybrid relaying is illustrated for 1 and 4 relays, respectively, when the relay is moving towards the cell edge (x-axial is distance and y-axial is energy per bit).

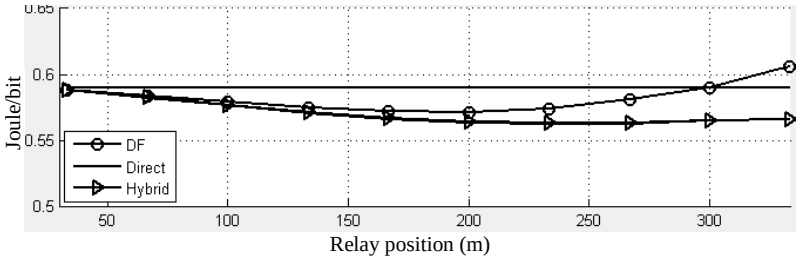

(a) Number of relay = 1

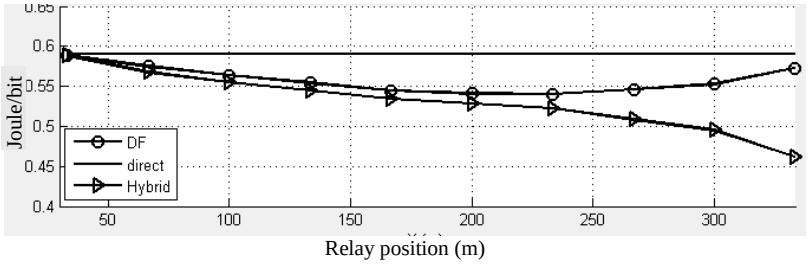

(b) Number of relay = 4

FIGURE 17. EE in cellular system.

As shown in the figures, hybrid relay achieves better EE performance than DF and the best EE performance is achieved at the cell edge. With 4 relays, although the overall energy consumption is increased compared to the 1 relay case, the system throughput is also greatly improved, thus leading to lower energy consumption for each bit. However, this does not mean the number of relays can be increased without limit. At some point, the disadvantage of more energy consumption will outweigh the benefit of improved throughput and causes more energy consumption for each bit. Based on these results, it can be conclude that the hybrid relay system that enables a pair of terminals (relay and destination) to exploit spatial diversity shows significant improvement in energy efficiency performance in terms of consumed energy per bit. However, compared with direct transmission, the cooperative strategy only shows improved energy efficiency when the destination is not very close to the source.

4.3. ENERGY EFFICIENT MIMO TWO-WAY RELAY SYSTEM WITH PHYSICAL LAYER NETWORK CODING

4.3.1. Background

Different wireless communication techniques can be combined together to realize their benefits to design energy efficient wireless systems. Cooperative relays, physical layer NC and multiple antennas at nodes are potential methods that can be used in this process. Relaying information through several hops reduces the need to utilize a large power at the transmitter, which in turn produces a lower level of interference [LanWor2000]. The Physical Layer Network Coding (PNC) reduces the number of time slots significantly to establish the full duplex communication between two nodes with the use of a relay [ZhLiLa2006]. Also, MIMO systems have distinct improvements over the single-input single-output (SISO) [Telata1999] and they also provide higher SE in the presence of multi-path fading channels [WiSaGi1994].

In the context of MIMO and PNC, authors in [XuHua2010] and [YaLeCh2007] have used MIMO two-way relaying schemes and discussed the detection and performance of such systems. A pre-equalizer before transmission is proposed in [KimChu2008] to use PNC at the relay.

Prior studies are not sufficient to have a broader understanding of system performances of MIMO PNC based two way relaying systems. Therefore, the bit-error-rate (BER) is evaluated by deriving upper and lower bounds. It is

understandable that the PNC reduces the number of transmit cycles and improve the energy efficiency of the systems. But energy efficiency is further improved by considering power allocation (PwA) scheme for such systems.

4.3.2. System Model

A basic two-way communication system model is considered with two nodes and a relay. Nodes 1 and 2 are required to transmit data between themselves with the assistance of the relay. All three nodes have *N* antennas. During the first time slot both node 1 and 2 transmit their corresponding modulated signals $\mathbf{S}_1$ and $\mathbf{S}_2$ to the relay as shown in FIGURE 18. Relay receives both signals at the same time and performs maximum likelihood detection [ZhLiLa2006] to estimate the summation of two signals. This estimation is used in PNC mapping and to find the exclusive or (XOR) of un-modulated message vectors $\mathbf{m}_1$ and $\mathbf{m}_2$ ($\mathbf{m}_1 \oplus \mathbf{m}_2$). During the second time slot, the relay broadcasts the modulated signal of the XOR message vector. Both nodes 1 and node 2 receive that and reconstruct the message using XOR operation with their own message at each node respectively. To facilitate this operation, zero-forcing precoders are used at node 1 and 2. Precoding matrices are selected as the pseudo inverse of the channel matrices.

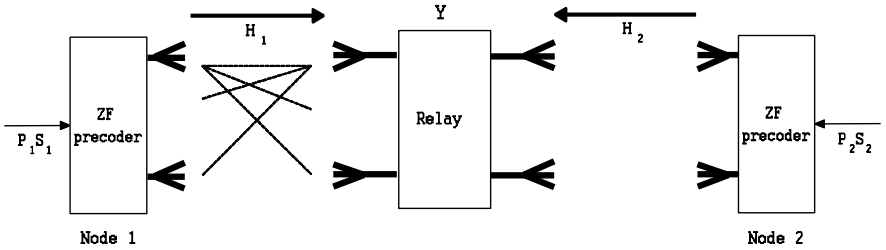

FIGURE 18. Multiple access stage.

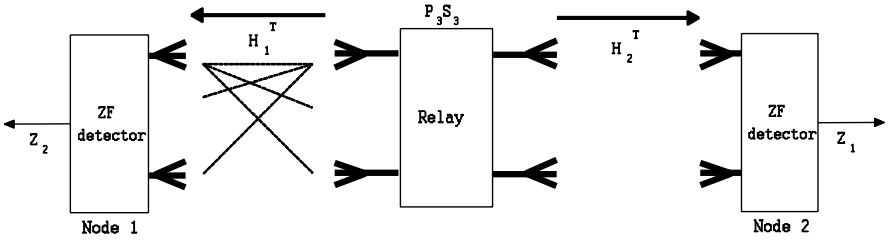

FIGURE 19. Broadcasting stage.

During the first time slot (multiple access stage), received signal vector **Y** at the relay is given by

$$\mathbf{Y} = \mathbf{P}_1\mathbf{S}_1 + \mathbf{P}_2\mathbf{S}_2 + \mathbf{n}, \tag{4-2}$$

where powers associated with the signals are defined by $\mathbf{P}_i = \mathrm{diag}\left(\sqrt{p_{i1}}, \sqrt{p_{i2}}, \ldots, \sqrt{p_{iN}}\right)$ and where $\mathbf{n} \sim \mathcal{CN}(0, \sigma^2\mathbf{I}_N)$. Each antenna at the relay receives different signal streams from node 1 and node 2. Received signal at i*th* antenna is given by

$$y_i = \sqrt{p_{1i}}\, s_{1i} + \sqrt{p_{2i}}\, s_{2i} + n_i, \tag{4-3}$$

There is no inter-symbol interference, since zero-forcing precoders are used. This leads us to consider MIMO PNC as *N* number of separate PNC operations. During the second time slot relay broadcasts $\mathbf{P}_3\mathbf{S}_3$ as shown in FIGURE 19. $\mathbf{S}_3$ is modulated signal of the XOR of two messages transmitted by the nodes. During the second time slot (broadcast stage), zero-forcing receivers are considered at node 1 and node 2.

4.3.3. Error Performance

Lower and upper bounds for the end-to-end average BER with binary phase shift keying (BPSK) modulation system are derived. A similar procedure is valid for the quadrature phase shift keying (QPSK). Here, both multiple access stage and broadcast stage errors are considered to derive bound on end-to-end average BER. Numerical analysis verifies these results and it is given in FIGURE 20. Analytical results are matching perfectly with the simulation at high signal-to-noise ratio (SNR). A noise variance as 1 is assumed. At lower SNR they provide relatively good bounds.

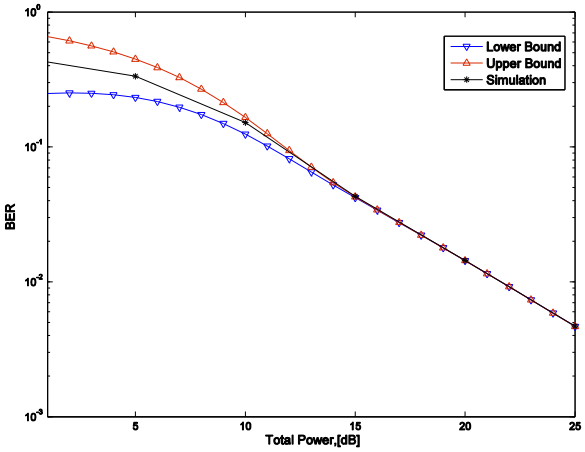

FIGURE 20. Comparison of simulation to upper and lower bounds of end-to-end BER.

4.3.4. Background Optimum Power Allocation

In this section the maximization of the sum-rate in the two-way communication is considered, by referring to the above described MIMO PNC system model. Here, the total transmit power is limited and we discuss an optimal PwA scheme. Basically, PNC operation combines both receive symbols into one symbol, which ultimately contains all the information. If the relay cannot transmit all received data without delay, then higher rates in the first time slot are not of any use. Therefore, the broadcasting rates should be higher than the multiple access rates for every spatial stream. Solutions of the following optimization problem give the optimum power values.

$$\begin{aligned}
&\text{maximize} \quad \sum_{k=1}^{N}\log_2\left(1+\frac{p_{1k}}{\sigma^2}\right)+\sum_{k=1}^{N}\log_2\left(1+\frac{p_{2k}}{\sigma^2}\right) \\
&\text{subject to} \begin{cases}
\log_2\left(1+\frac{p_{1k}}{\sigma^2}\right)\le\log_2\left(1+\frac{p_{3k}}{\left[\mathbf{H}_2\mathbf{H}_2^{H}\right]^{-1}_{kk}\sigma_1^2}\right), & k=1,\dots N \\
\log_2\left(1+\frac{p_{2k}}{\sigma^2}\right)\le\log_2\left(1+\frac{p_{3k}}{\left[\mathbf{H}_1\mathbf{H}_1^{H}\right]^{-1}_{kk}\sigma_2^2}\right), & k=1,\dots N \\
\mathrm{Tr}\left(\mathbf{H}_1^{\dagger}\mathbf{P}_1\left(\mathbf{H}_1^{\dagger}\mathbf{P}_1\right)^{H}+\mathbf{H}_2^{\dagger}\mathbf{P}_2\left(\mathbf{H}_2^{\dagger}\mathbf{P}_2\right)^{H}+\mathbf{P}_3\mathbf{P}_3^{H}\right)\le P_T.
\end{cases}
\end{aligned} \tag{4-4}$$

This is a convex optimization problem and closed form results are obtained using Karush-Kuhn-Tucker (KKT) conditions. The proposed PwA scheme is compared with a sub optimum PwA scheme and equal PwA scheme as shown in FIGURE 21 (a). Results confirm that the proposed PwA scheme provides much higher rates for a given total power constraint. Simulation is then extended by varying the relay location (see FIGURE 21 (b)).

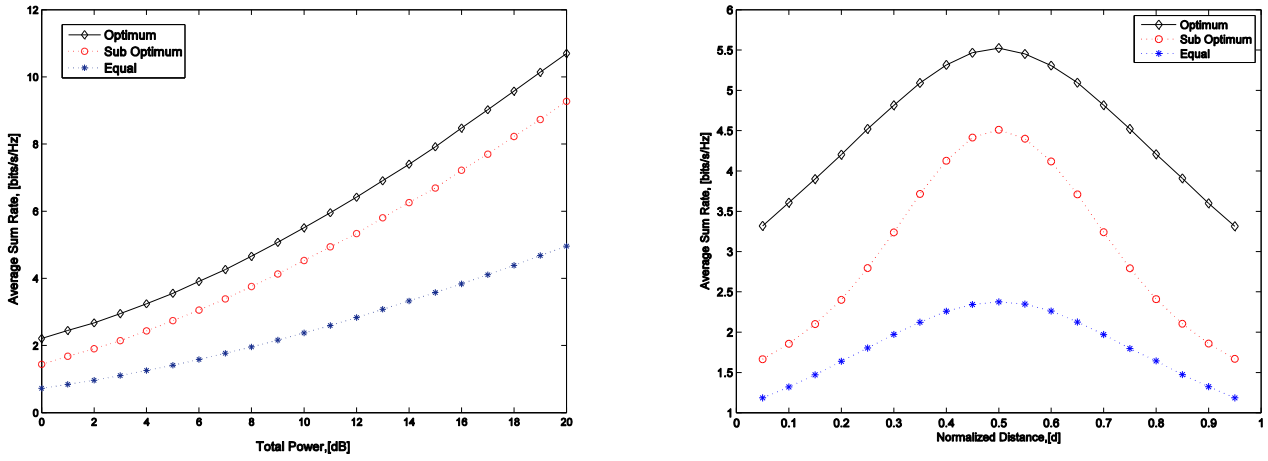

(a) (b)

FIGURE 21. (a) Sum rate with total power, and (b) Sum rate with varied relay location.

MIMO two-way relaying system with PNC has been considered. The system consists of zero-forcing precoders for the multiple access stage and zero forcing detectors at broadcasting stage. Analytical solutions for error performance bounds have been derived considering BPSK modulation system. Further, an optimal resource allocation problem to maximize the sum rate of the two-way relay communication under a total power constraint has been investigated. In the numerical analysis of error performance, bounds overlap with simulation results at higher SNR. Also the achievable sum rate variation with the total power in optimal PwA scheme shows that it is better than the sub-optimal strategy considered and the equal PwA strategy. Average sum rate variation with normalized distance suggests that the relay should be halfway between the two nodes.

4.4. IN-BUILDING COMMUNICATION

It has been shown in [HéImTa2011c] via an analytical analysis that in-building AF relaying can be an effective solution for increasing the EE of cellular system by reducing the consumed power. On the one hand, the use of relay would tend to increase the overall network energy consumption; on the other hand, avoiding to waste large amount of power for transmitting through walls could save a lot more of energy. Assuming an in-building scenario, where the relay to UE link quality is 20 dB higher than the BS to relay link, we have derived in [HéImTa2011c] the maximum achievable SE of the MIMO AF and combined it with the PCM of [EARTH-D2.3] for formulating the EE-SE trade-off of this in-building relaying system. This analytical expression has then been utilized for comparing the performances of our relaying scheme against classic P2P scheme both in terms of EE and SE. The results reveals that relaying can reduce the energy consumption in comparison with P2P communication, especially at low SE, when the quality of the BS to relay link is at least 5 dB higher than the quality of the BS to UE link (direct link). This is likely to happen in an in-building scenario since the user in a building is most likely to be in non-line-of-sight with the BS, whereas the BS is most likely to be line-of-sight with the relay. Results also indicate that even though transmitting with maximum power implies maximum SE, it does not imply maximum EE. Here, we refine our previous results using the power model proposed in Sections 4.1 and 4.5 for the urban relay node.

Assuming a two-phase transmission model, the total power consumption of the MIMO AF system can be characterized as

$$P_{\Sigma,AF} = P_{BS,Tr} + P_{RN,Tr} + P_{RN,Re} + 2P_{UT,Re}, \quad (4\text{-}5)$$

where $P_{BS,Tr}$, $P_{RN,Tr}$, $P_{RN,Re}$ and $P_{UT,Re}$ are the consumed power related to BS transmission, RN transmission, RN reception and UE reception, respectively. In [EARTH-D2.3], the total consumed power of several types of BS has been abstracted as

$$P_{BS} = t(\Delta_{P,BS} P_1 + P_{Ov,BS}), \tag{4-6}$$

where t is the number of transmit antenna at the BS, $\Delta_{P,BS}$ accounts for the PA inefficiency and $P_{Ov,BS}$ is the overhead power. In addition P_1 is the transmit power per PA, i.e. per antenna, at the BS and it varies from 0 to P_{max}. This linear abstraction can also be applied for either rural or urban RNs such that $P_{RN} = t(\Delta_{P,RN} P_2 + P_{Ov,RN})$, where P_2 is the transmit power per PA at the RN. Moreover, the same linear type of PCM has been used in [MiHiLi2010] for characterizing the power consumption of a UE. Assuming the linear power model of (4-6) for each node, the total consumed power of the system in (4-5) can be re-expressed as

$$P_{\Sigma,AF} = n(\Delta_{P,BS} P_1 + P_{Ov,BS}) + q(\Delta_{P,RN} P_2 + P_{Ov,RN}) + q\varsigma P_{Ov,RN} + 2r\varsigma P_{Ov,UE}, \tag{4-7}$$

where $1 \geq \varsigma \geq 0$ characterises the ratio between overhead powers use for transmitting and receiving. Intuitively, less overhead power will be necessary for receiving than for transmitting signals. The EE in bit/J/Hz of this system can then be simply defined as the ratio of its SE in to its total consumed power in (4-7) such that $C_J = C / P_\Sigma$, where C are approximated in closed-form in the appendix of [EARTH-D3.1]. For our simulation, the following values for the macro BS are considered: $\Delta_{P,BS}$ = 7.5, $P_{Ov,BS}$ = 375 W as well as $P_{max,BS}$ = 40 W such that P_{BS} = 1350 W when t=2 [EARTH-D2.3] and $\Delta_{P,RN}$ = 6.3, $P_{Ov,RN}$ = 6.45 as well as $P_{max,RN}$ = 1$ W such that P_{RN} = 25.5 W when t=2. In addition, $P_{Ov,UE}$ = 100 mW has been set according to [MiHiLi2010], and the ratio between transmission and reception overhead power as ς = 0.5.

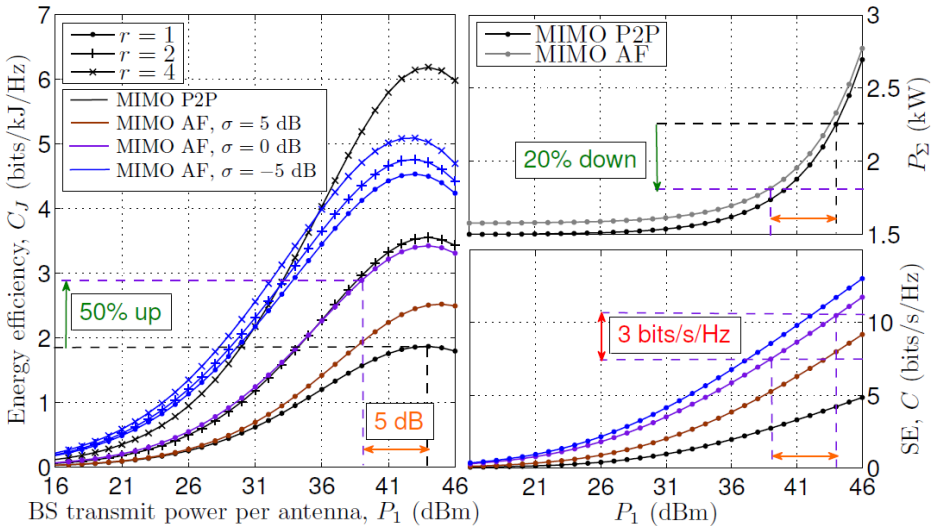

FIGURE 22. EE, SE and total consumed power of MIMO P2P as well as MIMO AF vs. the BS transmit power per antenna in dBm for various numbers of antennas and σ values.

In FIGURE 22, the EE, SE and total consumed power of MIMO P2P are depicted, as well as MIMO AF against the BS transmit power per antenna for various numbers of antennas and σ (SNR offset between the direct and donor links) values. In addition, four transmit antennas at the BS and RN are considered, P_2 = 1 W is fixed and the BS to UE SNR varies from -15 to 15 dB. In the left hand-side plot (EE plot), results first clearly show the existence of a maximum for the EE, which is not necessarily obtained for the maximum transmit power. Moreover, results indicate that MIMO AF EE gain over MIMO P2P increases as the number of receive antenna at the UE, r, decreases

(when comparing the blue with the black curves) and as the quality of the donor link increases in comparison with the quality of the direct link (when comparing the brown, purple and blue dotted curves with the black dotted curve for r = 1). Looking now at the upper right-hand side graph (P_Σ), it shows that the total consumed power of the MIMO AF as a function of P_1 is always greater than that of MIMO P2P, which is obvious due to the additional RN power consumption in MIMO AF. Thus, it implies that the better performances of MIMO AF against MIMO P2P in terms of EE (EE plot) are not due to power saving but SE improvement, as it is confirmed by the lower right-hand side graph (SE plot) where the SE gain of MIMO AF over MIMO P2P can be seen for different values of σ and r = 1. However, one can also look at these graphs in a different way. Assuming that we want to use MIMO AF to reduce the total consumed power by 20 % in comparison with MIMO P2P when σ = 0 dB and r = 1. It corresponds in the x-axis of the P_Σ plot to a reduction of 5 dBm in the BS transmit power per antenna, which in turn corresponds to an increase of 50 % for the EE (see EE plot). As a reminder of the existence of a trade-off between EE and SE, this power saving will come at the cost of a 3 bit/s/Hz reduction (see SE plot).

Overall, the results reveals that relaying can increase the EE in comparison with P2P communication by either power saving or SE improvement in an in-building scenario, especially when the number of receive antennas at the UE is lower than the number of antennas at the BS and RN as well as when the quality of the donor link is higher than the quality of the direct link. Results also indicate that even though transmitting with maximum power implies maximum SE, it does not necessarily imply maximum EE.

4.5. RELAY NODES PERFORMANCES IN HOTSPOTS OF TRAFFIC

As shown in Section 4.1, the performance of Relay Nodes in term of energy savings increases considerably if only the area covered by the Relay Node is considered. Therefore it is reasonable to assume that, if the traffic is not uniformly distributed in the whole cell, and there are areas where a higher concentration of traffic is expected, there is the possibility to use Relay Nodes to serve the traffic in those spots and provide a higher improvement to the overall energy efficiency of the system.

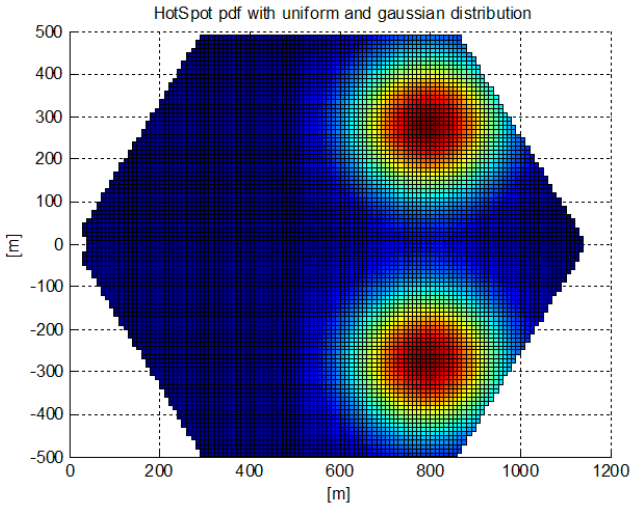

FIGURE 23. Traffic distribution with two hotspots covered by the Relay Nodes.

In order to investigate this scenario a hotspot traffic distribution has been considered, assuming that half of the traffic of the cell is uniformly distributed and the remaining half is concentrated under the two Relay Nodes considered in the cell deployment of the static simulator introduced in [EARTH-D3.1]. This part of the traffic is distributed according to a spatial Gaussian distribution whose variance has been chosen so that 95% of this traffic falls in the area that is served by the Relay Nodes. The resulting distribution in the case of a cell with ISD = 500 m is shown in FIGURE 23.

This kind of distribution has been used in order to weight the results obtained by the simulator for the various scenarios and traffic loads that are used as inputs to the E^3F framework, in order to evaluate the overall ECI for the network in presence of hotspots. Also in this case, long-term traffic variations for the high traffic profile defined in [EARTH-D2.3] have been considered.

The power models used in this study for the Macro BS and the Relay Nodes are those reported in TABLE 3, which represent a more realistic guess of the power model that can be expected to characterize network nodes available in 2014, as reasonable assumption under the hypothesis of a smooth evolution from current equipments.

TABLE 3. Updated parameters for different base and relay stations (2014 –estimation).

LTE node type	P_{max} [W]	P_0 [W]	Δ_P
Relay Rural 2014	5	28.5	5.6
Relay Urban 2014	1	19.9	5.6
Macro BS 2014	40	248	14.25

With these parameters, the results shown in FIGURE 24 have been obtained. The column relative to BS SOTA uses the same power model used in FIGURE 2 for SOTA BSs. Comparing this column with the same one obtained in FIGURE 2 for the uniform traffic distribution, it can be seen that in this case, the presence of hotspots near the cell edge impacts on the overall energy consumption, making it even worse, since more energy is needed to provide the service to these users that are near the cell border. However if RNs with a good power model (as the one reported in TABLE 3) are used to collect and serve this traffic a significant improvement can be obtained, lowering the overall energy consumption index of 20.8% in the case of 2-hop relay nodes, and of 5.6% in the case of multicast relay nodes.

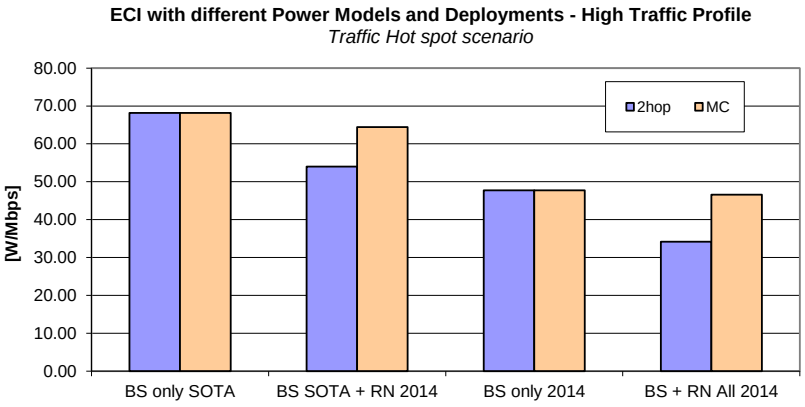

FIGURE 24. Overall ECI in the hotspot scenario, with different deployments (High Traffic Profile).

Note that in this case, while it can still be observed a better efficiency of 2-hop relays, also the multicast scheme proves to provide some benefits, not only from a capacity point of view.

As observed for the uniform traffic distribution, even higher gains can be obtained when also BSs are upgraded with a more efficient power model. As it can be seen from FIGURE 24 when newer BSs are deployed alone a good increase in energy efficiency is obtained, but the improvements granted by relay nodes still stack with this higher

performance, lowering the corresponding energy efficiency index of an additional 28.4% in the case of 2hop relays, and of 2.5% in the case of multicast relays.

It should be highlighted that these results are obtained considering the full E^3F framework, which assumes to deploy relay nodes in all the scenarios (macro, micro, etc.) and in all load conditions. However in certain cases, for example for low traffic condition and rural environment, deploying relay nodes can be not convenient, and it might be possible that higher results are obtained if relays are added and considered only in those scenarios where they are actually needed.

5. MIMO AND ADAPTIVE ANTENNAS

As cellular networks evolve to LTE-A and future RANs, the number of multiple antennas in a BS, correspondingly MIMO order, is expected to increase. LTE-A supports 8 transmission antennas and even larger numbers of antennas are considered for future RANs. This opens the possibility to use more complex multiple antenna techniques that have not been used commonly for Wideband Code Division Multiple Access (WCDMA) and LTE networks. They include high-order adaptive antenna techniques providing 2D or 3D beamforming and CoMP techniques that enable multiple BSs to jointly serve single or multiple users. This high-order MIMO in BSs is favourable for improving cell capacity and user throughput, however it may result in a less energy-efficient operation in cellular networks because it requires more RF transceivers and baseband processing units than a SISO does. This chapter provides an energy efficiency analysis of multiple antenna techniques and a new approach, which improves the energy efficiency of cellular networks by exploiting multiple antenna techniques.

5.1. MIMO VS. SISO: AN ENERGY EFFICIENCY ANALYSIS

EE can be interpreted as a ratio between the transmission rate and consumed power. Consequently, the EE gain between two systems can either result from an increase of SE (one of the system providing a better rate than the other, for a given transmit power) or a decrease in consumed power (one of the system consumes less power than the other, for a given transmission rate). The former definition of the EE gain is actually equivalent to the definition of the SE gain and, thus, it can be seen as an indirect EE gain, since the concept of EE is implicitly linked with power consumption and cost reductions. The latter definition of the EE gain is obviously more suitable for EE based analysis. Having derived closed-form approximations of the EE-SE trade-off for the SISO and MIMO Rayleigh fading channel in [HéImTa2012b], [HéImTa2011d] and [HéImTa2012a], we have used these expressions in [HéImTa2011b] and [HéImTa2012a] to study the effectiveness of MIMO for reducing power consumption over the Rayleigh fading channel for both idealistic and realistic PCMs.

5.1.1. MIMO vs. SISO EE gain : Idealistic PCM

The EE gain of MIMO over SISO due to power reduction, i.e., G_{PR} where PR stands for power reduction, can be expressed as in (30) of [HéImTa2012a] when assuming an idealistic PCM, i.e. when the total consumed power, P_{Σ}, is equal to the transmit power P. More interestingly, the study of the limits of this gain at low and high SE reveals that G_{PR} is always greater than the number of receive antenna and that it grows with the minimum number of antennas as well as the SE at high SE. These limits are given by [HéImTa2012a]

$$G_{\mathrm{PR}}^{0} = r \ \text{ and } \ G_{\mathrm{PR}}^{\infty} = \alpha\ t,r\ 2^{C\left(1-\frac{1}{m}\right)}, \tag{5-8}$$

where t and r are the numbers of transmit and receive antennas of the MIMO system, $m = \min\{t, r\}$, $\alpha\ t,r$ is a function of t and r, and C is the maximum achievable SE, or equivalently, the channel capacity per unit bandwidth. Similarly, the EE gain due to SE improvement, i.e. G_{SE}, can easily be defined by using (30) of [HéImTa2012a] and its limits at low and high SE are given by

$$G_{\mathrm{SE}}^{0} = r \ \text{ and } \ G_{\mathrm{SE}}^{\infty} \propto m\,. \tag{5-9}$$

Comparing equations (5-8) with (5-9) indicate that, at low SE/SNR, reducing the transmit power while keeping the same rate is equivalent to increasing the rate while keeping the same transmit power. This is consistent with the fact that in this SE region the rate scales linearly with the power and the number of receive antennas. However, in the high SE regime, the rate scales in a logarithm manner with the power and, hence, a larger EE gain can be achieved by reducing power instead of increasing SE. For instance, G_{PR}^{∞} increases with the SE (exponentially) as well as the number of antennas, whereas G_{SE}^{∞} increases only with the number of antennas. In order to cross-validated these analytical results with numerical results, we plot in FIGURE 25, G_{PR} and G_{SE} plot as a function of

the SE and number of antenna elements when n_{ant}= t = r. The results show that $G_{PR} \geq G_{SE}$ and confirm that G_{PR} grows both with the SE and number of antenna elements n_{ant}. Overall, these results indicate than MIMO has a great potential for EE improvement when an idealistic PCM is considered, especially for large numbers of antenna and high SE.

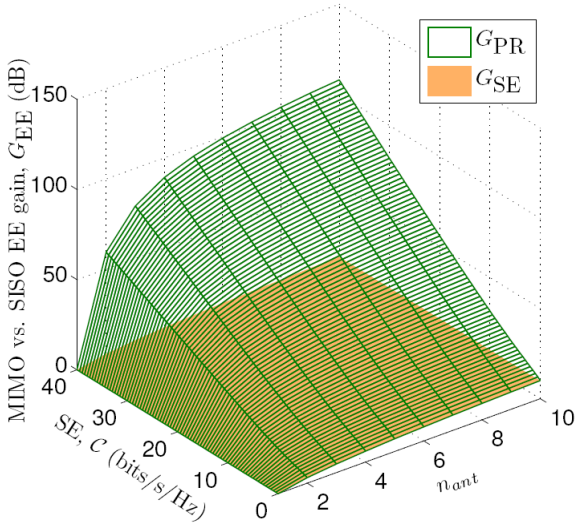

FIGURE 25. Idealistic MIMO vs. SISO EE gain due to power saving vs. SE improvement as a function of the SE and number of antenna elements when n_{ant}= t = r.

5.1.2. MIMO vs. SISO EE gain : Realistic PCM

Instead of considering that $P_\Sigma = P$, we now consider the realistic PCM of EARTH in [EARTH-D2.3] such that

$$P_\Sigma = t\ \Delta_P P/t + P_0\ , \tag{5-10}$$

for analysing the MIMO EE potential of improvement in a more realistic setting. In (5-10), Δ_P accounts for the amplifier inefficiency and P_0 is the overhead power. Under the assumption that both SISO and MIMO systems are affected by the same level of noise, G_{PR} can be simplified as $G_{PR} = P_{SISO}/P_{MIMO}$, where P_{SISO} and P_{MIMO} are the respective SISO and MIMO transmit powers. Then the EE gain due to power reduction can then be re-expressed as [HéImTa2012a]

$$G_{PR} = \psi + 1\ \ \psi / G_{PR} + t\ ^{-1}, \tag{5-11}$$

where ψ is the power ratio given by $\psi = \Delta_P P_{SISO}/ P_0$. It can be remarked in (5-8) that $G_{PR}^{\infty} \geq 1$ as long as $m > 1$ and, hence, the upper limit of $\hat{G}_{PR}$ can be formulated as [2012Héliot]

$$\hat{G}_{PR}^{\infty} = \psi + 1 \left[1 - \text{sgn}\ m-1\ \ \psi / \alpha\ t,r\ + t \right]^{-1}. \tag{5-12}$$

Similarly, the EE gain due to SE improvement can be re-expressed as

$$G_{SE} = G_{SE}\ \ \psi + 1\ \ \psi + t\ ^{-1}. \tag{5-13}$$

Comparing the high-SE limits of EE gain due to power reduction in the idealistic and realistic PCMs G_{PR}^{∞} in (5-8) with $\hat{G}_{PR}^{\infty}$ in (5-12), an interesting paradox can be observed. In the idealistic PCM, G_{PR} increases both with the SE and number of antennas; whereas, equation (5-12) indicates that $\hat{G}_{PR}$ decreases with the number of transmit antennas when considering a realistic PCM and m > 1. Hence, it implies that t = 2 is the most energy efficient

number of transmit antennas in the high-SE regime for a realistic PCM and $r > 1$. Moreover, equation (5-12) reveals that if $\psi < 1$ and $m > 1$, then MIMO cannot be more EE than SISO. Concerning, the EE gain due to SE improvement, it also decreases as the number of transmit antennas increases according to (5-13). These analytical results also indicate that contrarily to the idealistic PCM case where $G_{\mathrm{PR}} \geq G_{\mathrm{SE}}$, it is likely that improving the SE would be more EE than reducing the transmit power for certain SE and antenna configurations depending on the values of the parameters Δ_P and P_0. Given a set of PCM parameters, it would be energy efficient to deploy a MIMO system instead of a SISO if at least $\hat{G}_{\mathrm{PR}} \geq 1$ and even more if $\hat{G}_{\mathrm{PR}} \geq \hat{G}_{\mathrm{SE}}$.

Considering the values of the EARTH PCM for the 2x2 case in [EARTH-D2.3], i.e. $\Delta_P = 14.5$, $2P_0 = 712$ W and $P_{\max}/2 = 40$W (maximum transmit power per antenna), we depict the EE gain due to power reduction and SE improvement in FIGURE 26, as well as the maximum EE gain as a function of the SISO SNR when SISO transmit at full power., i.e. $P_{\mathrm{SISO}} = P_{\max} = 80$W and $P_{\Sigma,\,\mathrm{SISO}} = 896$ W. We also depict the total consumed power and SE values for the 2x2 MIMO system relative to these gains. The results show that at low SNR ($\gamma_{\mathrm{SISO}} < 0$ dB), EE cannot be achieved via power saving. Moreover for $\gamma_{\mathrm{SISO}} < 10$ dB, the maximum achievable EE gain is equal to the EE gain due to SE improvement. Thus, EE can be achieved by 2x2 MIMO even though more power is consumed, which is not desirable. When the SNR is large enough, EE can be achieved via power saving, but in order to get the maximum gain one has to trade-off rate for power. For instance at $\gamma_{\mathrm{SISO}} = 60$ dB, the maximum EE gain is obtained by increasing the power by 80 W in comparison with $\hat{G}_{\mathrm{PR}}$ and incurs a 6 bit/s/Hz loss in SE in comparison with $\hat{G}_{\mathrm{SE}}$, such that $\hat{G}_{\mathrm{EE,max}}$ is 36% and 45% higher than $\hat{G}_{\mathrm{PR}}$ and $\hat{G}_{\mathrm{SE}}$, respectively.

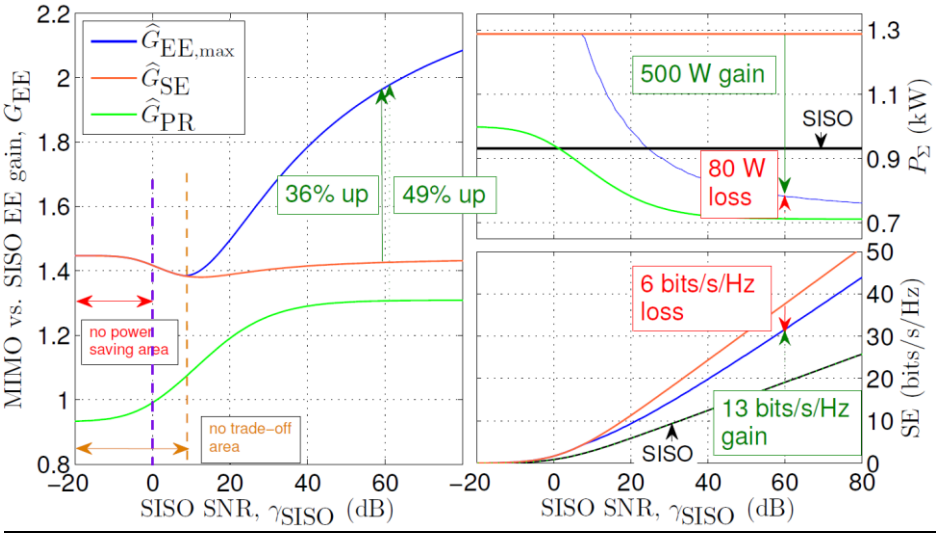

FIGURE 26. 2x2MIMO vs. SISO EE gains and their respective SE and total consumed power when considering a realistic PCM.

Overall, MIMO has a great potential for EE improvement over the Rayleigh fading channel in theory; in contrast, when a realistic PCM is considered, a MIMO system with two transmit antennas is not necessarily more EE than a SISO system and utilizing more than two transmit antennas is likely to be energy inefficient, which is consistent with the findings in [CuGoBa2004] for sensor networks.

5.2. ADAPTIVE MIMO

5.2.1. Introduction of MIMO muting

In BS architecture currently used for commercial services, the most power consuming part is an analog RF transceiver that includes PA, mixer, local oscillator, driving amplifiers. FIGURE 27 shows one example of energy

consumptions in each part of BS. More than 80% of overall energy consumption derives from RF transceivers, particularly PAs. This gets still valid or even more serious as the number of antennas in BS, i.e. MIMO order increases from 2 or 4 in WCDMA and LTE to 8 in LTE-A. In the design of advanced BS supporting high-order MIMO, all antennas with analog RF transceiver chain are dimensioned to provide the required capacity at load peaks, thus they are always operational even in low traffic conditions like mid-night in which only few users are connected to mobile networks. It has also been shown that current PAs are not flexible enough to adjust its transmission power to network traffic. Therefore, normal MIMO operation causes a significant energy waste to provide connectivity during low traffic situations.

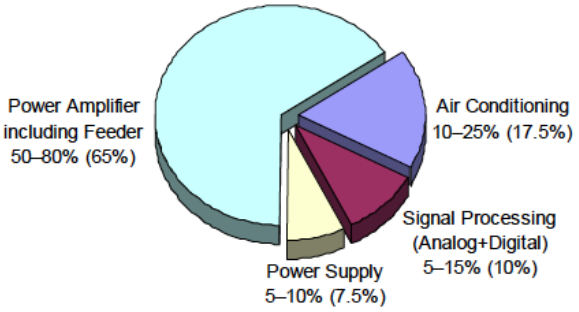

FIGURE 27. Energy consumption of components in BS.

MIMO muting, turning off one or several RF transceivers, would give us considerable amount of energy saving in low traffic situations. It does not completely switch off the whole BS but deactivate some of analog RF transceivers when traffic is low; therefore it is still possible to maintain cell coverage by keeping a BS operational. However, it imposes several problems for cellular network operations. First, MIMO muting may decrease total transmission power where detail number depends on hardware implementation. This causes cell edge users to suffer from worse signal-to-interference-plus-noise-ratio (SINR) than ones in normal operation. It also means that MIMO muting may generate more dead-zone (hole) that normal operation would not cause. This problem can be relaxed by introducing PA with adaptive bias control promising adaptive transmission power. In case that some PAs are switched off, other PAs which are still operational could increase its transmission power so that total transmission power can be equal to the transmission power normal operation would transmit.

5.2.2. Energy saving operation by advanced CoMP

Even with this solution, MIMO muting has drawback. Once MIMO muting is applied, it cannot adaptively activate antenna again if a UE requests high traffic. Even in low traffic scenario, a UE comes up and requests high traffic for high volume data transmission. MIMO muting has structural limitation to cope with such high traffic requests, particularly cell-edge users which would not be able to get high traffic due to low SINR. Our idea is to use advanced CoMP in order to provide UE with possibility to keep MIMO order as normal operation would offer. FIGURE 28 shows comparison between the normal operation in high traffic scenario and the energy saving operation we proposed in low traffic scenario.

Here is the detailed system concept for proposal. We consider a cellular network scenario where BSs are equipped with *N* antennas. Each antenna is connected to an analog RF transceiver module. Our proposal aims at switching off as many analog RF transceivers as possible at each BS according to total cell traffic, thus achieving high energy efficiency performance, while ensuring the QoS requirements of the users. In other terms, our algorithm is able to configure BS such that it can serve connected mobile users with the required QoS level, while using the minimum number of active analog RF transceiver module. The actions taken by our algorithm are triggered by the actual wireless traffic load present to the wireless cell. Over a long-time scale, when the number of users or user traffic demand decreases below a certain threshold, the algorithm starts looking for the most energy-efficient antenna configuration that is able to fulfil the QoS requirements of users. Once it goes into

MIMO muting mode, CoMP techniques are eventually used to achieve this goal in short-time scale. When a certain number of active antennas (equivalently active analog RF transceiver) is not able to fulfil the QoS requirements of users, cooperation with neighbouring BS is explored to exploit unused wireless resource blocks available at neighbouring BS. The right-hand side of FIGURE 28 shows the configuration that applies CoMP to support high traffic request by a UE. Our algorithm ensure the use of a minimal set of analog RF transceiver modules at each BS, while providing the required level of network service at the minimal energy cost.

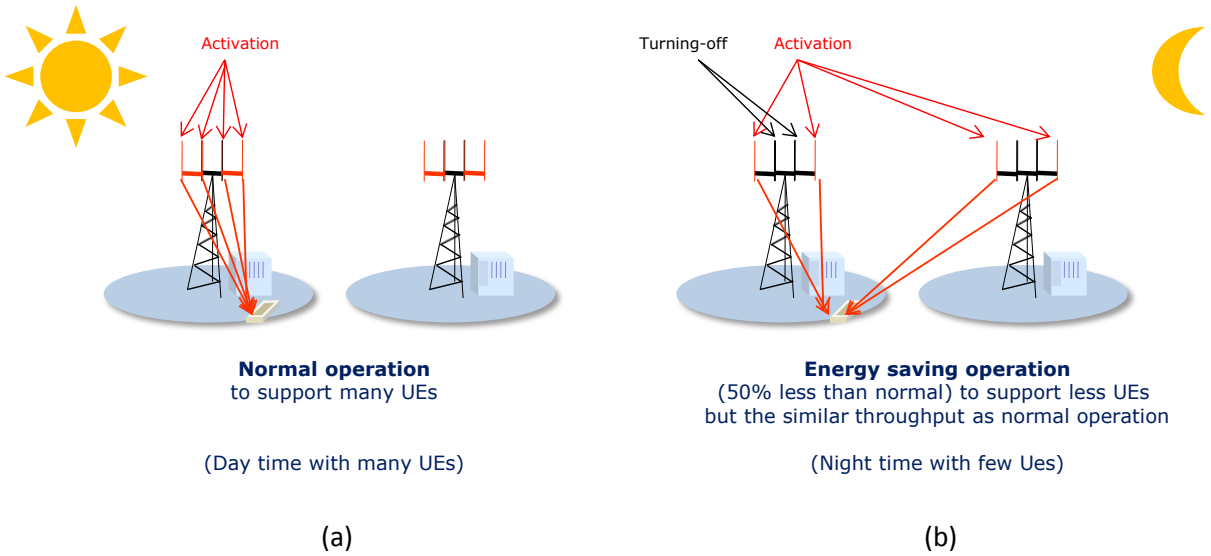

FIGURE 28. (a) normal operation and (b) proposed energy saving operation by advanced CoMP.

6. BASE STATION COOPERATION

Currently, two major development paths may be foreseen for mobile communication networks to cope with increasing future traffic and QoS demands: The use of more (and smaller) BSs and the use of coordination or cooperation between BSs also referred to as *Coordinated Multi-Point* communication, i.e. CoMP. While both concepts are not mutually exclusive and can very well complement each other, they may act differently on certain network characteristics. Both network densification as well as CoMP are able to achieve an increased network capacity as well as a more uniform distribution of user rates in the cell, however, they incur different costs in terms of consumed energy. Naturally, densification increases the network's energy need due to increased number of radio access points, and trade-offs between gains in cell throughput and increased energy consumption are investigated in Section 2 of this deliverable. CoMP schemes in uplink and downlink on the other hand require higher capacity backhaul connections between cooperating sites as well as additional signal processing at the BSs. In the following, we investigates the trade-offs between attainable gains in cell throughput obtained from CoMP schemes on one hand, and increased power dissipation of BSs due to higher complexity of CoMP processing and additional backhaul requirements on the other. In particular, we discuss both full blown *cooperation* schemes where BSs jointly transmit and receive users' signals in order to exploit interference as well as *coordination* schemes, in which BSs coordinate their transmission in the frequency domain in order to avoid interference.

Within this section an information-theoretic framework is presented, based on which the energy efficiency of uplink cooperation schemes is estimated. Here, results indicate that gains in energy effort (in J/Mbit) coming from *cooperative* detection are achieved only for cell edge users. Further, cooperation of more than 3 BS did not improve the energy effort (J/Mbit) of the system compared to non-cooperative reception if realistic power models are taken into account. This result coming from an information-theoretical framework is in line with earlier observations from system simulations in [EARTH-D3.1], where cooperation among more than 3 BS did increase the combined energy effort (J/Mbit) of uplink and downlink.

Investigations on the performance of cooperative transmission with noisy data backhaul reveal, that there is a distinct transmission power (resp. SNR) that minimizes the energy effort (in J/Mbit) required for data transmission.

Two further studies presented here suggest that *coordinated* transmission in the downlink yields reduced energy consumption of BSs on the order of 15-25% for a practical range of ISDs. Furthermore those gains are most pronounced in heavily loaded systems. Both results are intuitive since cooperation schemes target to improve the cell SIRs which are independent of ISD and most severe under full load.

The results presented in Sections 5.1 to 5.4 are based on power models either neglecting backhaul power or using a very simple backhaul power model. The study presented in Section 5.5 investigates in more detail on the energy consumption of today's practically most relevant backhaul technologies and provides a more detailed and complete modelling for future work. It concludes that the fraction of backhaul energy that can be accounted towards each BS is not negligible, especially for small cells. Among the technologies considered, passive optical networks (PONs) require the lowest power among.

6.1. ENERGY EFFICIENCY IN THE UPLINK OF COMP: AN ANALYTICAL STUDY

This work establishes in which scenarios CoMP can be used for improving cellular system EE. In our preliminary work of [HélmTa2011a], the EE-SE trade-off has been formulated by means of a computable formula and this formula have been utilised for analysing the downlink of an idealised CoMP system in terms of both EE and SE, when considering a simplistic backhaul PCM. Results have indicated that multi-BS cooperation is most likely to be efficient when the link quality between the BSs and UEs is weak, e.g. cell-edge communication. In addition, cooperative processing power should be kept low for CoMP to provide energy efficiency gain. Here our analytical study of CoMP is complemented by investigating the uplink of CoMP system. We have derived closed-form

approximations of the EE-SE trade-off for the uplink of MIMO CoMP when considering a theoretical (Wyner model) and a more realistic uniform user distribution in [OnHéIm2011a] and [OnHéIm2011b], [OnHéIm2012], respectively. We have then used these expressions for defining the EE gain of CoMP over classic non-cooperative system for both idealistic (when only the transmit power is considered) and realistic PCMs (mainly derives from [EARTH-D2.3] for the BS consumption and [FeMaFe2010] for the backhaul consumption). For more details about our work (EE-SE trade-off derivation, user model, PCMs, simulation settings), please see [OnHéIm2012].

In the uplink of cellular system, it turns out that CoMP is more EE than non-cooperative system by reducing the consumed power of the system when an idealistic PCM is considered. However, EE gain due to power reduction, can hardly been achieved when considering a realistic PCM for CoMP (including backhaulink effect). Indeed, in FIGURE 29 (a), we compare the EE gain of CoMP against conventional non-cooperative system due to power reduction (PR) and SE improvement when considering both an idealistic (denoted as G_{PR}, G_{SE}) and realistic PCMs (denoted as $\hat{G}_{PR}$, $\hat{G}_{SE}$), both for M = 3 and 5 cooperating BSs, ISD = 1 km and r x t = 2 x 2, where r is the number of antennas at the BS and t is the number of antennas at the UE. Moreover, the relative distance between each UE and its serving BS, denoted rd_{UE-BS}, is always greater than 0.05 (rd_{UE-BS} = 0/1: UE collocated with BS / UE at cell edge, respectively). Note also that a scenario in which only one UE is active per-cell at every time due to the use of an orthogonal multiple access scheme within the cell is here considered. Results indicate that when the idealistic PCM is considered CoMP is always more energy efficient than the non-cooperative system, i.e. the EE gain is always greater than 1, but a higher gain is achieved via reduction in power consumption, i.e. $G_{PR} > G_{SE}$. Whereas, for the realistic PCM, CoMP's EE gain can only be achieved through SE improvement and mainly for cell edge communication, i.e. when the relative distance between the UE and the BS, rd_{UE-BS}, is above 0.8, and small number of cooperating BSs, i.e. M =3. In addition, FIGURE 29 (a) shows that no EE gain can be achieved via power reduction in the realistic PCM.

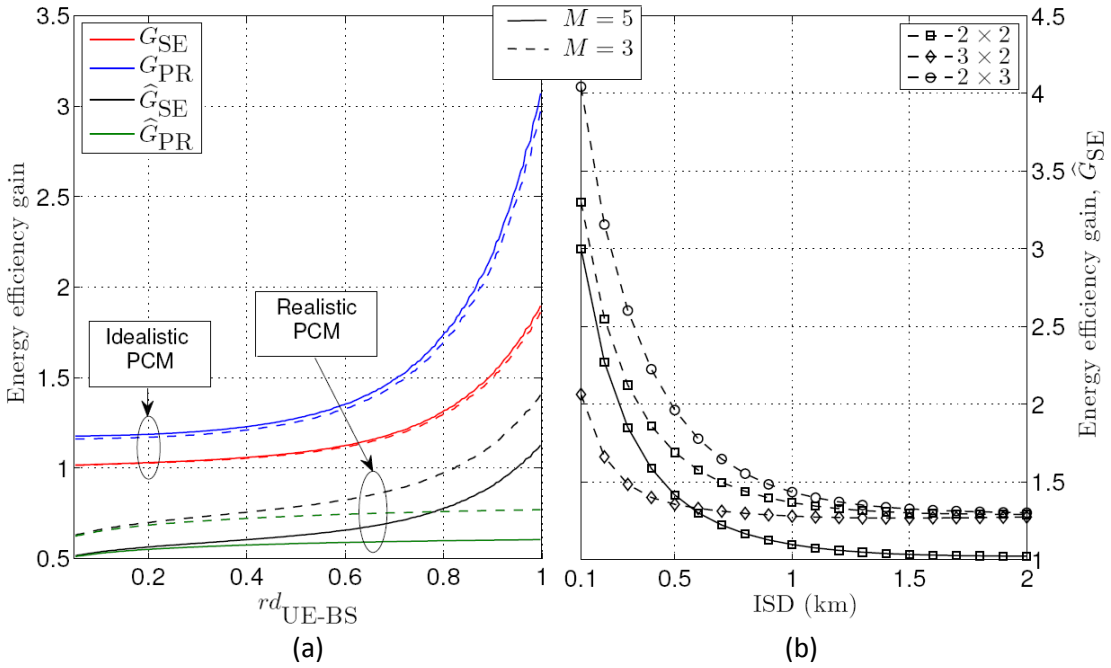

FIGURE 29. Various EE gains of CoMP against non-cooperative system as a function of (a) user relative distance and (b) the ISD for various number of cooperating BSs (M) and antenna configurations.

In FIGURE 29 (b), we plot $\hat{G}_{SE}$, which is the EE gain of CoMP over classic non-cooperative system when considering the realistic uplink CoMP PCM of [OnHéIm2012] (mainly derived from [EARTH-D2.3] [FeMaFe2010]), when UEs are placed at cell edge (rd_{UE-BS} = 0.95) for M = 3 and 5, and antenna configurations r x t. It can be observed that reducing the ratio, β, between the number of transmit antennas at the UE, t, and the number of receive antennas at the BS, r, i.e. $\beta = t / r$, from β = 1 in (2x2) to β = 2/3, in (3x2) results in a decrease of $\hat{G}_{SE}$ since

increasing r is beneficial in terms of SE for the non-cooperative system, whereas CoMP performance is only slightly increased. In addition, increasing β from β = 1 in (2x2) to β = 3/2 in (2×3) leads to an increase in $\hat{G}_{SE}$ since no improvement in SE is achieved by the non-cooperative system when increasing β beyond 1, whereas CoMP performance increases. Furthermore, increasing the number of cooperating BSs leads to a reduction in the EE gain as a result of the sharp increase in both the backhaul and processing powers of CoMP, whereas, the SE increases marginally especially for M > 3 in the conventional circular cellular grid layout. It can finally be noticed on this graph that CoMP can be up to 4 times more energy efficient than non-cooperative system for M = 3, a 100 m ISD and a 2x3 antenna configuration.

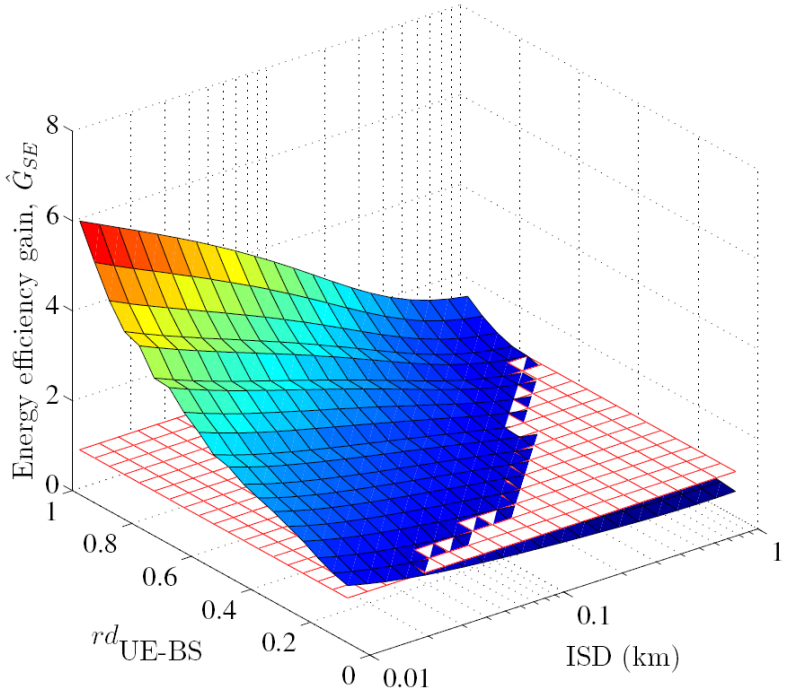

FIGURE 30. Realistic EE gain of CoMP against non-cooperative system due to SE improvement as a function of the user relative distance and ISD for *M* = 3 and *t* = *r* = 2.

From our analytical analysis, we can conclude that CoMP is most likely to be more energy efficient than traditional non-cooperative cellular system for cell-edge communication and/or small cell deployment, as it is summarized by FIGURE 30. Moreover, using more than 3 BSs for cooperation is unlikely to be beneficial in terms of EE. Finally, in the uplink, EE can mainly be achieved via improvement in SE as a result of macro-diversity.

6.2. BASE STATION COOPERATION UNDER LIMITED BACKHAUL CAPACITY

In this study, we address for a single user scenario the energy efficiency of two BSs cooperation under limited backhaul capacity. In order to evaluate the EE metric, we provide an information-theoretical analysis based on the outage probability. Then, we identify by numerical results the cooperation scenarios that can save energy depending on the backhaul capacity [SarKam2012].

6.2.1. System Model

We consider a downlink transmission from two BSs with a single antenna each to a single user with one receive antenna. The user is located between both cells as presented in FIGURE 31. The BSs are assumed to be perfectly synchronized in time and frequency. They are connected via limited capacity backhaul link with capacity C_b bit

per channel use (bit/cu). This latter condition limits the number of bits that can be sent over the backhaul link per transmission block. . A transmission rate of R bit/cu is considered and BS1, BS2 are transmitting with power P_1 and P_2 respectively. A sum power of $P = P_1 + P_2$ is fixed, with $P_1 = \alpha P$ and $P_2 = (1-\alpha)P$, α denoting the ratio of the total sum power used by BS1. Note that only the transmission power from the BSs is considered, the backhaul power is not included in our power model.

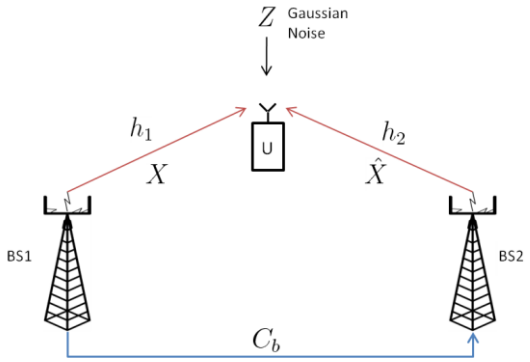

FIGURE 31. Downlink BS cooperation.

We assume that the transmission happens over a slow flat Rayleigh fading channel where the channel remains constant over a transmitted block and varies independently from one block to another. The channel fading coefficients h_1, and h_2 are respectively between BS1, BS2 and the user and are only known at the receiver side. They are modeled as i.i.d. complex Gaussian random variables with zero mean and unit variance $\sim \mathcal{N}_c(0,1)$. White Gaussian noise Z is added to the transmitted signal $\sim \mathcal{N}_c(0,\sigma^2),\ \sigma^2 = 1$. Thus, the received signal is given by

$$Y = \sqrt{P_1}h_1 X + \sqrt{P_2}h_2 \hat{X} + Z. \tag{6-14}$$

Quantization over the Backhaul link: For cooperation between BSs, and since the backhaul link has finite capacity C_b, BS1 performs quantization of the signal X to be transmitted to the user. It forwards then the quantized version to BS2 via the backhaul. We assume that we transmit over this backhaul independent complex Gaussian variables $X \sim \mathcal{N}_c(0,1)$, and not the modulated symbols. Thus, the transmission is subject to quantization noise based on the rate-distortion theory. It is defined by $D(C_b) = 2^{-C_b}$. The backhaul can be modeled by a forward test channel of the form $\hat{X} = c(X+\eta)$, where X and η are independent and η represents the quantization noise with variance $\sigma_\eta^2 = \frac{2^{-C_b}}{1-2^{-C_b}}$ and $c = 1 - 2^{-C_b}$ a constant. Thus, the received signal can be redefined as

$$Y = \sqrt{P_1}h_1 X + \sqrt{P_2}(1-2^{-C_b})h_2(X+\eta) + Z = \left(\sqrt{P_1}h_1 + \sqrt{P_2}(1-2^{-C_b})h_2\right)X + N, \tag{6-15}$$

where $N = \sqrt{P_2}(1-2^{-C_b})h_2\eta + Z$ is the equivalent noise with variance $\sigma_N^2 = P_2 2^{-C_b}(1-2^{-C_b})\left|h_2\right|^2 + \sigma^2$.

6.2.2. Information Theoretical Energy Efficiency Analysis

In the case of slow fading channel, a transmitted codeword with finite length spans only one channel realization, and a suitable capacity metric is then defined by the outage probability for a target data rate R as

$$P_{\text{out}}(P,R) = \Pr\{C(H) < R\}. \tag{6-16}$$

Based on this outage probability, we use an EE metric that was proposed to measure the energy efficiency of slow MIMO fading channels by optimizing the PwA policy [BelLas2009]. It is defined as the ratio between the expected throughput (the benefit function) and the average consumed power. The expected throughput can be seen as the average system throughput over many transmissions. For the BS cooperation model with fixed total transmission power P and under limited backhaul capacity C_b, this metric is given by

$$\xi(P,R,C_b)=\frac{R\left(1-P_{\text{out}}(P,R,C_b)\right)}{P}. \tag{6-17}$$

In order to evaluate it, we first derive the outage probability of the virtual multiple-input single-output (MISO) channel, where the user terminal and each BS have single antennas. The outage probability can be then defined by [SarKam2012]

$$\begin{aligned}P_{\text{out}}(P,R,C_b)&=\Pr\left\{\log_2\left(1+\frac{\left|\sqrt{P_1}h_1+\sqrt{P_2}(1-2^{-C_b})h_2\right|^2}{P_2 2^{-C_b}(1-2^{-C_b})\left|h_2\right|^2+\sigma^2}\right)<R\right\}\\&=\Pr\left\{\left|\sqrt{P_1}h_1+\sqrt{P_2}(1-2^{-C_b})h_2\right|^2-\lambda P_2 2^{-C_b}(1-2^{-C_b})\left|h_2\right|^2<\lambda\sigma^2\right\}.\end{aligned} \tag{6-18}$$

We identify that $P_{\text{out}}(P,R,C_b)$ represents the probability that the difference of two correlated χ^2-distributed variables, *i.e.* the difference of two Bivariate Gamma variables, falls below a given threshold. We find that this difference follows Type II McKay distribution according to [HolAlo2004]. In Rayleigh case, the outage probability has a reduced expression. It is computed as [SarKam2012], [HolAlo2004]

$$P_{\text{out}}(P,R,C_b)=1-\frac{1-c}{2}\exp\left(-\frac{1+c}{b}\lambda\sigma^2\right) \tag{6-19}$$

with the following parameters,

$$\begin{aligned}&b=\frac{2\lambda\sigma_1^2\sigma_2^2(1-\rho)}{\sqrt{(\sigma_1^2+\lambda\sigma_2^2)^2-4\lambda\sigma_1^2\sigma_2^2\rho}},\quad c=-\frac{\sigma_1^2-\lambda\sigma_2^2}{\sqrt{(\sigma_1^2+\lambda\sigma_2^2)^2-4\lambda\sigma_1^2\sigma_2^2\rho}},\quad \lambda=(2^R-1)\\&\sigma_1^2=P_1+P_2(1-2^{-C_b})^2,\quad \sigma_2^2=P_2 2^{-C_b}(1-2^{-C_b}),\quad \rho=\frac{P_2(1-2^{-C_b})^2}{P_1+P_2(1-2^{-C_b})^2}.\end{aligned}$$

6.2.3. Numerical Results

In this section, we evaluate the Energy Efficiency of the BS cooperation model with limited backhaul capacity $C_b$and fixed total transmission power P via numerical results. The EE performances are represented in terms of (Joule/Mbit) versus the backhaul capacity C_b bit/cu or the transmit power P expressed in terms of the SNR in (dB). For all the results, we consider a transmission rate of $R=2$ bit/cu, and a distance between the BS and the user equal to $d=200$ m for the path loss computation.

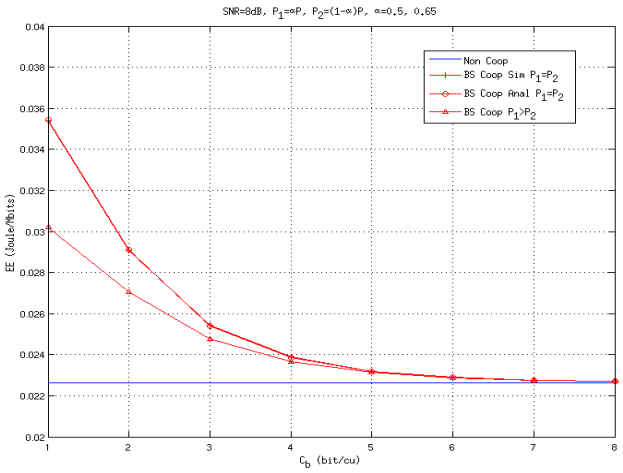

(a) EE vs. C_b for a fixed SNR.

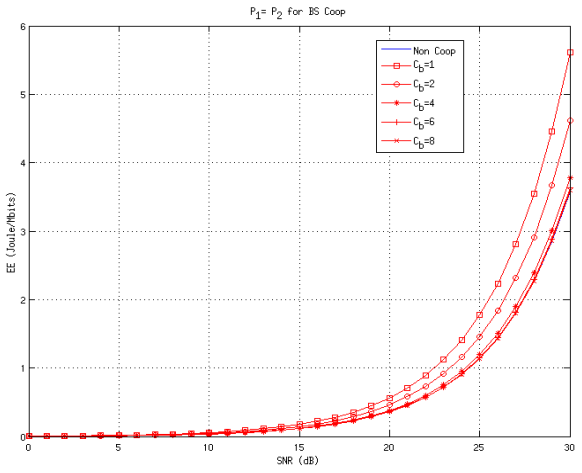

(b) EE vs. SNR for different C_b and $P_1=P_2$.

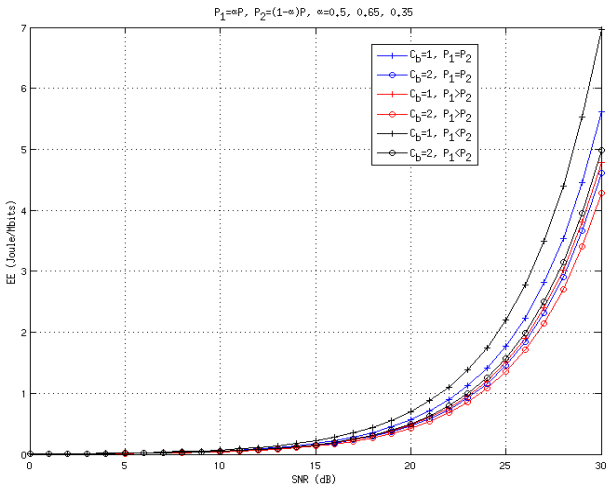

(c) EE vs. SNR for limited C_b.

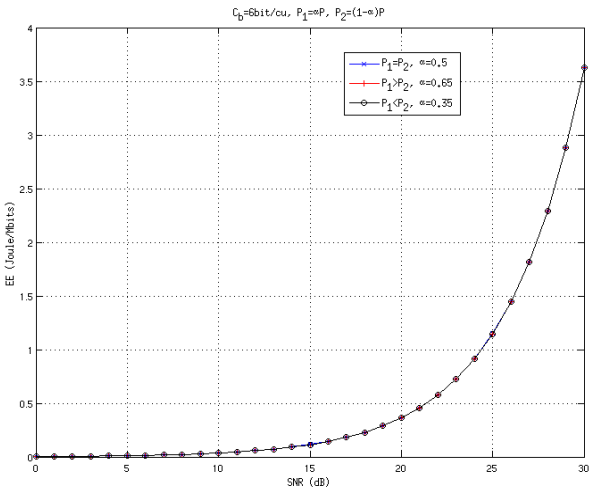

(d) EE vs. SNR for unlimited C_b.

FIGURE 32. EE numerical results.

FIGURE 32 (a) demonstrates the accuracy of the analytical EE metric by comparing to simulation results. In addition, it compares the BS cooperation model to a non-cooperative model where only BS1 is transmitting to the user with the total power$P$. It is evident that cooperation with any PwA policy between BS1 and BS2 $P_1 = P_2$ or $P_1 > P_2$ $(P_1 = 0.65P)$ cannot be as energy efficient as non-cooperation unless the backhaul capacity is unlimited (perfect backhaul). FIGURE 32 (b) focuses on the case of uniform PwA between BS1 and BS2 for different C_b values. We can see that cooperation with low capacity C_b increases the EE in Joule/Mbit. In fact, the P_{out} is increased, so we need more energy to transmit reliably the same number of bits. Finally, comparing the PwA between BS1 and BS2, we can observe in FIGURE 32 (c) that with limited C_b, BS1 transmitting at a higher power $P_1 > P_2$ is more energy saving than both BSs transmitting at the same power or BS2 transmitting at $P_2 > P_1$. It is obvious that this last case is subject to more outage events since C_b is low. Increasing the power at BS2 then results in wastage of energy. Whereas, with unlimited backhaul capacity, for instance $C_b = 6$ bit/cu, all the power configurations are equivalent as it is illustrated in FIGURE 32 (d).

We conclude from numerical results that BS cooperation can be energy saving for limited C_b in asymmetric configuration where $P_1 > P_2$, while all power configurations behave similarly under perfect backhaul.

6.3. FRACTIONAL FREQUENCY REUSE

Fractional frequency reuse (FFR) has been proposed as a competitive strategy to mitigate the interference in Orthogonal Frequency Division Multiple Access (OFDMA) networks with single frequency reuse deployments [DasVis2006], [Ericsson2005]. The basic idea of FFR is to divide the whole bandwidth into two types of sub-bands. One sub-band is dedicated to the users that are close to their BS (inner zone). This sub-band is exploited with single frequency reuse planning. The other sub-bands are occupied with a larger frequency reuse factor (2, 3 or more) and are attributed to the users that are located in the cell edge area (outer zone). In the conventional use of FFR strategy, the BSs are handled equally without considering the difference in the traffic load between them. This case can be handled easily with a static solution for the bandwidth splitting. However, if the load is unbalanced between the neighbouring BS then the overloaded cell starts to increase the transmit power in order to compensate the lack of spectrum resource until the maximal allowed power is reached. This will generate more interference and practically waste the energy. Thereby we propose to mitigate the impact of traffic imbalance on the energy consumption by using a dynamic approach. With the proposed solution, the bandwidth allocation

(BwA) follows the number of users located in each cell, and the power is allocated in each sub-band based on the relative narrowband transmit power (RNTP) indicators available in LTE networks. This solution gives more bandwidth to the users that are located in the edge of overloaded cells. In order to be efficient, the adaptation has to be as fast as possible.

For clarity of illustration, we consider the simple case of two neighbouring BSs BS_1 and BS_2 in a downlink scenario. Taking into account the 3GPP LTE terminology, the total bandwidth is divided into three slices: N_0 physical resource blocks (PRBs) are utilized with a frequency reuse factor of 1 for both sites, N_1 (respectively N_2) PRBs are utilized by BS_1 (respectively BS_2) exclusively for users that are located in the cell edge area (see FIGURE 33). For a general deployment, the total bandwidth is divided in three slices, one slice is utilized with a frequency reuse of 1 (centre of the cell), and the others are utilized with a frequency reuse factor of 3.

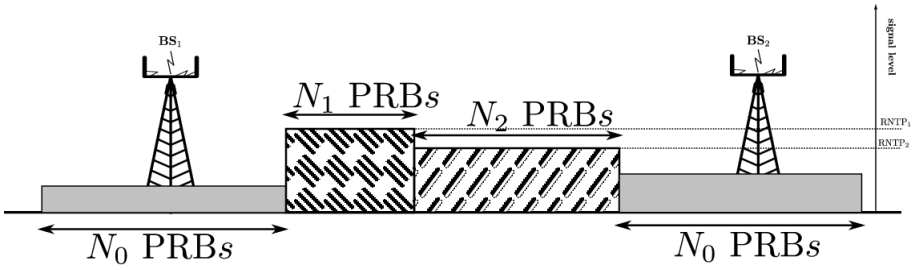

FIGURE 33. Adaptive FFR scenario with two BSs.

Based on RNTP indicators [3GPPTS423-890], N_0, N_1 and N_2 are adapted to the number of users in each cell according to the following procedure: BS_1 allocates power and frequency resources in its cell using the optimization method proposed in [SeMoCi2006][1]. Two limits for the signal amplitude are considered in this optimization: one for the inner zone, and another for the outer zone. The signal level limit that is used in the outer zone is sent to the neighbouring base-station BS_2 using RNTP indicators. This level allows the neighbouring cell to estimate the level of interference generated by BS_1 and to allocate the resources accordingly. After few iterations, both BSs agree on the frequency and power resources that are allocated in outer zones. Compared to the static approach where N_0, N_1 and N_2 are fixed, the proposed adaptation increases the energy efficiency of the system by reducing the required transmit power to satisfy a certain rate demand. As a consequence, when taking into account the transmit power, the average cost of correctly transmitted bits (in J/bit) is improved. FIGURE 34 draws the energy saving ratio between an adaptive approach and conventional static strategy for both base-stations (FIGURE 34 (a)) and for the cell experiencing the highest load (FIGURE 34 (b)) when the rate demand of users varies between 0 and 10Mbps. All users in both cells ask the same rate, and the number of users served for each TTI is 5 for BS_1 and 3 for BS_2. Note that the results are independent of the number of users that are served, and are only sensitive to the aggregated rate that is requested by all users in each BS. For high rate demand, FIGURE 34 shows that 15% of energy saving for the cell with highest number of users and 8% for the sum power of both BSs.

[1]Note that other optimization approaches with lower complexity can also be used

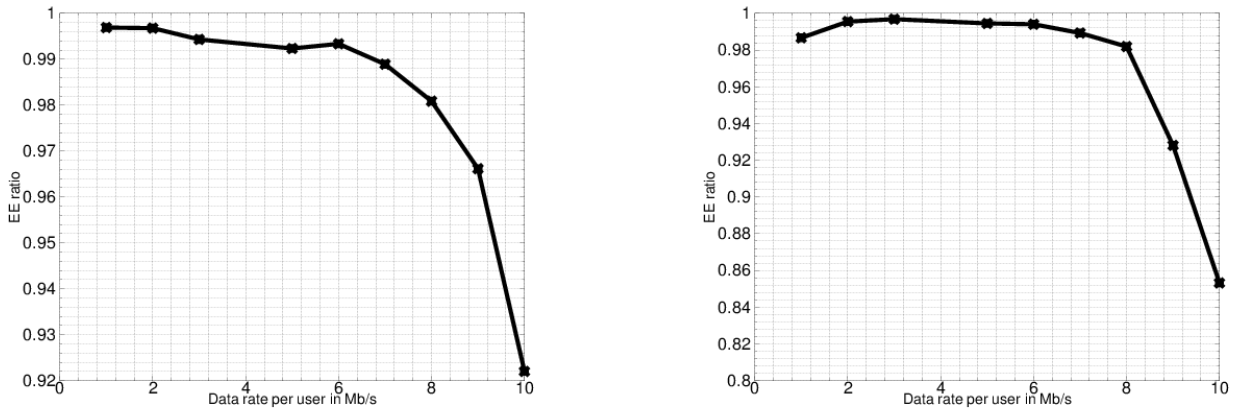

(a) (b)

FIGURE 34. Energy saving gains with adaptive FFR (ratio between energy consumption using adaptive FFR and energy consumption using static approach).

The energy saving of adaptation could be enhanced by increasing the number iterations for bandwidth adaptation. However this comes at the cost of higher signalling overhead.

6.4. MULTI-CELL SCHEDULING

This work proposes an energy-efficient based resource allocation (bandwidth and power) for the downlink of a coordinated multi-cell system. In the conventional resource allocation schemes, resources are kept orthogonal between the interfering cells. This approach, which is obviously tailored for interference limited scenarios, is far from optimal in the case of spatially well separated P2P transmissions, where reuse of the resources is more justified. In addition, if resources are reused within the adjacent cells the need for coordination in the radio resources becomes even more justified. To this end, short-term time-frequency allocation through coordinated scheduling has been considered in [ROCKET-4D2] for improving the SE of cellular system. In this work, a general framework for sequential coordinated resource sharing and allocation between interfering sectors of adjacent BSs has been proposed and evaluated. In the downlink scenario, different BSs take turns to sequentially allocate the resources leaving specified margins for “the BSs to follow in the sequence” and respecting the allocation of the “preceding BSs”. The order of the BSs in the sequence is changed over time to ensure fairness. Following the same idea, we propose here an energy-efficient RRM scheme for the downlink of a multi-cell coordinated system.

Multi-cell coordination, which relies on single cell signal processing and detection, avoids very complex multi-cell detectors or precoders in comparison with multi-cell cooperation, but incorporates efficient procedures to limit the negative effects of other adjacent cells’ operations. This approach will only require sharing a part of the global channel state and the extra backhaul load will be limited in comparison with joint multi-cell processing methods. The coordinating BSs (more specifically the adjacent sectors of three coordinating BSs, as it is depicted in FIGURE 35) exchange the channel state (channel gain) on all sub-bands for all the users. In the case that the information is available for the channel with the adjacent (non-serving) cell, it is also reported back to the serving cell and can be exchanged with other cells during coordination. The BSs then take turns to allocate the full pool of available resources to a fixed number of served users and pass over the allocation control to the next BS in the schedule. In this manner, the first BS to have the chance of the resource allocation has the advantage to make the best use of all available resources and is called the primary BS. However, this BS is constrained to keep only a limited number of resources and free up the resources for the subsequent BSs for their use. The second BS is called secondary and the third is called tertiary BS. The secondary and the tertiary BSs allocate the limited left over resources. Since

the first BS gets an advantage in this allocation scheme, we change the schedule in round robin fashion to ensure fairness by giving equal chance for all BSs to be in this advantage situation. We also consider the orthogonality of the band allocation within each cell, and that the interference caused by the other cells on the band of a given cell depends on the BwA-PwA outcome of the other cells and the associated channel gain norms of the interfering other-cell UEs.

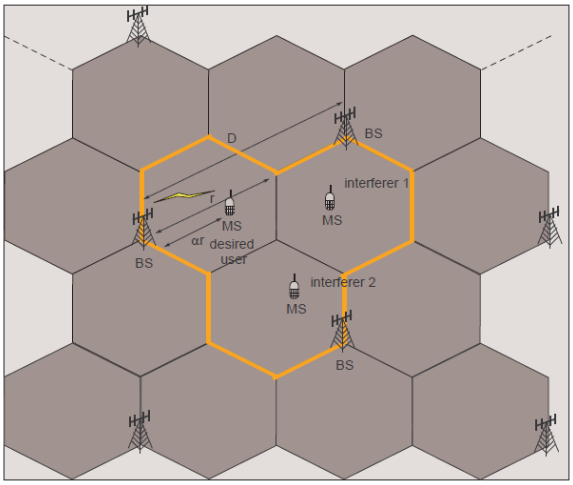

FIGURE 35. Adjacent sectors of three BSs coordination model.

The results in FIGURE 36 compares 3 types of BwA-PwAs for the scenario depicted in FIGURE 35 (coordination of 3 sectors) when considering that each BS has one transmit antenna, each UE has one receive antenna; full buffer traffic, 10 users per sectors, and the simulation and PCM parameters as described in [EARTH-D2.2] and [EARTH-D2.3], respectively. However, we did not take into account the extra requirement of backhauling for coordinating the BSs. In the orthogonal reuse baseline system (BLS), each user of the different sectors uses different sub-band, the BwA is performed via proportional fair scheduling and the PwA is based on water filling for maximizing the sum-rate. In full reuse non coordinated BLS, the same BwA and PwA are considered as for the first scheme but only one bandwidth is shared among the three sectors and no coordination is performed. Finally, in full reuse coordinated EE-BwAPwA, we apply our coordination for allocating in an EE way both bandwidth and power. The results clearly show that our scheduling method can reduce the energy effort by 40% when compared to the non-coordinated traditional scheduling method. This energy effort gain is mainly due to power saving as it is shown in the top right part of FIGURE 36.

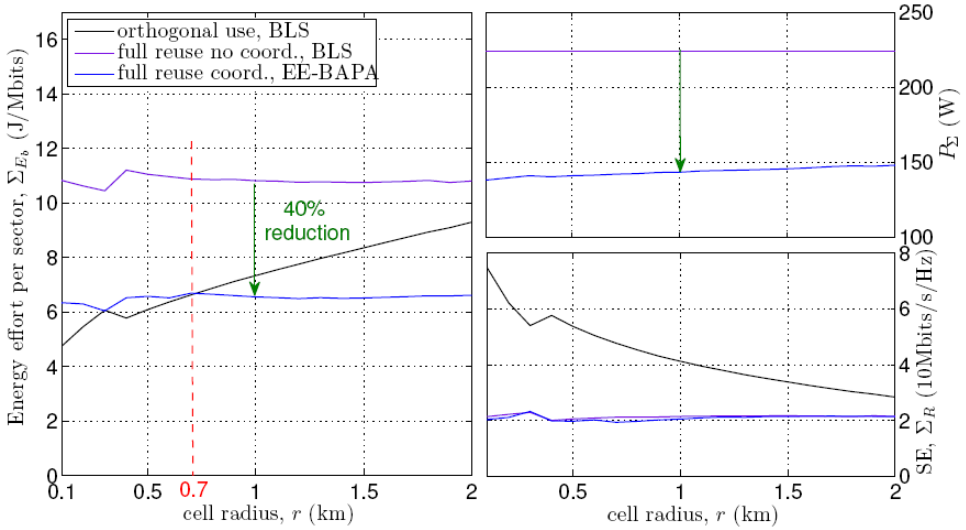

FIGURE 36. Energy effort, sum-rate and total consumed power per sector for three types of scheduling methods.

Intuitively, if interference occurs, reducing power will reduce the interference, which in turns will counterbalance the loss of rate due to power reduction and hence decrease the energy effort. For instance let us considers a simple numerical example to illustrate this point and cross-validate the results in FIGURE 36. Let us assume the scenario of FIGURE 35 with one user per cell placed in the middle of the cell (α=0.5) and r = 250 m such that the distance of the user to its desired BS is d_1 = 125 m and to its non-desired BSs is d_2 = $((\alpha r)^2 + D^2 - 2\alpha r D\cos(\pi/6))$ = 396.7 m. Using the EARTH link budget in [EARTH-D2.2], d_1 and d_2 corresponds to a channel gain coefficient of about $g_1 = 5.10^{-9}$ and $g_2 = 3.11^{-11}$, while the noise power for a bandwidth of 10 MHz is roughly equal to $N = 3.11^{-13}$. Using the Shannon capacity formula $C = \log_2\left(1 + \frac{Pg_1}{N + 2Pg_2}\right)$ reveals that transmitting at full power, i.e. P = 20 W, provides a maximum SE of C = 20.7 bit/s/Hz, whereas transmitting at $P = 5.10^{-3}$, which in the process makes the interference power equal to the noise power, gives a SE of C = 18.7 bit/s/Hz. Meanwhile, considering the abstraction of the EARTH PCM in [EARTH-D2.3], where $P_{BS/sector} = P\,\Delta_P + P_0$, where 20 W ≥ P ≥ 0, Δ_P =4.7 and P_0 = 130 W, the energy effort at full power is E_b = 10.8 J/bit/Hz, whereas the energy effort at $P = 5.10^{-3}$ is E_b = 6.95 J/bit/Hz. Thus, by willing to trade-off 10% of SE in this example, one can obtain a gain of 35% in energy effort by saving power and reducing interference. From, this numerical example and the results of FIGURE 36, coordinated scheduling can save energy especially if the interference level is high in comparison with the noise level.

Note that prior to defining our EE-based resource allocation for the downlink of multi-cell system, we first have developed a resource allocation method for the single cell scenario with residual interference in [HéImTa2012c], which acted as a stepping stone for this work.

6.5. IMPACT OF BACKHAULING TECHNIQUES

CoMP techniques rely on inter BS signalling and eventually user data exchange. Therefore, BS cooperation poses specific requirements on the backhaul network infrastructure. The choice of a certain backhaul technology depends on the capacity and latency demands that the mobile operator requires. In addition, the use of CoMP scheme raises the performance expectations of the backhaul network in terms of capacity and latency on the X2 interface [BiScCh+2011]. In our study we consider four backhaul deployment possibilities, each of them offering different trade-offs in terms of cost and performance, and most importantly in this extent, power consumption. We consider PON, fibre-to-the-node (FTTN), microwave (MW) and active optical network (AON) backhauling solutions (see FIGURE 37). For each of them, we provide a PCM and calculate power consumption related to each connected BS, as well as the overall backhaul power in realistic deployments where a number of BSs is required.

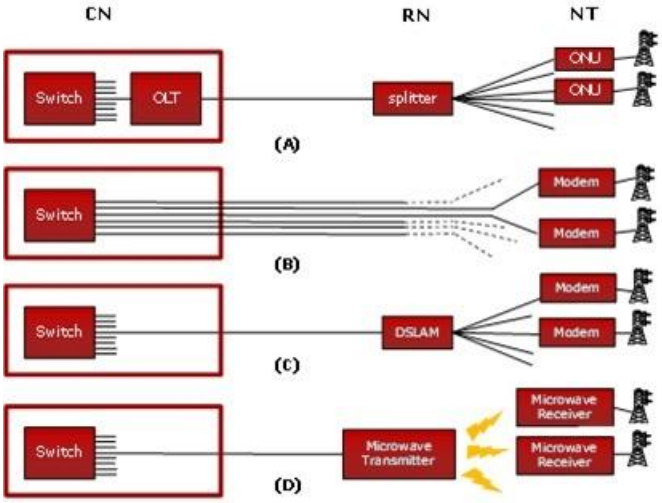

FIGURE 37. Backhaul networks (A) Passive Optical Network (PON) (B) Active Optical Network (AON), also referred to Point-to-point (P2P) (C) Fibre-to-the-node (FTTN) (D) Microwave links.

We refer to a general model that defines the power consumption per BS P_{BS}, and then we consider the total number *N* of BSs in a certain area *A*. This approach is used also in [GlLaLe2008], [BaAySo+2009] and [SkLiDa2010]. The PCM is reported on equation (1), which describes the power required to connect one BS and the total backhaul power for a given number of BSs. P_{NT}, P_{RN} and P_{CN} represent respectively the power consumed at the network terminal (NT), the remote node (RN) and the connection switch (CN). N_{RN} and N_{CN} indicate how many users share the RN and the CN, respectively. We assume that one BS is attached to the network termination. Cooling and power supply at certain network elements are accounted by means of a factor 2. The network termination, which is collocated with the BS, does not include this factor since it is assumed the cooling and the power supply are shared with the BS. Both the CN and the RN have a specific data rate we refer to as R_{CN} and R_{RN} respectively. In our formula, two additional multiplicative terms appear, α and β. The term α represents a scaling factor that accounts for the additional number of remote nodes needed to accommodate a number of NTs exceeding that allowed by the RN factory settings. Similarly, the term β represents the number of additional CNs needed to accommodate a number of RNs exceeding that allowed by the CN factory settings.

$$P_{BS} = \left(P_{NT} + 2 \cdot \frac{P_{RN}}{N_{RN}} \cdot \alpha + 2 \cdot \frac{P_{CN}}{N_{CN}} \cdot \beta \right) \qquad (6\text{-}20)$$

$$P_{tot} = N \cdot P_{BS} \quad .$$

In our analysis, we first look at the power consumption per BS without considering any realistic backhaul deployment. We take into account the characteristics of each technology and then we consider the power consumed for connecting each BS. For this purpose, the terms α and β are set to 1. Later, we consider a variable number of BSs. In this case, the two terms α and β need to be updated according to the network technology.

PON

In a PON-based network, the RN is a passive element which does not consume any power. Therefore, P_{RN} is set to 0. In a PON, the bandwidth is shared amongst the NTs, or optical network units (ONUs) in this case. Traffic aggregation is considered by means of a factor *a*. The rate per BS R_{BS} is jointly offered to the optical line terminal (OLT) collocated with the CN, resulting in an uplink traffic equal to $(N_{CN} \times R_{BS})/a$. Since the uplink traffic is also expressed as $R_{CN} - N_{CN} \times R_{BS}$, if *a* is equal to 1 (no aggregation, then highest power consumption) the quantity N_{CN} is given by $R_{CN}/2R_{BS}$. Notice that if the overall traffic offered by the PON network is 1 Gbps, only one port of the CN is used (and powered) if the maximum rate per port, R_{port}, is equal to 1 Gbps [LanGla2009].

AON (also referred to P2P) Similar considerations apply for the AON, also referred to P2P link. In this case, no OLT is present and the BS is directly connected to the CN. The uplink is expressed by $R_{BS} \times N_{CN}/a$. On the other hand, the uplink rate is also expressed as $R_{CN} - N_{CN} \times R_{port}$. With a = 1, N_{CN} thus results equal to $R_{CN}/R_{BS} + R_{port}$.

FTTN

In this scenario, both the CN and the RN are present. We calculate the values of N_{CN} and N_{RN} as follows. We observe that the role of the CN is played by the RN from the BSs' perspective. Then, it turns out that, similar to the previous AON case, with a = 1, N_{RN} can be expressed as $R_{RN}/R_{BS} + R_{port}$. The quantity N_{CN} undergoes the same considerations as in the PON case: the incoming traffic from is $N_{CN} \times R_{BS}/a$. At the same time, assuming $a = 1$, we express this traffic as $R_{CN} - N_{CN} \times R_{BS}$, thus obtaining the same expression for N_{CN}. Same considerations apply to the MW architecture.

TABLE 4 reports the power consumption figures and other parameters related to the technologies we considered here. FIGURE 38 shows the backhaul power consumption per BS and for the total backhaul network with a varying number of BSs. In this case, the factors α and β are accounted. Considering a maximum port number of 60, as soon as the number of BSs increases, more switches will be necessary, based on the amount of traffic each BS requires (FIGURE 38 (a)).

TABLE 4. Backhaul network characterstics.

	P_{NT} (W)	P_{RN} (W)	P_{CN} (W)	Range (Km)	R_{max} (Gbps)	N_{RN}	Per BS (Gbps)
PON	5	-	112	20	1	32	0.03
FTTN	10	85	466	1 (from DSALM)	0.1	16	0.05
AON	4	-	466	15	1	60 (switch ports)	1
MW	10	40	466	15	0.170	1	0.17

Two important considerations are drawn. The PON backhaul is more efficient compared to the other technologies, in absolute terms. On the other hand, as soon as the number of connected BS increases, the AON becomes more competitive and can potentially provide better power consumption performance as soon as the required bandwidth requirements per BS get higher (FIGURE 38 (b)). This is an important parameter to account for, since BS cooperation is likely to introduce an elevate amount of traffic on the X2 interface, thus requiring high bandwidth in the backhaul links.

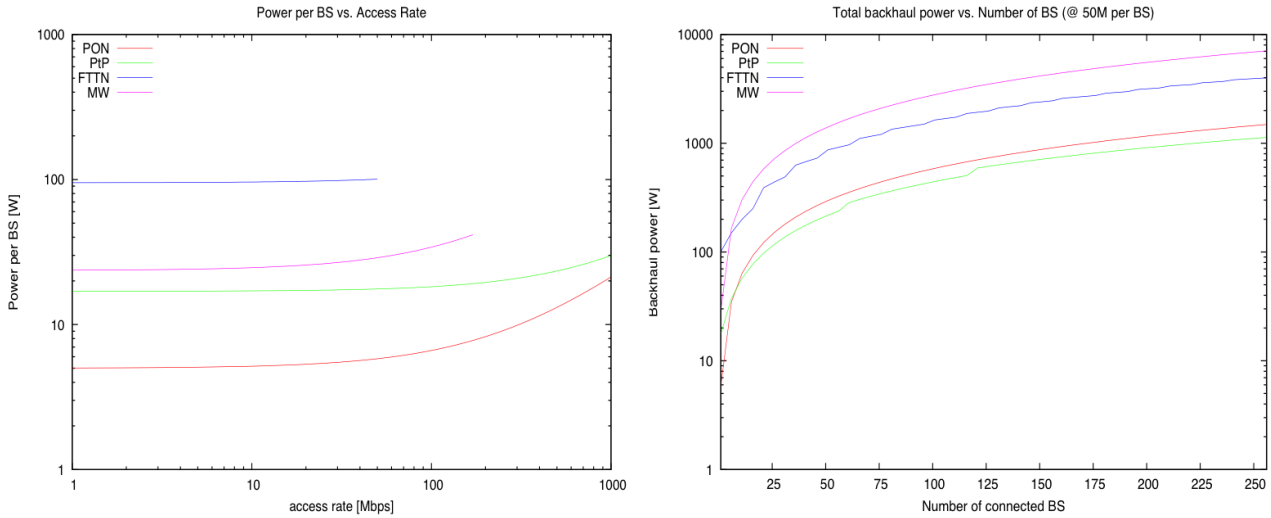

FIGURE 38. (a) Per BS power consumption vs. access rate; (b) Overall backhaul power consumption vs. number of BSs.

7. ADAPTIVE NETWORK RECONFIGURATION

Analysis of traffic in current networks and the predictions of its growth trend show that BSs will keep using only a small fraction of their capacity [Auer+2011]. The strong requirements on low latency and low blocking probability demand that even during busy hour resources are on average not fully utilized. Besides, the analysis of daily variation of the data traffic in today's networks [Auer+2011] and [Sandvine2010] shows that there are long periods during a day in which the average load of the network can be 5 or 10 times smaller than the peak values in the busy/peak hours. A good deal of the daily energy consumption is thus spent for providing the full system capacity, even when the actual traffic demand is much lower.

Smart management tries to reduce such over provisioning in order to save energy. A promising way to reduce the energy consumption of the mobile networks is to dynamically reduce the number of active network elements to follow adaptively the daily variation of the traffic. In particular, four techniques are presented.

Dynamic bandwidth management is based on a stepwise adaptation of the bandwidth usage to the required traffic load, i.e. by an adaptation of the maximum number of resource blocks that are used during each LTE subframe. The total transmitted maximum output power can be decreased when less resource blocks are used for scheduling user data. Then the operation point of the adaptive PA can be modified by reducing the supply voltage so that the PA operates more closely to its most efficient operation point. In addition the reference signal overhead can be reduced. We have found that this technique provides approx. 25% energy saving and combines well with radio hardware improvements [EARTH-D4.2] providing more than 50% energy saving. This idea is discussed in Section 7.1.

Dynamic sectorisation of BSs is already applicable to currently operational RATs [HevGod2011]. This energy saving technique also suits RATs with a frequency reuse of one. In urban networks, the macro BSs are close to each other and capacity might be limited by interference in busy hour periods. In lightly loaded situations, when interference is low, the receivers typically operate with a high margin over thermal noise. In such cases, some extra loss on the radio links can be tolerated and macro BSs can switch to fewer but larger sectors, for instance, from three-sector to omni-cell configuration. By switching off sectors, radio units can be switched off as well, and the energy saving potential is the largest in case of macro BSs. We have found that this technique provides 13-30% energy saving without considerable impact on coverage or average user throughput. This idea is discussed in Section 7.2.

Beyond the scope of sectorisation, low traffic conditions allow to save power by switching off a number of BSs if the BSs remaining on can serve the demands from the users. The viability of turning off BSs relates to the dense BS deployment that is done in order to be able to cope with the peak-traffic demands. In these cases, the coverage is not limited by the transmit power. Cell sizes are deliberately reduced since the limiting factor is the BS capacity and not its power budget. In such cases, we have found that the idea of **cell on/off in single layer networks** provides approx. 14% energy saving. This idea is discussed in Section 7.3 together with the application of the solution in vehicular machine-to-machine (M2M) scenarios.

The great increase of traffic and MBB penetration calls HetNets that are in the focus of network modernization especially in densely populated urban environments. In such HetNet networks there is a coverage layer dimensioned to serve conversational services and low data traffic, and a capacity layer dimensioned to serve high data traffic demands and large user throughput. Consequently, if the coverage layer forms a solid layer covering the given urban area, then one can expect that the capacity layer in most of the time is inevitably underutilized [VidGod2011]). We have found that the idea of **cell on/off in HetNets and multi-RAT networks** can provide 25-40% energy saving (or even approx. 50% in case of relaxed capacity of the coverage layer) and even more gain can be achieved in case of RRH (up to additional 7%). The idea is discussed in Section 7.4 together with the impact of application of macro BSs with RRH in the coverage layer and the impact of capacity of the coverage layer.

Note that all of the above techniques combine well with radio hardware improvements [EARTH-D4.2] forming solid basis for the integrated solutions to be defined in EARTH deliverable D6.2b and D6.3 later on.

7.1. DYNAMIC BANDWIDTH MANAGEMENT

Dynamic bandwidth management is based on a stepwise adaptation of the bandwidth usage to the required traffic load, i.e. by an adaptation of the maximum number of resource blocks that are used during each LTE subframe. The total transmitted maximum output power can be decreased when less resource blocks are used for scheduling user data. Then the operation point of the adaptive PA, which is described in [EARTH-D4.2], can be modified by reducing the supply voltage so that the PA operates more closely to its most efficient operation point. In addition the reference signal overhead can be reduced.

System level simulations have been performed with a hexagonal cell layout containing 19 macro BSs each serving 3 cells as defined in [EARTH-D2.2]. For all simulations wrap around has been applied to avoid cell edge effects. Other common parameters are the usage of a carrier frequency of 2 GHz, a 3D antenna model for SISO, a video streaming application with constant bit rate of 2 Mbps per user, as well as shadowing with a correlation distance of 50 m and a correlation of 0.5 between sites. Furthermore, an ISD of 500 m and 1732 m and a user mobility of 3 km/h and 30 km/h have been implemented for dense urban and rural scenarios, respectively.

The power consumption per area unit of a cell has been calculated by applying the EARTH E^3F [EARTH-D2.3]. This includes the daily EARTH traffic load model for dense urban and rural scenarios as well as the EARTH power model for macro BSs according to the year 2012. The calculated power consumption per area unit along a day (left side) as well as the daily energy savings as function of the peak system throughput (right side) is depicted in FIGURE 39 and FIGURE 40 for dense urban and rural scenarios, respectively.

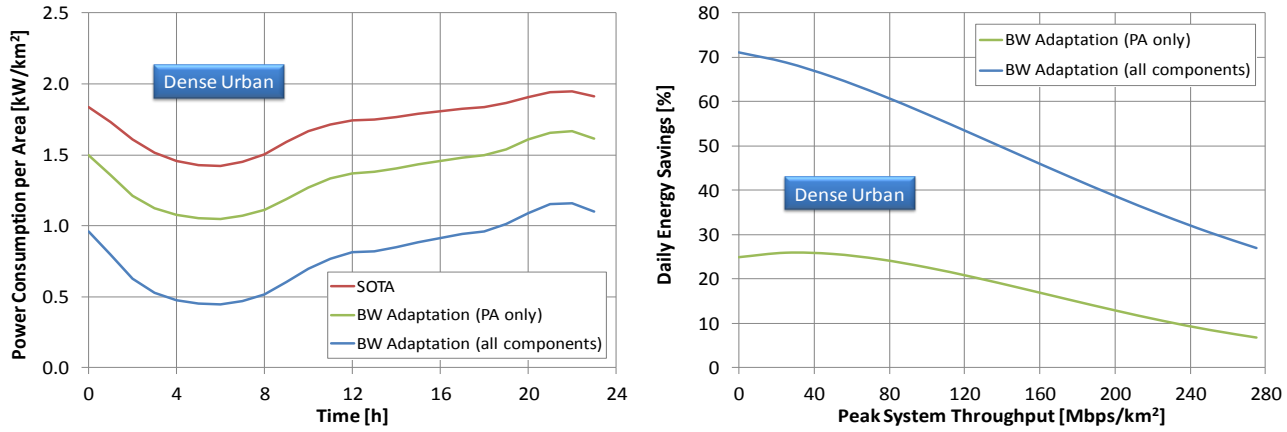

FIGURE 39. Dense urban scenario: Power consumption per area unit along a day for peak system throughput of 120 Mbps/km^2 (left) and daily energy savings vs. peak system throughput (right).

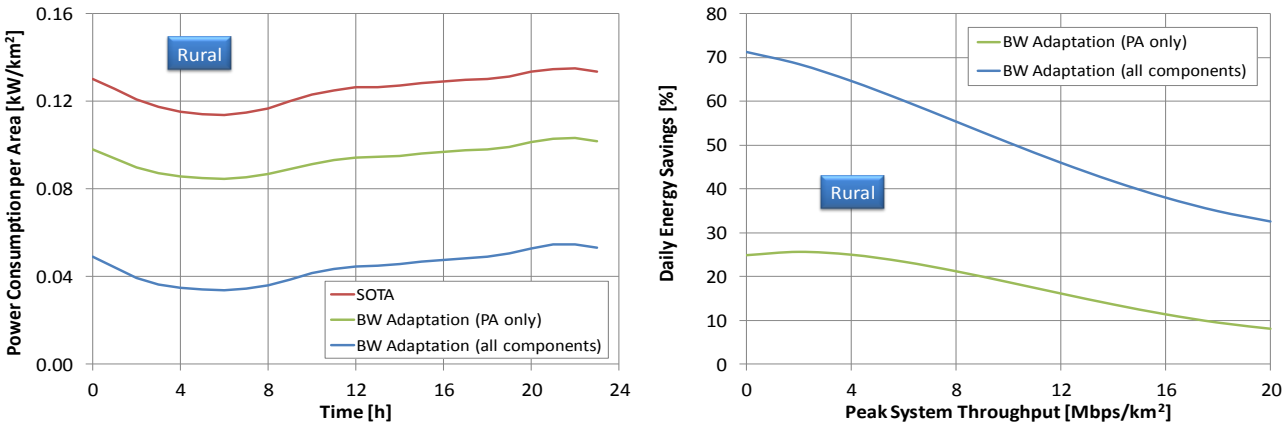

FIGURE 40. Rural scenario: Power consumption per area unit along a day for peak system throughput of 4 Mbps/km^2 (left) and daily energy savings vs. peak system throughput (right).

Depending on the peak system throughput of a day energy savings up to 26% can be achieved by bandwidth adaptation when the SOTA PA is replaced by the adaptive PA developed in [EARTH-D4.2]. When also other components of the BS (i.e. base band processing, the RF part, the limited efficiency of DC-DC conversion, AC-DC power supply, and cooling) are able to adapt to the lower load, additional energy savings can be achieved. The aggregated gain of an integrated solution of BW adaptation and all EARTH hardware improvements provides up to 70% savings. In this case a RRH without active cooling has been considered which reduces the power consumption by around 10%.

Daily energy savings have been evaluated for macro BSs in areas of dense urban and rural deployments under consideration of high data traffic profiles [EARTH-D2.3]. Energy savings of 20.9% and 53.6% along a day can be achieved in dense urban scenario at a peak system throughput of 120 Mbps/km^2 under consideration of the PA only and all other components including the PA, respectively. For the rural scenario the daily energy consumption can be reduced by 25% and 64.7% at a peak system throughput of 4 Mbps/km^2.

Dynamic bandwidth management can be improved in terms of energy savings by minimization of inter-cell interference. This is achieved by coordinating the unused part of the bandwidth between next neighbour BSs. As a limiting case, we consider a scenario which completely avoids interference of next neighbours. Therefore, system level simulations have been performed by using a reuse factor of 3 for the above determined daily traffic profiles in dense urban and rural scenario in combination with the bandwidth adaptation approach. For these investigations a full reuse scheme with factor 3 has been considered, i.e. an allocation of 3 x 10 MHz bandwidth according to 3 neighbour cells. FIGURE 41 illustrates the daily energy savings as function of the peak system throughput for dense urban and rural scenarios.

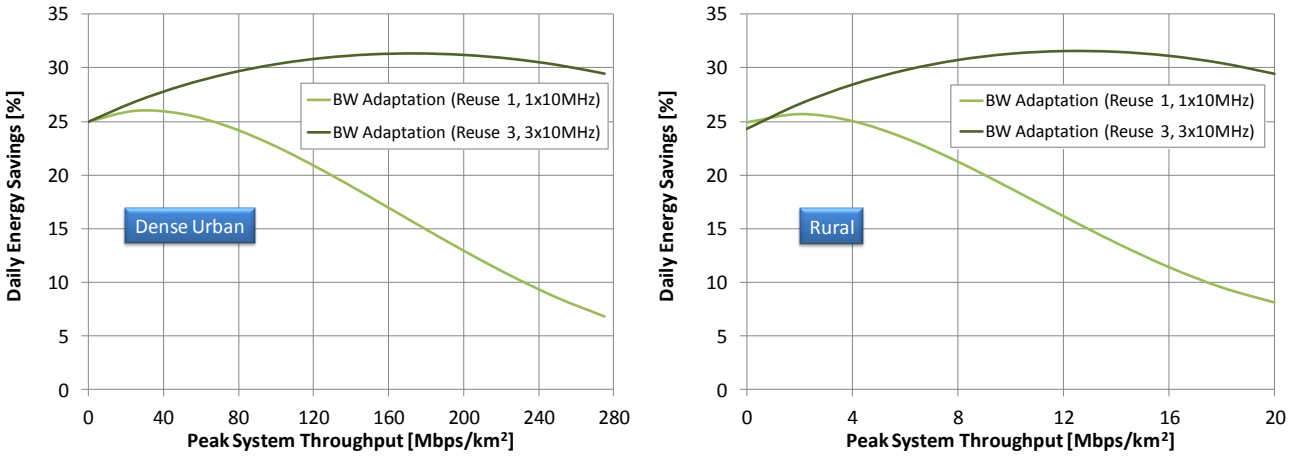

FIGURE 41. Daily energy savings of bandwidth adaptation approaches in combination with different reuse schemes for dense urban (left) and rural scenarios (right) based on improvements by the PA only.

The results show that higher energy savings can be achieved if a reuse scheme with factor 3 is applied. The daily energy savings are increased for dense urban scenarios at a peak system throughput of 120 Mbps/km^2 from 20.9% for reuse 1 to 30.8% for full reuse 3, if improvements of the PA only are considered. Similar improvements can be observed for the rural scenario at a peak system throughput of 4 Mbps/km^2. In this case daily energy savings are increased from 25% for reuse 1 to 28.5% for full reuse 3. Higher daily energy savings can be achieved when considering higher peak system throughputs. Improvements of all components show also much higher savings: 64.9% for full reuse 3 compared to 53.6% for reuse 1 in dense urban scenario and 68.2% for full reuse 3 compared to 64.7% for reuse 1 in rural scenario. Especially dense urban scenarios show that much higher daily energy savings are achievable when a full reuse scheme with factor of 3 is additionally implemented.

For realistic deployments a full reuse scheme with factor of 3 is not applicable, because the available spectrum of operators is often restricted. However, this scheme is used as reference scenario showing nearly the limit that can be achieved by minimization of inter-cell interference. A more practical and realistic scheme based on a partial

reuse scheme with factor of 3 is planned for future investigations, i.e. only 1 x 10 MHz bandwidth is allocated to all cells. In this case each cell of a RAN is assigned to use first a preconfigured set of resource blocks for scheduling. If the preconfigured resources are exhausted, the resources of the next neighbour cell are employed. Next the resources of the last neighbour cell are allocated, until all resources are used up at maximum bandwidth usage of 10 MHz. In this allocation schemes interference is not completely eliminated at higher load. It is expected that the achievable savings are between the reported values of the standard LTE reuse scheme with factor 1 and the full reuse scheme of factor 3.

Higher energy savings are expected when combinations of green scheduling strategies are considered. Promising solutions are combinations of procedures based on bandwidth adaptation with micro DTX or capacity adaptation with micro DTX. The potential of these combinations have been investigated in [EARTH-D4.2]. Therefore, system level simulations will be used to confirm these results and to show enhancements with the above mentioned partial reuse scheme. These approaches are also suitable for an integrated EARTH solution. In this case carrier aggregation procedures, which are currently under discussion in 3GPP, can be considered to realise fast bandwidth adaptation procedures in a RAN.

7.2. DYNAMIC SECTORIZIATON

Dynamic sectorisation of BSs is already applicable to currently operational RATs [HevGod2011]. This energy saving technique also suits RATs with a frequency reuse of one. In urban networks, the macro BSs are close to each other and capacity might be limited by interference in busy hour periods. In lightly loaded situations, when interference is low, the receivers typically operate with a high margin over thermal noise. In such cases, some extra loss on the radio links can be tolerated and macro BSs can switch to fewer but larger sectors, for instance, from three-sector to omni-cell configuration. By switching off sectors, radio units can be switched off as well, and the energy saving potential is the largest in case of macro BSs.

An operator can estimate the SNR margin of lightly loaded BSs from long-term user terminal measurements and can identify the nodes where dynamic sectorisation can be applied without the risk of service degradation.

Sectorisation switching in a network can be governed by predictions, when the switching times are determined from long-term traffic observations, or by short-term evaluation of instantaneous load and service quality in active sectors. A technique for each method is described by the next two subsections.

7.2.1. Adaptive, prediction-based sectorisation

In this work, we propose a novel energy-aware adaptive sectorisation strategy, where the BSs are able to adapt themselves to the temporal traffic variation by switching off some sectors and changing the beam-width of the remaining sectors. Adaptation is performed while taking into account the target QoS.

In the cellular system we considered, each BS consists of three sectors and each sector is defined as a hexagon. Sectorised antenna is employed in each sector. We assume the spatial traffic density is uniform throughout the whole system.

When traffic demand is at high level, all three sectors within one BS are activated. When traffic demand is low, in previous network management schemes some of the cells are turned off to save energy. The users attached to those silent BSs are taken care of by the remaining BSs. However, if the transmission power of the remaining cells keeps unchanged and the ISD is relatively large, this turning off action will cause severe coverage problem. Therefore, we propose to turn off sector 1 (it can be sector 2 or 3 and this selection does not make any difference. Here for simplicity, we assume sector 1 is switched off) of each BS instead. Handover is performed throughout the system. The users in the silent sector, i.e. sector 1, will be assigned to other sectors or even other BSs based on the long term received signal strength, i.e. summation of pathloss and shadowing loss. Apparently, those users in the silent sectors will suffer from lower coverage because of the weaker received power. To maintain the coverage level of the silent sector, we need to change the antenna pattern of the other two sectors.

In order to cover the silent sector, the antennas of the two remaining sectors should cover 180 degree instead of 120 degree and the beam-width of these sectors should be increased from 65 degree to 95 degree as shown in FIGURE 42.

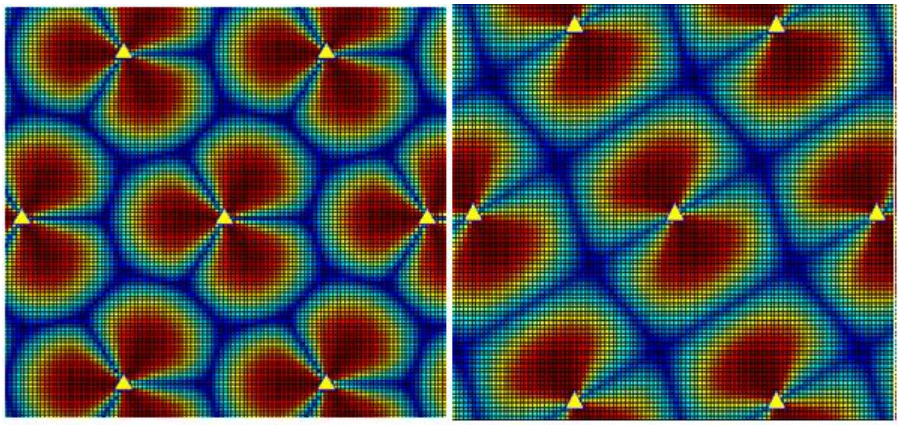

FIGURE 42. SINR map.

Establishing a practical and accurate power model is essential to the evaluation of energy saving. In [EARTH-D2.3], a well defined macro cell power model based on measurement is presented, where the power consumption in Watts is estimated individually for each sub-system. One BS consists of PA, main supply, DC part, RF link, base band and cooling equipment. If one sector is switched off, the energy saving is not straightforward 1/3. PA and RF link consumption can be reduced by approximately 1/3. The other power consumption associated with DC, baseband processing and cooling will not be significantly reduced. Succinctly, the overall power consumption can be reduced by approximately 21%.

Turning off one sector not only brings the coverage problem, it also increases the traffic demand of the remaining active sectors due to the new users handed over to them and might increase the blocking probability. To analyze this problem, we need to establish an event based traffic model instead of a full buffer model. Here we assume that the user arrival process is a continuous-time Markov process with rate λ_s. Each user can generate multiple data connections with certain amount of data to transmit, arriving according to Poisson process with rate λ_d. For s users the data connection arrival rate is $s\lambda_d$. This traffic can be modelled by a MMPP/M/1/D-PS queue (a single-server Processor Sharing queue, with MMPP arrival process, Markovian service time) as in [NeierH1989] and [SinDat2004]. We define the situation that a new user cannot be registered or a new data connection cannot be admitted as a blocking event.

As shown in FIGURE 43, the user arrival rate per km^2 is changing in the temporal domain. Note that since the data connection arrival rate is constant, the temporal traffic variation is purely demonstrated by the fluctuation of the user arrival rate per km^2. When the traffic demand in terms of user arrival rate is low, one sector is switched off to save energy. The coverage area of the remaining two sectors is then increased to 1.5 times of its original size, which means that the user arrival rate for each active sector is 1.5 times of its original value now. In the mean time, the average system throughput is degraded. As a consequence, the blocking probability increases. However, if we carefully choose the switching off point, we can guarantee that it is still below the target value. Apparently, the longer the sector is silent, the better energy efficiency we can achieve. Actually, the switching point is chosen where the blocking probability is exactly the same as the target value to maximize the energy saving. We define the energy saving ratio μ_{sav} as the ratio of the overall system energy consumption with sectors switching off over that without switching off. The results show that if we do not switch off sectors when the traffic demand is low, the blocking probability is unnecessarily lower than the target, which means that resources are actually overpaid to provide much better QoS than expected. If we switch off one sector, the two active sectors are now serving all the users and there is a jump for the blocking probability because of the sudden increase of the user arrival rate. However, as we mentioned, by wisely selecting the switching point, the blocking probability is still below the

target. If we do not change the beam-width of the remaining sectors, the users in the silent sector suffer from weak received signals and therefore the coverage target cannot be achieved. On the contrary, if we employ the adaptive sectorisation by widening the beam-width, the coverage level is well maintained (just 1% reduction). The overall energy consumption is saved during the silent period of sector 1 (from time h2 to h18, total 16 hours). Generally speaking, the overall energy consumption can be saved about 13% in each day (from h0 to h24).

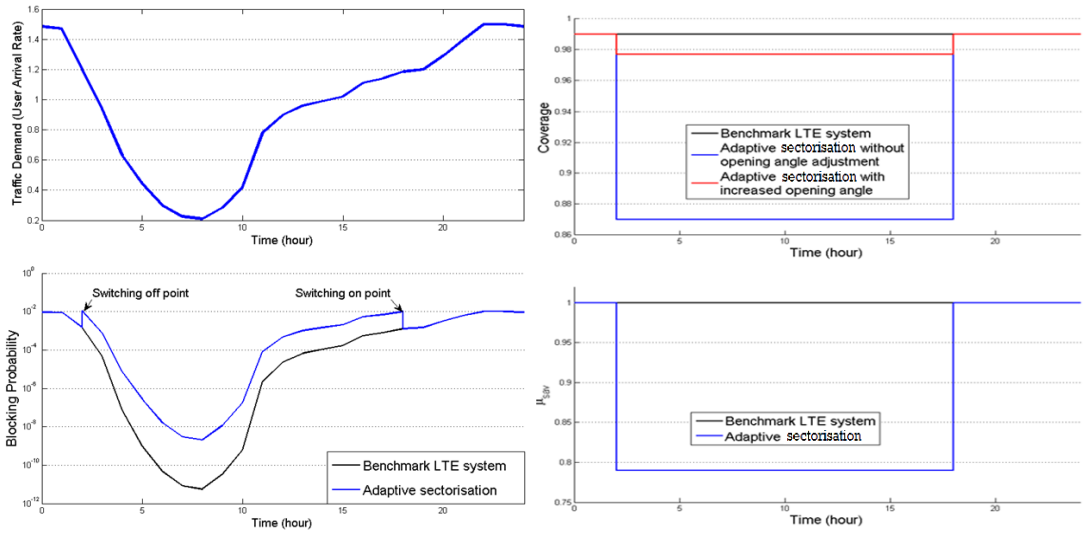

FIGURE 43. Traffic demand, blocking probability, Coverage and μ_{sav}.

7.2.2. A fast algorithm for dynamic sectorisation of base stations

The main objective of mobile operators is to maintain a guaranteed service level over the service area possibly in busy hours as well; hence the perceived user performance should be the conditional target of any network optimization including the optimization of energy efficiency. So cells, sectors, or radio resources in general, can be switched to low-power modes only if network throughputs are expected to remain safely above target level. In the same time, radio resources should be reactivated upon detecting that user throughput drops below target level.

We have compared three network configurations to analyze the impact of dynamic sectorisation on energy consumption and performance. These scenarios are: a) all BSs are always in 3-sector mode, b) all BSs are always in omnidirectional (1-cell) mode and c) when the mode of each BS is adaptively switched between omnidirectional and 3-sector depending on the system load. A dynamic LTE simulator was used to compare the three configurations. The creation, motion and traffic demand of users were identical in the simulation scenarios, while the performance (the number of completed download sessions and the achieved session bit rates) depended on the particular scenario. First the adaptive switching algorithm is described, and then the performance comparison is presented.

Adaptive sector switching

We propose a closed-loop control mechanism to switch between 3-sector and omnicell mode. The algorithm can work autonomously in each BS and it requires the following two measurements from all active cells as input: a) the average number of users with active buffer content and b) the median of buffer serving rates at medium access control (MAC) level. The operation of the algorithm is as follows:

- An omnicell BS is upgraded to a 3-sector BS if the omnicell cannot schedule all users and, in average, more than 1 user remains in the queues after scheduling and, at the same time, the median MAC-layer serving rate in the omnicell is below a predefined threshold, e.g. 1 bps/Hz.

- A 3-sector BS is downgraded to an omnicell if all users can be scheduled and, at the same time, the median serving rate at MAC level is above 1.5 bps/Hz. One of the two conditions should be fulfilled in all 3 cells in order to trigger the desectorisation of BS.

FIGURE 44 (a) shows the MAC-level service rate and the sector switching control signal for one particular BS in the network. FIGURE 44 (b) shows the corresponding load in the main (non-switching) and its neighbour (switching) cells. The switching algorithm is based on these two measurements.

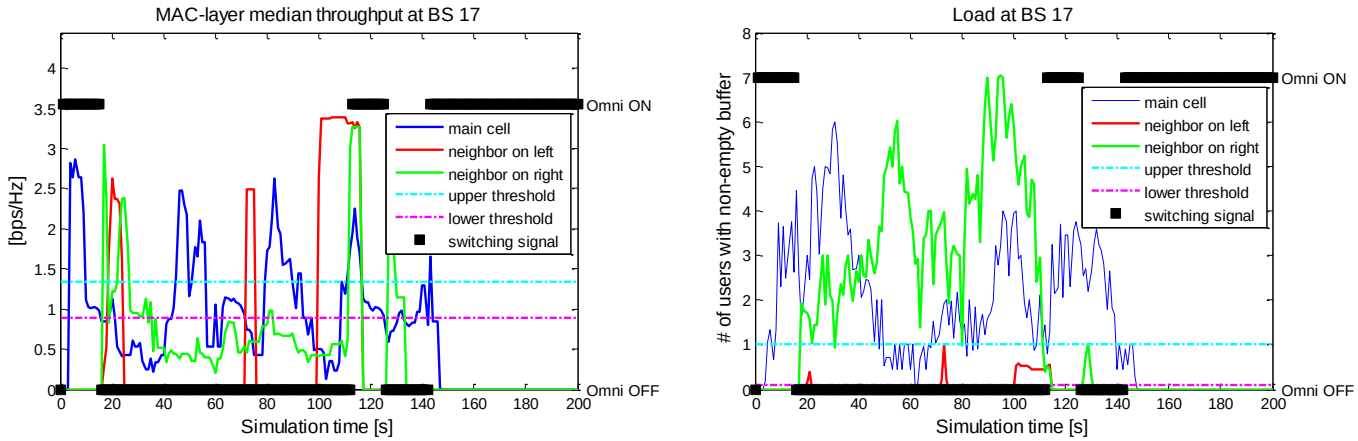

(a) The MAC layer service rate for the 3 cells of a BS in the network.

(b) The corresponding load measurements for the same cells.

FIGURE 44. Cell level analysis of switching pattern.

Performance evaluation

The simulation experiments are implemented in a dynamic LTE simulator over a 19 x 3-cell homogenous layout with an ISD of 1500m. The spatial and temporal traffic variation is induced by a group of users moving across the arena with the same motion in all scenarios. The users repeatedly conduct file transfer protocol (FTP) downloads of 1 MB files, and the sum traffic offered to the network is according to the typical daily variation. Consequently, the download service rates often cross the throughput thresholds that are established for sector activations and deactivations.

The reference case is the scenario with constant, 3-sector BSs. The fully-powered radio network obviously provides the best performance among the tested configurations and the goal is that the network with dynamic sector switching approached this level of performance with less power, by saving the power consumption of 2 radio units on desectorised BSs. The third scenario, where all BSs are in omnicell mode, is also examined in order to obtain the worst-case performance as reference.

FIGURE 45 (a) shows the network performances in the three scenarios, i.e., the number of completed download sessions (x-axis) in ascending order of session throughput (y-axis). The more download sessions are completed, the better the network performance is. A wide range of session bit rates occurs in all 3 scenarios, since the load in individual cells varies between extreme values both in time and space. There are always cells with heavy and light load regardless of the particular network configuration.

The achieved bit rates in the dynamic sector switching and constant 3-sector simulation scenarios are identical up to session throughputs of 1.8 bps/Hz, and there are only slightly fewer high-speed downloads in the dynamic sector switching scenario than in the 3-sector BSs scenario. This indicates that mostly the well-situated users are impacted, but they still receive good service quality. With slightly fewer peak-rate users, the overall network performance expressed in the number of completed downloads slightly drops compared to the constant 3-sector scenario. So compromising the peak-rates in the network is the price paid for the energy savings.

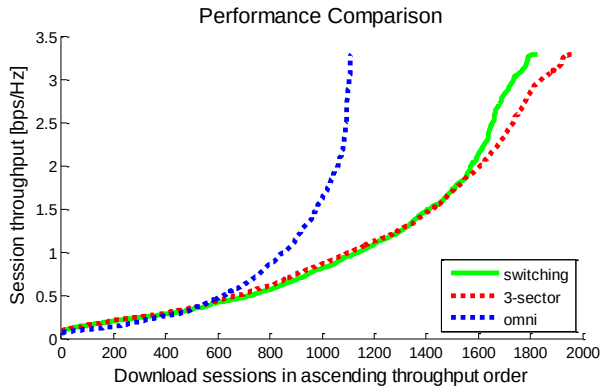

(a) Performance of dynamic sectorisation.

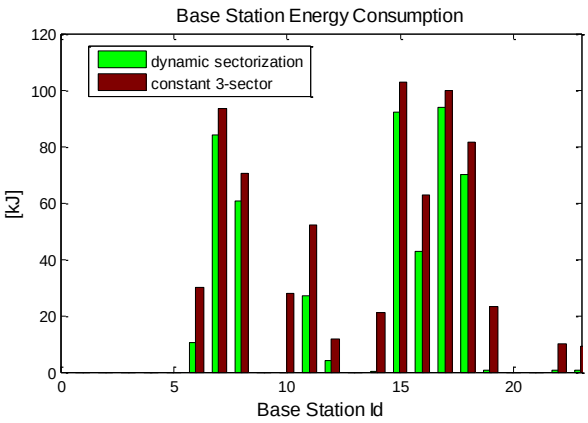

(b) Energy consumption with dynamic sectorisation.

FIGURE 45. Analysis of performance and energy consumption with dynamic sectorisation.

FIGURE 45 (b) compares the energy consumption of BSs in the dynamic switching and constant 3-sector scenarios. The estimates are based on the evaluation framework and macro base-station reference power model proposed by the EARTH project [EARTH-D2.3]. The temporal and spatial variation of network load strongly influences the achievable power savings. So in the presented example, only the BSs and only the service periods that have active user connection are counted. The adaptive sectorisation results in a power savings of 30% on network level (see FIGURE 45 (b)), while the compromise in peak bit rates causes a drop of 7.6% in system throughput meanwhile having negligible impact on average users.

7.3. CELL ON/OFF SWITCH SCHEMES IN SINGLE-LAYER NETWORKS

In this section, we introduce how to save power by switching off a number of BSs when the load conditions are such that the BSs remaining on can serve the demands from the users. The viability of turning off BSs relates to the dense BS deployment that is done in order to be able to cope with the peak-traffic demands. In these cases the coverage is not limited by the transmit power. Cell sizes are deliberately reduced since the limiting factor is the BS capacity and not its power budget. Upon application of this management scheme the users in the coverage of sleeping BSs can be served by the remaining active BSs which only have to increase in a few watts the emitted power, something negligible in the total BS energy consumption. The scheme proposed would allow configuring, on a given network and taking into account the traffic profile this network has to handle, a number of sites that can be put into idle mode. While powering down completely a BS accounts for an important save in terms of energy, the power increment that is necessary for the BSs that remain active to compensate the absence of switched off sites in terms of geographical coverage is negligible. Since the optimal configuration can be defined in advance based on system layout, no further coordination is necessary between BSs but defining which BSs have to go down and when they have to power down and up.

It is quite important to keep in mind that in real networks it is not possible to switch off any random number of BSs, but it is restricted by their configuration. This study uses a few typical schemes for geometry and site positioning, proven valid upon results obtained after going through several theoretical studies. Working with hexagonal cells, omnidirectional antennas and Macro BS, the analysis will be focused on evaluating 1/7 and 1/19 schemes. For instance, 1/7 means that in a regular hexagonal deployment a centre node is kept on while all the six surrounding cells are switched off, meanwhile the rest of the network is not affected by this operation. In [EARTH-D3.1] it has been shown that the energy saving potential of such techniques is 25%. Furthermore, the proposed scenario does not count with any fixed sectors, so it is completely decentralized and dynamic.

In order to increase the complexity and evaluate more properly the effectiveness of the proposed algorithm, improving along the way its performance, a new decision factor is introduced, consisting in a Linear Predictor which will act the moment the data curve surpasses some previously determined thresholds (corresponding to the two schemes aforementioned). In order to do so, instantaneous and historical data regarding load conditions in the network will be combined.

After collecting theoretical energy savings in simplified and linear worlds, the next step consists in evaluating what potentials are in real networks. In this study, we are focusing on a M2M environment, specifically one represented by an automotive use case, acting over the multiple vehicles that drive on a highway during a specific amount of time.

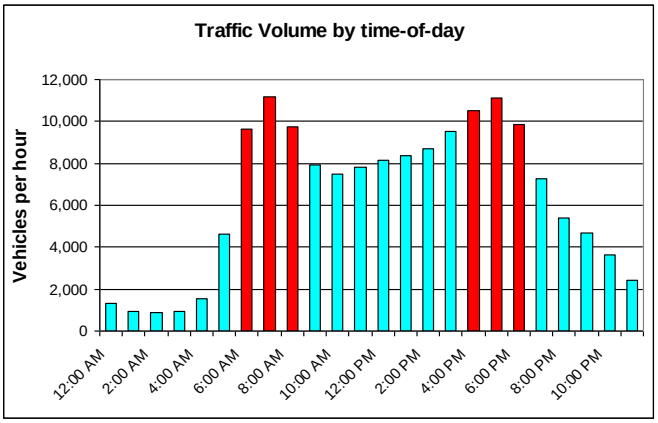

FIGURE 46. Observed number of vehicles on highway during a day © [NRC_US2010].

The idea relies on the fact that vehicle density among the day on highways follows quite a similar trend compared to data and voice calls' distribution in cellular networks (FIGURE 46). These kinds of curves are based on two peaks and two valleys during each 24 hour periods. Each peak and valley may vary its amplitude and duration depending on multiple factors. In the highway use case, for instance, there will be certain peaks quite higher and during more time on toll barriers or zones where traffic jams are most likely to occur. It is possible to simulate this behaviour and apply the dynamic ON-OFF mechanism in order to obtain the theoretical achieved savings derived from its application and evaluate the convenience of deploying this solution in the real world.

Envisaged practical use cases have been simulated trying to adjust the behaviour of a network of 17 cells to a highway use case. Two main use cases have been simulated so far

- The first one emulates a flat distributed traffic scenario. That means that each cell is supposed to carry the same traffic as its neighbours. This way, the selection of 7-cell cluster is totally flexible, and all possible groups of cells have the same probability to be switched-off. The expectations consist in obtaining the best saving under these constraints. Very high traffic curves are the ones selected for performing the simulation.
- Trying to study in depth the possibilities of this scenario, some new constraints are added, like including a couple of toll barriers in the road, as seen in FIGURE 47, which lead to new results but not so different as the ones previously noted, since there are still important savings peaks in certain cases. Four different cell models have been taken into account, depending on the envisaged vehicle traffic they are supposed to handle during the day:
    - Very High traffic cells, corresponding to those cells adjacent to toll barriers. They will support the normal traffic of the highway plus potential traffic jams on busy hours due to the delay introduced by people paying at the barriers. This constraint is simulated with higher throughputs (up to 120Mbps) and longer lasting peaks (about two hours).

- High traffic cells, matching the standard highway cells. They will carry out the daily traffic of the road, but they are not likely to support traffic jams, as they are not close to the barriers. In order to simulate that situation, peaks up to 100 Mbps lasting for 1.5 hours have been introduced on the software.
- Low traffic cells, simulating the behaviour of secondary roads or entrances/exits to the highway. On this kind of cells, the amount of traffic is clearly lower than the one in the highway case. Thus, the parameters introduced for emulating these cells are 70 Mbps maximum curves with just 1 hour lasting peaks.
- Very low traffic cells, corresponding with cells with no roads. On that situation, only the traffic generated by walking people will be carried out. Curves up to 60 Mbps and half an hour lasting peaks are used as model.

In accordance, four different traffic load curves have been employed, modelling the behaviour and trend followed by the diverse cell types present in the scenario. They all respect the characteristics observed in real world measurements and are depicted in FIGURE 47.

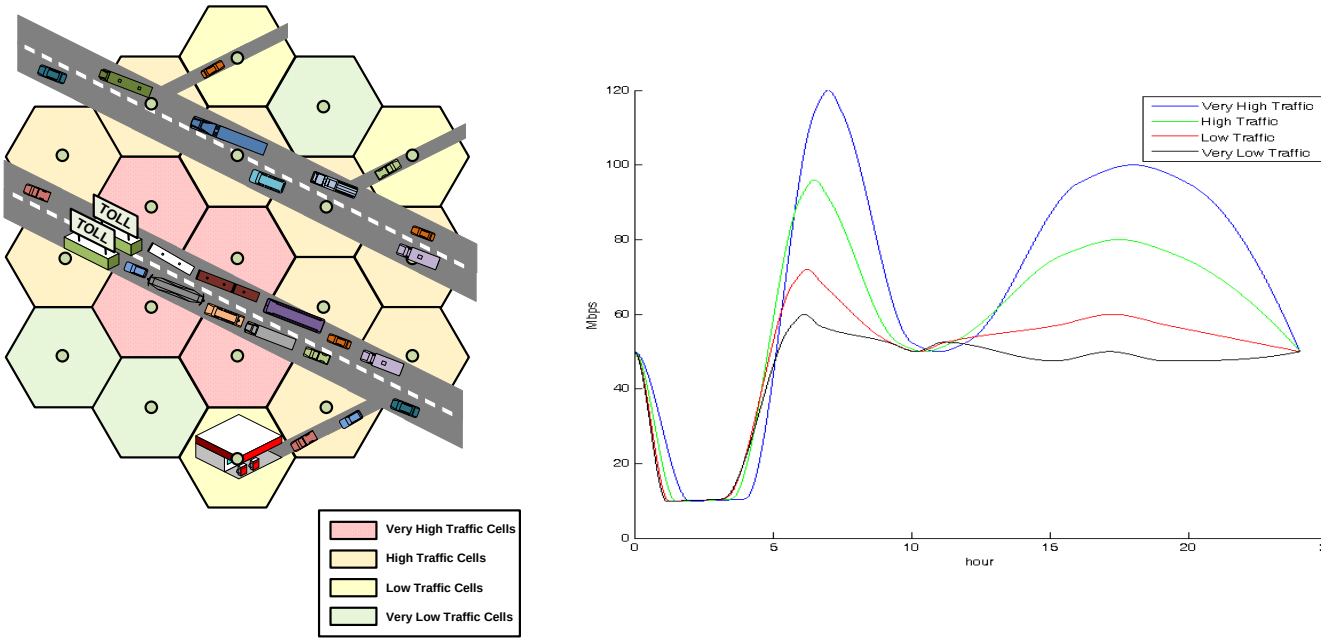

FIGURE 47. Different cell classification on the simulated scenario and their corresponding curves.

As an extra constraint, trying to adjust the simulations to a real behaviour, random noise is introduced on each curve. This random noise will introduce changes on the amplitude of the signal (it can decrease the maximums up to 75% of its value) and short time variations on the signal, simulating the real-life bursty curves related to data traffic.

The results showed that up to 25% peak energy saving can be achieved (on the homogeneous cell type distribution, and slightly less percentages when using the 4-kind approach), meanwhile the average areal energy saving is 14% in the case of the aforementioned randomized daily traffic curves. These results are very similar to the ones obtained when using voice or data traffic, so we can conclude that this particular application handling data traffic from vehicles on a highway is suitable to implement ON/OFF schemes.

The way forward implies a deeper investigation in these real world behaviour constraints and how they have any influence in the algorithm performance and what is more in the achieved savings. Moreover, some other M2M use cases (different from this one of automotive) could be considered. The best preliminary candidates may be:

- Smart metering use case, on specific human-oriented applications (periodic sampling is not a valuable use case as the ON/OFF would not be able to use any low-load period).
- E-Health, as the info transmitted is more likely to follow similar trend curves as the ones used for data calls.

In addition, it is worth noticing the necessity to address the issue raised by operators regarding the kind of information that should be distributed among the neighbouring nodes when the ON-OFF scheme is applied. In a first approach, it could be solved as long as the deployed algorithm includes some data in charge of updating the tables stored in each node, acting over the decisions taken by the RRM.

7.4. CELL ON/OFF SCHEMES IN HETNET AND MULTI-RAT NETWORKS

7.4.1. Efficiency Analysis of HetNets

The traffic and MBB penetration in cellular mobile radio networks greatly increases year-by-year, so the HetNets are in the focus of network modernization especially in densely populated urban environments. In such networks there is a *coverage layer* dimensioned basically to serve conversational services and low data traffic, and a *capacity layer* dimensioned to serve high data traffic demands and large user throughput. As a consequence, if the coverage layer forms a solid layer covering the given urban area, then one can expect that the capacity layer in most of the time is inevitably underutilized [VidGod2011]. The system model can be seen in TABLE 5 assuming three different levels of MBB penetration to be served by the capacity layer, i.e., 25%, 50%, 75% (corresponding to low, mid and high scenario) and the population is served by 3 operators. We have compared how much impact the capacity of coverage has, so we have compared 1Mbps (today's requirement) and 100kbps (limited to background traffic by that the coverage layer could be greatly reduced).

TABLE 5. HetNets coverage and capacity layers' system parameters.

Layer	BS type	System, band	Cell edge requirement	Served users by the layer	ISD
Coverage layer	3-sector macro	HSPA, 900 MHz	1 Mbps	75%	292m
				50%	357m
				25%	500m
			100 kbps	75%	848m
				50%	982m
				25%	1212m
Capacity layer	omni micro	LTE, 2100 MHz	10 Mbps	25%	128m
				50%	112m
				75%	104m

In order to evaluate how much the capacity layer of the HetNet is utilized, besides system model the users' distribution needs to be modelled, as well. Two distributions are considered, namely, the homogeneous and the inhomogeneous user distributions. The homogeneous spatial user distribution in the area is modelled as a homogeneous Poisson point process, while the inhomogeneous case is modelled according to a modified Matern process [StLeHe+2002]. In the Matern process cluster centres are determined first according to a homogeneous Poisson process. Then, the number of points (i.e. users) around each cluster centre is again Poisson distributed, and these points are uniformly distributed within a predefined radius around the centre (e.g., with 80m^2 cluster/hotspot size in our case, like the size of a café). It can be shown that the probability that a cell does not contain active users in the inhomogeneous case (P_I) is always below than that of the homogeneous case (P_H), and a lower limit for P_I compared to P_H is $P_I \approx 0.63\ P_H$. Given that how many cells of the capacity layer are empty (i.e., there is no user to be served) at a given time, it can be calculated that how much of the sites can be put into power saving mode. The daily average and peak utilizations as network average measures are given in TABLE 6.

TABLE 6. Utilization of small cells and energy saving potential by switching off empty small cells.

User distribution	Scenario	Utilization of capacity layer		Energy saving							
				1Mbps in coverage layer				100kbps in coverage layer			
				Macro normal		Macro RRH		Macro normal		Macro RRH	
		Daily ave.	Peak hour	Daily ave.	Peak hour	Daily ave.	Peak hour	Daily ave.	Peak hour	Daily ave.	Peak hour
Homogeneous	Low	33%	51%	25%	17%	32%	23%	56%	41%	59%	44%
	Mid	45%	67%	29%	17%	35%	21%	49%	30%	51%	31%
	High	53%	75%	34%	17%	38%	20%	44%	23%	45%	24%
Inhomogeneous	Low	31%	44%	26%	19%	33%	26%	58%	46%	61%	49%
	Mid	40%	54%	32%	23%	39%	28%	54%	41%	56%	43%
	High	45%	59%	40%	20%	44%	32%	51%	38%	52%	39%

It can be seen that more than half of the cells are empty on average and even in peak hours a great portion of the cells are not utilized. There is also significant difference between homogeneous and inhomogeneous user distributions. That is, the utilization of nodes in the inhomogeneous case is 2-8% less in daily average and 7-16% less in peak hours compared to the homogeneous case.

Based on the above utilization figures and the EARTH linear BS power model (see [EARTH-D2.3]), the energy saving potential by switching off empty small cells of the capacity layer is shown in TABLE 6 including both the traditional macro coverage and the macros with RRH. Depending on the capacity of the coverage layer, one can achieve 25-40% or 44-58% areal energy saving in 1 Mbps and 100 kbps cell bitrate guaranteed coverage layer, respectively. Note that relatively more gain can be achieved in case of RRH (up to 7% on daily average), since in that case the energy consumption of the coverage layer is greatly reduced, so any adaptive reduction of the capacity layer has greater impact on the total system wide energy consumption.

The above results illustrate that if the coverage layer is not limited to some very specific hot spots, but forms a solid layer covering an urban area, then considerable energy can be potentially saved not just in daily average, but even in peak hours.

7.4.2. Operational proposal and implementation aspects

In order to efficiently switch on and off the small cell of the capacity layer, the network management system should collect information about the position of the users. The source of this information is based on whether

- Capacity cell is active: if the load in an active cell drops below a given level, or there are no active users in the cell, then management system can hand over the inactive and low-traffic users to the coverage layer and switch off the particular cell.
- Capacity cell is in sleep mode: if the load in the coverage layer is high and the position of the users identifies a given sleeping cell, then the management system should wake up the sleeping cell and hand over the active users this cell. (Note it is enough to identify the position of the users in the "granularity" of the capacity layer.)

3GPP has introduced X2 control plane functions dedicated to energy saving [3GPPTS36.300]. This function allows decreasing energy consumption by enabling indication of cell activation/deactivation. Two functionalities can be used as primary functions indicating sleep mode to neighbouring cells and requesting waking up sleeping cell. Note that 3GPP uses the term "dormant" for sleep modes. These procedures are illustrated in FIGURE 48.

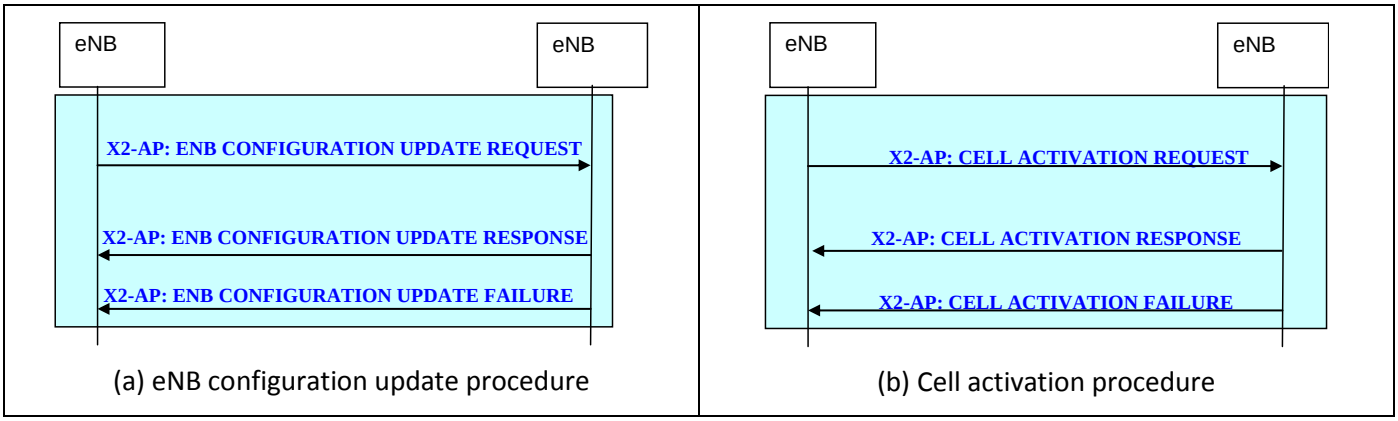

FIGURE 48. Configuration and activation procedures

Cell switch-off

The decision on cell switch-off is typically based on cell load information. The eNB may initiate handover actions in order to off-load the cell being switched off and indicate its reason. All peer eNBs are informed by the eNB owning the concerned cell about the switch-off actions over the X2 interface, by means of the eNB Configuration Update procedure.

The **eNB Configuration Update procedure** is illustrated in FIGURE 48 (a). The purpose of this procedure is to update application level configuration data needed for two eNBs to interoperate correctly over the X2 interface [3GPPTS36.300]. This procedure also includes the indication of cells entering dormant state for energy saving purposes [3GPPTS36.300].

The details of the ENB CONFIGURATION UPDATE, ENB CONFIGURATION UPDATE ACKNOWLEDGE and ENB CONFIGURATION UPDATE FAILURE messages can be found in [3GPPTS36.423].

Cell re-activation

ENBs may request a cell re-activation over the X2 interface if capacity needs in their cell(s) demand to do so. This is achieved via the *Cell Activation procedure*.

The **Cell Activation procedure** is illustrated in FIGURE 48 (b). The purpose of this procedure is to enable an eNB to send a CELL ACTIVATION REQUEST message to a peer eNB to request the re-activation of one or more cells, controlled by the peer eNB and which had been previously indicated as dormant. Upon receipt of this message, the peer eNB should activate the cell/s indicated in the CELL ACTIVATION REQUEST message and shall indicate in the CELL ACTIVATION RESPONSE message for which cells the request was fulfilled.

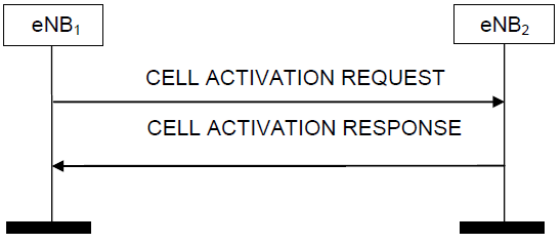

Upon receipt of this message, eNB2 should activate the cell/s indicated in the CELL ACTIVATION REQUEST message and shall indicate in the CELL ACTIVATION RESPONSE message for which cells the request was fulfilled. If the eNB cannot activate any of the cells indicated in the CELL ACTIVATION REQUEST message, it shall respond with a CELL ACTIVATION FAILURE message with an appropriate cause value.

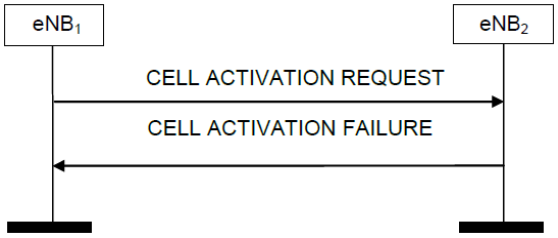

All peer eNBs are informed by the eNB owning the concerned cell about re-activation by an indication on the X2 interface.

The details of the CELL ACTIVATION REQUEST, CELL ACTIVATION RESPONSE and CELL ACTIVATION FAILURE messages can be found in [3GPPTS36.423].

Note that above described framework can be applied to the generic cell ON/OFF techniques described in Sections 7.2 and 7.3 after the appropriate technical changes.

8. ADAPTIVE SCHEDULING

Traditionally, RRM is concerned with maximizing outcome in terms of user satisfaction at a fixed power cost using a set of levers that include transmit power, radio channels, transmission delay, modulation or coding. In contrast, 'green' RRM provides fixed outcome at a minimal power cost leveraging the same set of parameters. Most existing RRM strategies and algorithms are designed around the full load or peak traffic assumption. They apply when large numbers of terminals are competing for high data rates. In fact, some techniques specifically address situations in which the capacity requirement is higher than the available capacity (overload). While these techniques can still be applied in low load they carry little benefit in this setting and does not address power consumption. In contrast, an RRM strategy that is sub-optimal or spectrally inefficient at high loads may be able to fulfil capacity targets at much higher EE. In this section, we approach green RRM from four points of view:

1. In the first approach, we exploit the dynamics in scheduling by putting the BS in sleep mode by utilizing MBSFN frames, where we can potentially disable both Data and Control signalling. This approach is very useful as it is backward compatible with LTE standard. The main idea here is to dynamically configure the MBSFN frame ratio according to the traffic conditions. The more the traffic, the lesser is the ratio of MBSFN frames whereas we utilize more MBSFN frames without data/control signalling in lightly loaded scenarios. This scheme can bring about a gain of about 20-30% with respect to the scenario where no MBSFN scheduling is used in terms of Joule/bit.

2. In the second approach, we propose algorithms utilizing adaptive DTX and power control where we study techniques such as using sleep modes or reducing transmit power or combinations of both. The proposed technique can have a gain of as much as 45% with respect to the case when no power control and DTX is used especially in very low load scenarios and this gain decreases linearly with the traffic load of the system.

3. In the third approach, we trade-off SE with energy efficiency especially in lightly loaded scenarios. In particular, we exploit the delay characteristics of a specific application to reduce the transmit power. Such a technique increases the delay experienced by the application, but this is acceptable as long as it is within the delay constraints of the QoS requirements. This approach can bring about gains from anywhere from 0-20% with respect to the case when no adaptive scheduling is used depending on the traffic load in the system.

4. Finally, we approach the RRM from the multi-RAT management point of view. Since, different RATs have different energy efficiencies of delivering their payloads, it is quite obvious that there exists a trade-off in which we can adapt the users camped on a particular RAT based on the traffic load of the system. The main idea here is to use vertical handovers (VHOs) to migrate users from one RAT to another depending on the traffic load of the system. Such a dynamic migration of users can bring a maximum gain of about 45% with respect to the scenario in which we don't utilize inter-RAT handovers for improving EE. The gains from such an approach come mostly in low traffic scenarios.

8.1. EE SCHEDULING FRAMEWORK BASED ON MBSFN SUBFRAME SWITCHING

In this work, we study an adaptive scheduling algorithm able to exploit the system dynamics in order to provide an improvement in terms of energy efficiency, working at a millisecond timescale. Lessons learned from past simulations showed that there is a fundamental trade-off between fairness (or, in general, QoS) and Energy Efficiency [EARTH-D3.1]. In particular, we showed with the help of dynamic system level simulator in a multi-cell environment that at full load the energy efficiency of the system (expressed in [J/bit]) is limited by the SE (depending on the adopted packet scheduler). In particular, at full load conditions simulation results showed good

performances of Max carrier-to-interference ratio (C/I) scheduler in terms of both spectral and energy efficiency (while the counterpart is offered by the fairness); in this sense, when comparing different scheduling algorithms both aspects (J/bit metric minimization and fairness/QoS guarantee) should be taken into account. For that reason, an additional $ECI_{[W/user]}$ metric is considered when assessing the system performances, expressed in terms of consumed power per satisfied user ([W/user], where a satisfied user is defined as a user for which QoS requirements are fulfilled by the system [EARTH-D2.4]. For the scope of the present study we consider all different load conditions present in the daily traffic variation, and it is worth noting that these considerations (valid for full load) can be applied also in other specific conditions: in fact, also when the average cell load is low, it can happen that instantaneously the traffic present in users queues can be enough to fill all resources available in one or more adjacent subframes, so that in these intervals the scheduler works at saturation point (i.e. in similar conditions w.r.t full load). More general, the instantaneous scheduler behaviour is conditioned by this particular traffic (and channel) situation, and due to the bursty nature of several traffic sources, an instantaneous saturation condition could be experienced even with just one active user. Following these considerations the idea is to design an adaptive scheduling algorithm, able to react to dynamic traffic conditions and provide the best instantaneous energy efficiency (at even lower and higher loads), while guaranteeing the quality for the users present in the system (not only long term fairness, but also short term QoS requirements).

Moreover, in order to enhance the scheduler performances in terms of energy efficiency, a solution aware of the hardware capabilities is seen as promising, especially if the algorithm is able to trigger special saving features according to instantaneous scheduling decisions. In particular, in the context of the present study the impact of a potential MBSFN switching mechanism has been investigated in terms of energy savings achievable by means of the triggering of sleep mechanisms during the data region of MBSFN subframes (containing neither cell specific reference symbol (CRS) nor data). Let us note that the assumption to consider this kind of sleeping conditions is seen as realistic and practically feasible already from first LTE equipment availability, in analogy with switching time requirements present in 3GPP specifications [3GPPTS36.104] for LTE time-division duplex (TDD) system (about 17 μs for both on-off and off-on transitions).

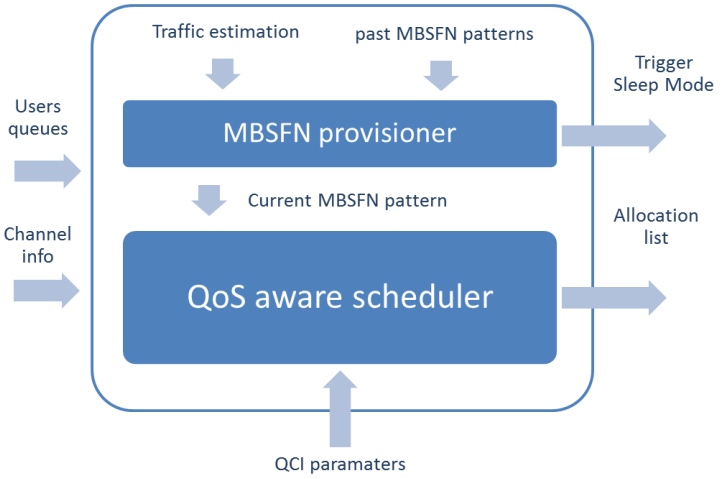

FIGURE 49. Overall architecture of the EE scheduling framework.

The proposed overall EE scheduling framework (depicted in FIGURE 49) is composed of two functional blocks (described in the following subsections): the first block called *MBSFN provisioner* (performing the MBSFN subframe switching mechanism and providing the triggers to sleep mode events), and the second block (the *QoS aware scheduler*) having in charge the maximization of EE/SE mitigated by a proper QoS management (and subjected to the specific MBSFN subframe switching decisions provided by the first block).

8.1.1. MBSFN provisioner

This block aims to maximize savings by allocating the maximum possible number of MBSFN subframes, according to traffic estimation and feedback coming from past switching decisions.

Regarding the MBSFN operation in a Rel.8 eNB and related time granularity, MBSFN subframes can be signalled via radio resource control (RRC) within a period of 4 radio frames (corresponding to an interval of T = 40 ms). FIGURE 50 shows two possible examples of MBSFN patterns, where at most 6 subframes over 10 are eligible for MBSFN operation (these subframes can be either active or inactive).

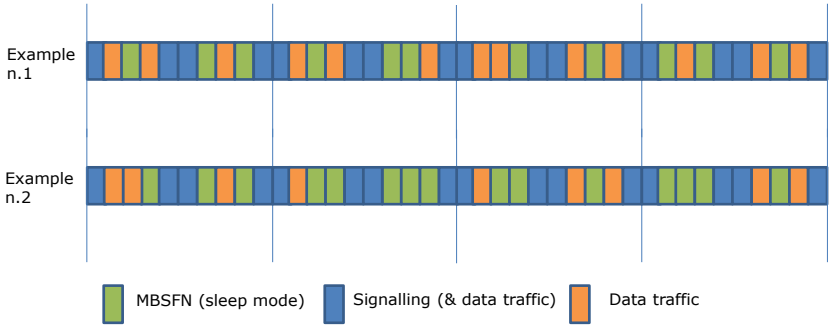

FIGURE 50. Examples of MBSFN provisioning in a period of 4 radio frames (T = 40 ms).

According to current 3GPP standards [3GPPTS36.331], MBSFN switching can be applied in a semi-static way, i.e. by providing updated MBSFN patterns with a period that depends on the UE RRC state:

- for RRC_IDLE terminals, the shortest time possible to change an MBSFN configuration is every 640 ms (modification period), linked to the UE reception of change notification via paging messages;
- RRC_CONNECTED terminals will be able to read more frequently the information, at least every 80 ms, i.e. the minimum period of scheduled system information (SI) message, always readable since transmitted in downlink shared channel (DL-SCH).

In general the optimal choice of MBSFN pattern depends on two main factors: on one hand packet arrivals vary over time, both because the number of traffic sessions changes in time and because traffic flows are inherently non-homogeneous (e.g., compressed multimedia flows, web browsing, etc.); on the other hand UE channel status (hence the transmission rate to each UE) varies as well; this may also influence the arrival rates in some cases (it is in fact well known that transmission control protocol (TCP) sources adapt to the available bandwidth). In this sense a dynamic MBSFN switch is seen as promising, but it would imply the need to consider more advanced mechanisms also at scheduler level (e.g. for managing Rel. 10 terminals, while keeping backward compatibility with legacy terminals) or even a possible impact on standardization (Rel. 11) in order to foresee additional messages to dynamically signal MBSFN pattern switch.

8.1.2. QoS aware scheduler

The goal of the scheduling block is to allocate system resources according to constraints provided by the first block (that introduces a piloted saturation point for the scheduler). The idea is to consider a Max C/I–like tuneable algorithm able to, on one hand, efficiently allocate system resources at saturation point in order to properly manage traffic peaks (while taking into account the QoS, according to operator's policies), and on the other hand, capable to concentrate scheduled resources in few subframes, in order to enable as much as possible the exploitation of sleep modes present at the transmitter of the eNB [EARTH-D4.2].

From the scheduler point of view, the provisioning of a particular MBSFN pattern correspond to a limitation of system resources, and for that reason the provisioner is driven by an adaptive traffic estimation, in order to avoid imposing too stringent constraints to the scheduler. On the other side, the scheduler itself is designed to work especially in saturation conditions (where optimal resource exploitation is more challenging). In other words, the

two blocks can be seen as two complementary parts of an overall scheme designed to improve the EE of the system while taking into account QoS requirements.

8.1.3. Current Results

System level simulations have been conducted in an Urban Macro scenario and at different traffic levels, considering for each case a different number of video streaming users in the LTE system (traffic characteristics are listed in TABLE 7 below).

TABLE 7. Simulation parameters.

parameter	value	comments
Simulated system	LTE, 10 MHz	
Number of antennas	2x2	Rank adaptation (TxD, SM)
Time windowing for MBSFN switching	80 ms	Rel.8 switching mechanism, users in connected state
Traffic type	Video Streaming	
Coding format	MPEG-4	Trace length = 1213 s
QCI index	6	(see [3GPPTS23.203])
Packet Delay Budget (PDB)	300 ms	< 100 ms for a better quality
Typical Data rate	168 kbps (low resolution) 307 kbps (high resolution)	

Simulation results showed that the proposed scheduling framework is capable to provide capacity performances similar to Max C/I (by definition the most efficient scheduler) while guaranteeing QoS requirements and giving significant energy savings, especially in low load conditions (see FIGURE 51 showing the trend of the ECI expressed in terms of $ECI_{[J/bit]}$ metric).

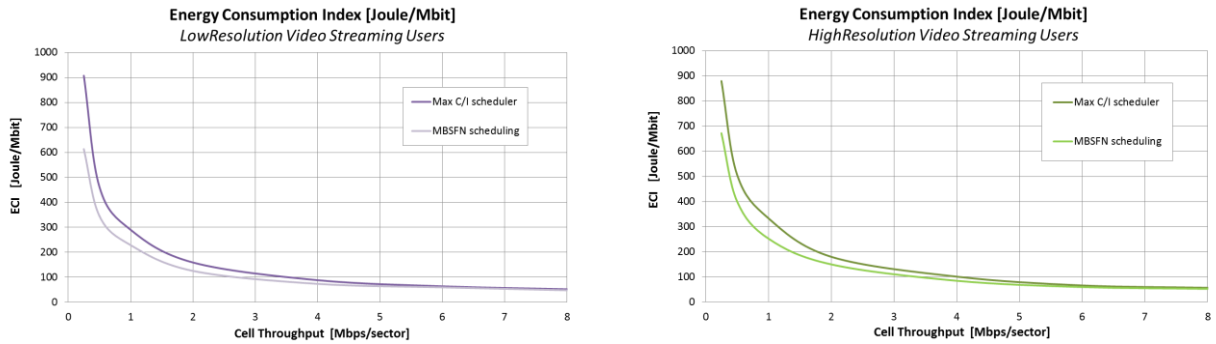

FIGURE 51. ECI of the proposed MBFSN scheduling framework (low and high resolution video streaming users).

In particular, it can be seen that at very low load (i.e. 0.25-0.5 Mbps/cell) the proposed scheduling framework provides EE gains (see FIGURE 52 below) of about 20-30% in terms of [Joule/bit] metric, corresponding to the 57% of sleep subframes activated in the system.

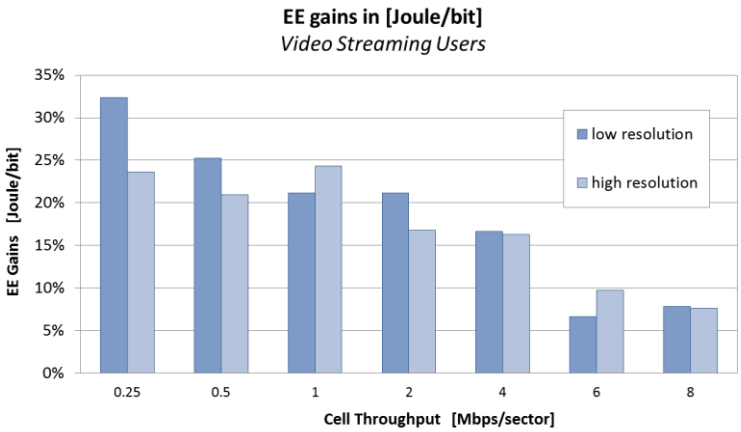

FIGURE 52. EE gains (expressed in [Joule/bit]) with respect to Max C/I scheduler

When considering also the additional $ECI_{[W/user]}$ metric already introduced in [EARTH-D2.4], the total number of satisfied users is taken into account, giving also an implicit guarantee of the fairness of the system. FIGURE 53 shows that EE gains computed with this metric are about 25% at low loads (as for the $ECI_{[J/bit]}$ metric) and decrease at higher loads, even giving a more stable trend with respect to the previous one (FIGURE 52 above).

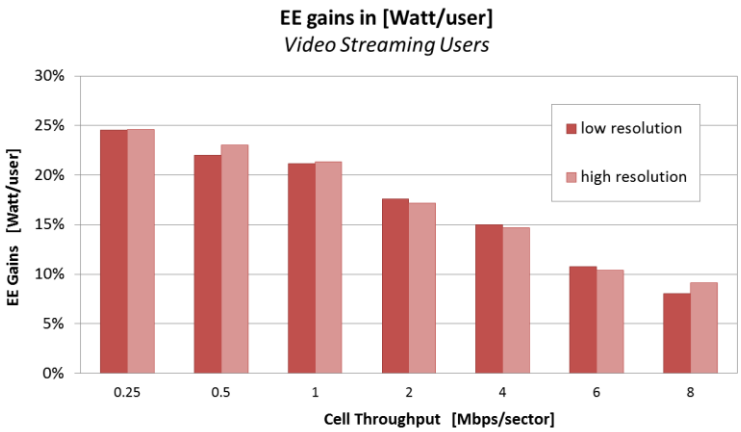

FIGURE 53. EE gains (expressed in [Watt/user]) with respect to Max C/I scheduler

In definitive, power savings techniques consisting of joint usage of micro DTX and MBSFN switching are considered as important tools in order to improve the EE behaviour at low load in first LTE deployment phases (Rel.8 compliant mechanisms).

8.2. DTX & POWER CONTROL

The EARTH power model states that overall consumption depends on the transmission power and that – when no transmission occurs – sleep mode consumption is lower than idle consumption [EARTH-D2.3]. Interpretation of this behaviour suggests two power saving strategies: Either aim for low transmission powers or for sleep modes. For a data packet, lower transmission powers can be achieved by increasing transmission duration. For sleep mode exploitation it is advantageous to have short transmission durations which allow for more time spent in sleep. In this track, the energy saving potentials of both strategies is investigated. It was found that both strategies can be optimized jointly and that in a minimum consumption solution both apply. The track described

in [EARTH-D3.1] has been extended by an analytical foundation and the extension of the two-user model to a multi-user system.

The average rate on a link i over some time interval T under optimal modulation depends on the transmission power $P_{\mathrm{Tx}} \leq P_{\max}$ and the actual transmission time t_i allocated to link i. For instance, if i=1 then clearly P_{Tx} is minimised for $t_i = T$. However, when sleep modes are available overall power consumption $\overline{P}_{\mathrm{supply}}$ (including static circuit consumption) is not minimized at long transmission times. The opposing strategy of minimising P_{Tx} is to transmit with $P_{\mathrm{Tx}} = P_{\max}$, thus minimising t_i. Both strategies can be combined into a transmission where $P_{\mathrm{Tx}} \leq P_{\max}$ and $t_i < T$. Formally, this optimization problem reads as [HoAuHa2011]:

$$\begin{aligned} \underset{\mu,\nu}{\text{minimize}} \quad & \overline{P}_{\mathrm{supply}}(\mu_i) = \left[\sum_{i=1}^{N_{\mathrm{L}}} \mu_i \left(P_0 + m \frac{N_i}{G_i} \left(2^{\frac{\bar{R}_i}{W_i \mu_i}} - 1 \right) \right) \right] + \nu P_{\mathrm{s}} \\ \text{subject to} \quad & \sum_i \mu_i + \nu = 1, \quad \nu \geq 0, \quad \mu_i \geq 0 \ \forall i \\ & 0 \leq P_i = \frac{N_i}{G_i} \left(2^{\frac{\bar{R}_i}{W_i \mu_i}} - 1 \right) \leq P_{\max} \end{aligned} \tag{8-21}$$

where m denotes the slope of the trajectory that quantifies the load dependence, $P_{\max}$ is the maximum transmit power, P_0 and P_{s} account for the stand-by and sleep mode consumption of the BS, respectively. Furthermore, t_{s} is the time spent in sleep mode, N_{L} the number of links served, target average rate $\bar{R}_i$, normalized duration $\mu_i = t_i / T$, normalized duration spent in sleep mode is $\nu = t_{\mathrm{s}} / T$, and W_i is the transmission bandwidth. The noise power is defined by $N_i = W_i k \vartheta$ with Boltzmann constant k and operating temperature ϑ in Kelvin. This problem is convex and can be solved, for example, by using the interior point methods [BoyVan2004].

This power and sleep mode allocation strategy has been simulated according to the scenarios defined in [EARTH-D2.2] and by assuming the 2010 power model and one RF chain in the BS with ten users in the system.

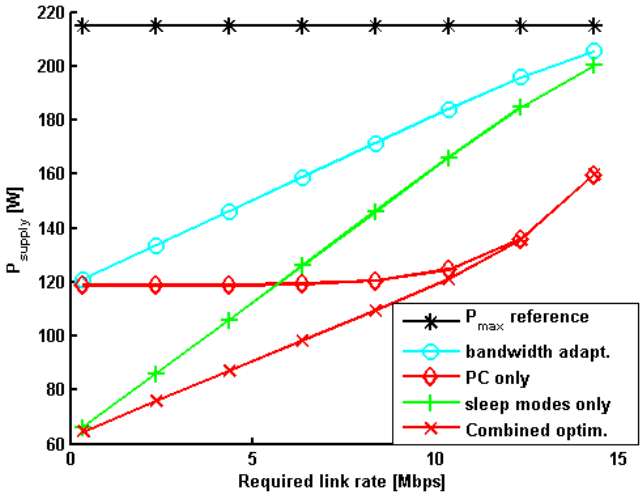

FIGURE 54. Simulation results. (Bandwidth adaptation represents a traditional BS.)

It was found that including sleep modes in the resource allocation strategy can provide large gains when low rates are required. This is due to the fact that in a very sparsely loaded system, the static consumption of a BS contribute the most to the overall power consumption and can be significantly lowered by switching to a sleep

mode. Power control (PC) is only marginally effective at low rates, since the saving potential of power control in a low-power regime is clearly limited. In contrast, at higher rates the effectiveness of power control is much larger due to the fact that transmission powers are very large in this regime and even slight adaptation can strongly affect the overall consumption. The simulation results are shown in FIGURE 54.

Although it is a promising energy saving technique, downlink power control is not available in the current standards. Here, a technical challenge is the linearity of the PA over a large range of transmission powers and the resulting adjacent carrier leakage ratio. The success of power control resource allocation strategies is therefore tightly linked to the advances in adaptive PA biasing. Until such Green Radio considerations are included, this technique may also be applied on the Uplink where power control is available, but since this is a power saving method for the mobile terminal, it is beyond the scope of this project. With regard to the applicability of sleep modes, pilot requirements in the standard have to be adhered to in order to guarantee that mobile terminals are not negatively affected. On-going work is the application of this strategy in a network simulator under the consideration of MIMO transmission.

8.3. PRIORITIZED SCHEDULING

In this section, we describe how new scheduling strategies become available when the high capacity requirement is relaxed. Low load implies unused spectrum and/or time slots which can be exploited opportunistically. Delay-tolerant data can be scheduled to radio channels which are power efficient, e.g., by the earliest deadline first (EDF) algorithm applied to OFDMA [ChiSiv1998]. EDF scheduling rule allocates packets according to their remaining time to lives (TTLs), thus granting priority to traffic flows with stringent QoS time constraints regardless to their momentary channel quality. Hence, the goal here is to reduce the overall downlink energy consumption while adapting the target of SE to the actual load of the system in order to meet the QoS requirements.

8.3.1. Algorithm Description

Detailing this idea, an efficient multi-user scheduling algorithm is designed, which can be applied to heterogeneous traffic scenarios. In [CalGre2010], the Green Scheduling algorithm is proposed which splits the resource allocation process into four steps. In the first step, it is identified which entities (packets) are rushing and which are not rushing. We classify the “rushing” users based on the TTL of the packets. In step two, the resources are assigned only to entities that have high probability of missing their QoS requirements regardless of their momentary link quality and their potential to save energy. Then, if any chunks are still unscheduled, in a third step resources are allocated to users (non-rushing) with highest momentary link quality, regardless of their QoS constraints. Finally, in the fourth step energy efficient link adaptation is performed to save downlink energy. We trade throughput (lowering the transmission SE and allocating a larger number of chunks to UEs) with downlink power by limiting the power budget on each chunk. In this way, downlink transmission power is minimized over a time window, which provides significant additional flexibility to the scheduling algorithm. In addition to throughput, both latency and SE enter in the trade-off.

8.3.2. Implementation Aspects and Operation Proposal

FIGURE 55 describes the implementation architecture for the proposed Green Scheduling algorithm. The incoming traffic for all the users arrives at call admission control (CAC), which then classifies the traffic based on the delay tolerance. After that, Green scheduling algorithm schedules the traffic to reduce the downlink transmit power, which in turns reduces the input power consumption of the base-station. The applicability of this algorithm is best at low/moderately load scenarios which have potential to trade SE with energy efficiency.

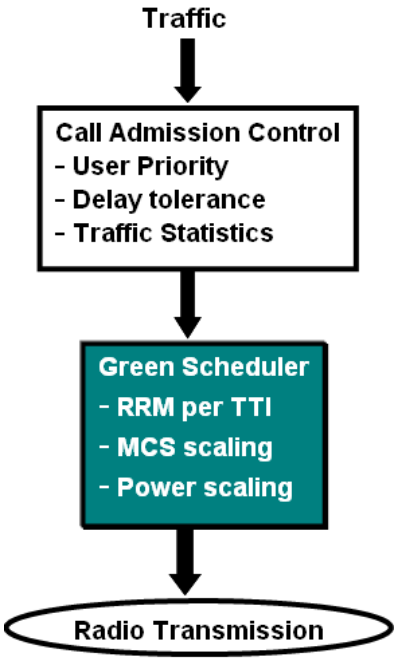

FIGURE 55. Green scheduling Architecture.

8.3.3. Simulation results

We show the results for Green Metric, in terms of Joule/bit defined in [CalGre2010] for web based traffic based on system simulation scenario in [EARTH-D2.3] in FIGURE 56. We can see from the system simulations that the maximum gain for the green adaptive scheduler (GAS) comes from the moderately loaded scenarios and it diminishes for high and low load scenarios. The system power gain for our proposed algorithm is from 0-20 % based on the traffic load present at the base-station.

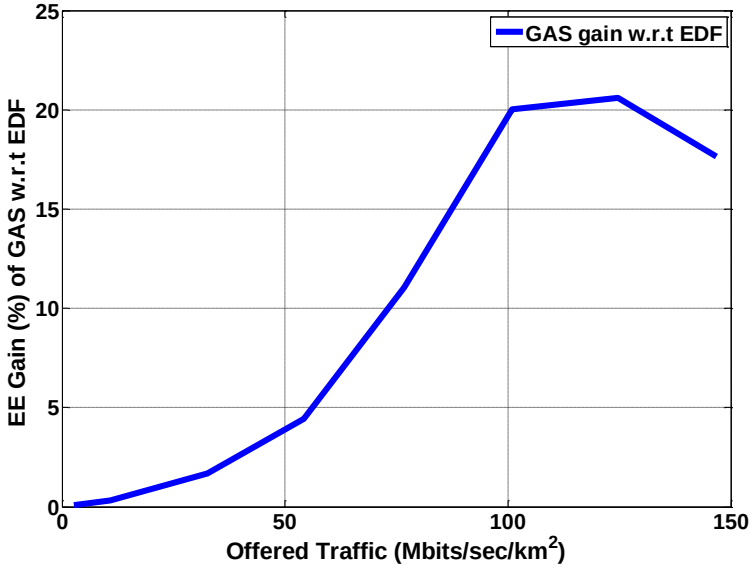

FIGURE 56. Green Metric Performance.

8.4. VERTICAL HANDOVERS

This section explores the relation between services and RATs heterogeneity from the energy efficiency point of view. In general, transmission of user data is accompanied by additional network signalling. As already defined in [EARTH-D3.1] in some cases, even in an "empty" network, radio beacons transporting network information must be continuously transmitting useful data (e.g., BS identification) to standby UEs. Therefore, in the end, the relation between real user data and overhead is relevant when discussing energy efficiency and the relation between transmitted bit and power. Additionally, the energy cost can be established, being assumed as the energy cost of a given BS and associated RAT. Thus, the total power cost C_U required to transmit user data is given by:

$$C_{U\ \mathrm{W/bit}} = \frac{P_{T\ \mathrm{W}}}{V_{D\ \mathrm{bit}}}, \tag{8-22}$$

where V_D is the user information volume related and P_T is the total power required to transmit user data and associated network signalling.

This power cost C_U is a key metric to measure the EE of a given BS, however, appropriate RRM decisions should be taken based in opportunistic time scale, being crucial to evaluate BSs efficiency, and therefore, C_U can also be measured in W/bps. This metric is computed by a cost function (CoF) defined in [SerCor2007a] and [SerCor2007b], being used in this work only with the operator component. Different CoFs may be computed for each different RAT type. Each one of these "sub CoFs" is weighted with different values, enabling the implementation and evaluation of different policies by RRM algorithms over each type of RAT.

8.4.1. Algorithm Description

Based on the previous metric C_U and using the algorithm to trigger VHOs defined in [PerezR2007] (the so called Fittingness Factor (FF)), the most energy efficient BS/RAT for each UE/service is provided. This algorithm is divided into two parts, one for new connections, and one for already set up ones. An integrated parameter is defined by the FF algorithm, the final cost factor $F_{u,p,s,r}$, which reflects the degree of adequacy of a given RAT to a given user: it takes each cell of the *r* RAT for each *u* user, belonging to the *p* customer profile, requesting a given *s* service. The RAT selection algorithm is considered differently, depending on whether the selection is done at session set-up or during an on-going connection.

For a user requesting service *s*, (see FIGURE 57 (a), the procedure is:

- Measure the $F_{u,p,s,r}$ for each candidate cell k_r of the *r* detected RAT.
- Select the RAT *r* having the cell with the highest $F_{u,p,s,r}$ among all candidate cells:

$$R = \arg\max_{r} \ \max_{k_r} F_{u,p,s,r} \ \ k_r \tag{8-23}$$

- In case that two or more RATs have the same $F_{u,p,s,r}$ value, then, the less loaded RAT is selected.
- Run the CAC procedure in the RAT *j*. If admission is not possible, try the next RAT in decreasing order of $F_{u,p,s,r}$, provided that its $F_{u,p,s,r}$ is higher than 0. If no other RATs with $F_{u,p,s,r}$ higher than 0 exists, block or delay the connection.
- For on-going connections, (see FIGURE 57 (b), the proposed criterion to execute a VHO algorithm based on the FF assumes that the UE is connected to the RAT denoted as "servingRAT" and cell denoted as "servingCell". In this case of on-going connections, the procedure is:
- For each candidate cell and RAT, monitor the corresponding $F_{u,p,s,r}$ (k_r). Measures should be averaged during a period *T*.
- If condition

$$F_{u,p,s,r} \quad k_r \quad > F_{u,p,s,servingRAN}(servingCell) + \Delta_{VHO} \tag{8-24}$$

holds during a period T_{VHO}, then a VHO to RAT r and cell k_r should be triggered, provided that there are available resources for the user in this RAT and cell. Δ_{VHO} is the required difference to performance the handover.

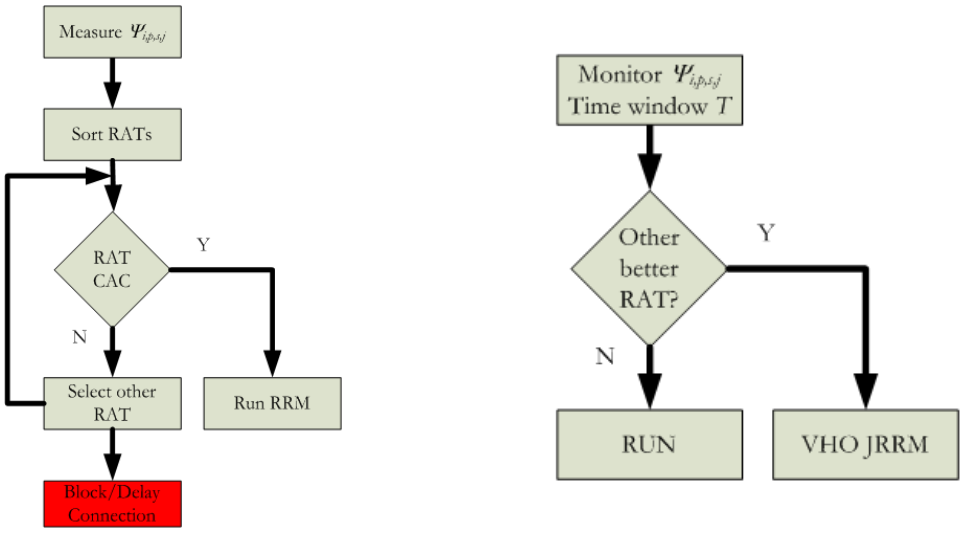

(a) New connections (b) On-going connections

FIGURE 57. FF BS/RAT selection algorithms.

8.4.2. Implementation Aspects and Operation Proposal

To implement and execute the previous algorithm in a multi-RAT environment the existence of a central and common entity with full access to the multiple RATs/BSs radio indicators is required. From the network architecture view point, this algorithm should be distributed between BSs/controllers and by central mobility entity. BSs or BSs controllers should report the metric to the central point in a second time-scale basis, then the proposed algorithm should be executed by the mobility management entities, and in some cases decide to attach MTs to the most energy efficient BSs/RATs in the first connections request or execute VHOs for ongoing connections. In the LTE network this algorithm can be handled by the Mobility Management Entity. From the signalling traffic load view point this process is not very demanding since it only requires information sent in second time scale for each active UE.

8.4.3. Scenarios and Simulation Results

In order to assess the impact on EE performance produced by the previous algorithms, the first approach is based on micro-cell BS power and traffic models are used to design a reference scenario proposed in [EARTH-D2.2] and used in this study.

TABLE 8. Model parameters for Micro-cells.

BS type	P_{max} [W]	P_0 [W]	Δ_P
Micro	**6.3**	**106**	**6.35**

The BS equipment power model consumption corresponds to a typical commercially available BS in 2010, used in this work as a reference for simulations and for system level energy gains. TABLE 8 presents values for the BS, being used to compute the system level power levels using EARTH power model.

Different services are also under test, because different RATs present different radio bearers, since they handle services in a different manner (e.g., voice in circuit switch or data in packet switch networks).

The reference number assumed for the users' density is 1000 user/km^2, which corresponds to a Low (L) traffic case; in order to assess the traffic load impact on EE, users density is increased by 25 and 50%, corresponding to Medium (M) and High (H) traffic load cases, respectively. In the reference scenario, one assumes two BSs, WCDMA and High Speed Downlink Packet Access (HSDPA), with a 500 m radius, WCDMA being considered the legacy RAT in which EE may be enhanced. The considered service set is defined according to TABLE 9, where reference parameters are provided for each service, arrival rate λ, session time τ or volume V_D are defined. These services correspond to two different classes, voice being of the Conversational type, while web browsing and file transfer of the Interactive one, following 3GPP classification. The average number of active users is valid for the Low traffic situation and for both BSs.

TABLE 9. Services and traffic (Reference).

Services	Average number of active users	λ	τ [s]	V_D [MBytes]
Voice	**15**	**0.31**	**90**	**-**
WWW	**6**	**0.5**	**-**	**0.1**
FTP	**6**	**0.1**	**-**	**10**

Based on this reference scenario, different simulations were performed, results being presented for each individual service (all active users are performing only this particular service), as well as the combination of all services.

The first step to obtain energy efficiency gains start by computing the BS RF power level, by comparing two different cases: the EE and FF algorithm being OFF and ON. The G_{RF} defined has the power gain savings achieved at BSs RF level is shown in FIGURE 58 (a). Results for EE gains at system level, G_{SL}, are presented in FIGURE 58 (b); this was computed based on the EARTH power model and on the previous RF gain.

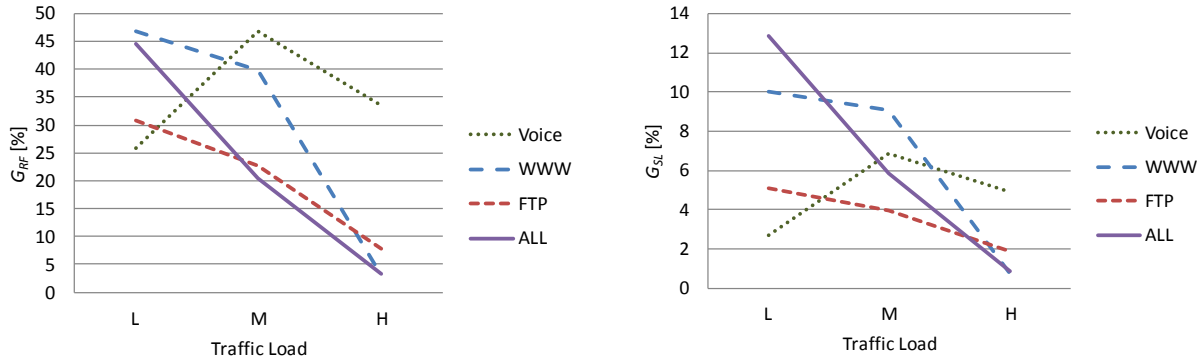

a) RF EE gains for WCDMA and HSDPA

b) EE at system level gains for WCDMA and HSDPA

FIGURE 58. EE gains for WCDMA and HSDPA.

When traffic raises, EE decreases, since the VHO power reduction effect become less relevant. Other effects become important, e.g., handover receiving RATs become more loaded, therefore, less power efficient, since more intra-cell interference becomes also significant. Another effect is in the communication distance, since HSDPA networks, by comparison with legacy networks, may become less power efficient for long range communications or high bit rate services become out of coverage, leading potential VHO situations to be less interesting or impossible.

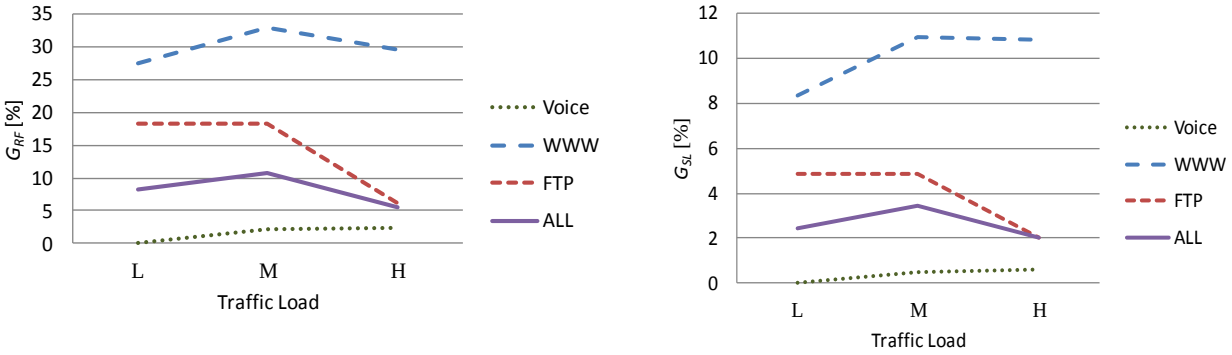

a) RF EE gains for WCDMA and LTE

b) EE at system level gains for WCDMA and LTE

FIGURE 59. EE gains for WCDMA and LTE.

By observing FIGURE 59 (a), one concludes that only the voice service increases its EE for the Medium load case. This happens because voice has less impact on the network load (compared to data), providing a margin to increase EE even in Medium load case; however for the High case, voice users trigger VHOs, providing less EE gain.

For the World Wide Web (WWW) and FTP services, differences on EE gains curves are due to their session density, duration, or burstiness intrinsic natures.

The results from FIGURE 59 (b) follow the previous RF gains, but for same cases the non-linearity of the model can be observed (Δ_P EARTH power model factor); for example, in the Low case, when all services are combined it presents higher gains compared to the WWW single case. Anyway, for the all services case, EE ranges from about 1 up to 13%.

When all services are simulated simultaneously, the RF EE gain decreases with the traffic load, but it can achieve relatively high gains in the Low traffic case, because, in this traffic scenario VHOs have some power margin, producing EE gains (being coherent with WWW and FTP trends).

The low (L), medium (M) and high (H) traffic cases follow the EARTH load levels.

9. ARCHITECTURES IN THE FUTURE

Most of the existing mobile radio communication systems, such as WCDMA/HSPA and LTE, have been designed with the ambition to deliver high user data rates and high SE. The energy efficiency of the networks, however, especially during periods when no user data is transmitted, has not been highly prioritized. Even though several means to enhance the energy efficiency of existing mobile communication systems exist, some of which are discussed in the previous Sections of this document, those solutions are often at least partly constrained by the system specifications and the capabilities of the networks.

As energy consumption is becoming more and more important it is likely that low energy consumption will be included among the design objectives of future mobile communication systems. Moreover, new systems standards may also include some novel technology solutions that were not available (or, mature) when the existing standards were determined.

This section discusses some promising ideas and technologies that may be considered as candidate solutions for future mobile communication systems and enablers for low energy consumption. To steer clear of one of the disadvantages of the existing standards, namely that the energy consumption during idle periods is unnecessarily high, Section 9.1 discusses the idea of logically decoupling the transmission of data and control information. Section 9.2, furthermore, provides on assessment of how mobile multihop relaying can be used to enhance coverage and facilitate that selected nodes in the fixed infrastructure can be turned off during low traffic periods to save energy. The numerical results indicate possible energy saving in the order of 30 %. Section 9.3 discusses a concept referred to as a cloud RAN, in which geographically separated nodes are connected to a central controller. The solution is well suited to handle HetNet deployments, radio remote heads and active antenna systems (AASs) and the results indicate a significant potential in terms of SE. In Section 9.4, finally, the energy efficiency of network coded transmissions is compared to traditional packet retransmission strategies in a multicast scenario. Here, the results show that in terms of energy efficiency NC provides the largest benefits when the SNR is low and with no or little error correction. For high SNR and a high level of error correction, however, the traditional packet retransmission strategy is associated with lower energy consumption.

9.1. LOGICAL DECOUPLING OF BASIC SYSTEM FUNCTIONALITY AND DATA TRANSMISSION

In order to design an energy efficient system there are two, seemingly obvious, challenges that needs to be addressed: The first one is to be energy efficient when transmitting data, and the second is to be energy efficient when not transmitting data. When data is being transmitted, high data rates (that enables us to stop transmitting and receiving quickly) and beam-forming (that enables us to focus the transmitted energy to the intended user) are key improvement areas for enhancing energy efficiency.

When data is not being transmitted, the key thing is to enable the network to operate in a low power mode with DTX and Discontinuous Reception (DRX) as much as possible. Current cellular systems (GSM, WCDMA/HSPA, and LTE) were never designed with the second challenge in mind, and consequently the amount of energy a cellular network consumes depends very little on the amount of data traffic in the system. Instead energy consumption in current cellular systems is by far dominated by mandatory transmissions of system overhead when no data is transmitted. If we are to effectively reduce energy consumption in cellular networks then we must take a closer look on what type of system overhead we have today and what can be done to reduce it. The reason why we need to broadcast system overhead at all in cellular systems is that we need to provide in-active mobile stations (MSs) with information on how they can access the system. An in-active MS needs at least the following support from the network:

Access information: A MS needs to know how to contact the network whenever it wants to initiate a service. This procedure is commonly known as random access, and the MSs need to know how the random access channel is configured (e.g. which pre-ambles, time slots etc. that are used).

Mobile station measurements: In-active mobiles need to perform mobility measurements and possibly also measurements related to positioning. Based on such measurements the MSs perform location update signalling with the network which is needed for paging to work.

System presence: In principle the MS could test if a system is available by transmitting a probe and checking for a network response. However, it is typically not considered acceptable with MSs transmitting in any frequency band before they know that they are allowed to do so (the MS may e.g. be in a country where these frequencies are used for another service). Therefore, in practice, in-active MSs need to first detect that a system is present before they can transmit anything.

System overhead in current cellular systems is transmitted from each individual cell in the entire network. This is a legacy from the first and second generation voice centric systems (Nordic Mobile Telephone (NMT) and GSM), but for third and fourth generation data centric systems (HSPA and LTE) this is starting to become a problem. Distribution of system information can be much more efficiently solved if we view it as a broadcast problem. In Orthogonal Frequency Division Multiplexing (OFDM) based systems, such as LTE, the natural solution to provide broadcast services is to make use of single frequency network transmission techniques. Furthermore, the concept of having fixed cells becomes more and more difficult to motivate with the ongoing introduction of more advanced system features such as Beam-forming, MIMO, multi-carrier, CoMP, multi-RAT, and reconfigurable antenna systems. This calls for a reinterpretation of the cell concept. It is more fruitful to view the cell as something dynamic that is specific for a single MS rather than something static that is common for all MSs in a given area. By also letting go of the idea that the coverage of the system information broadcast channel and the data channels need to be identical we can enable a much more efficient system operation. This is illustrated in FIGURE 60, where all MSs receives access information from a Broadcast Channel provided by the BSs RBS_1-RBS_4. The mobile station MS_1 is configured to received data from a MIMO capable cell provided by RBS_5; MS_2 communicates with a CoMP cell corresponding of signals from the BSs RBS_1, RBS_3, and RBS_9; the mobile station MS_3 is communicating with a cell with an omni-directional antenna pattern provided by RBS_4; the BSs RBS_4, RBS_6, RBS_7, RBS_8, RBS_{10}, and RBS_{11} are not used for transmission of system information nor packet data and are idle in this example. The decision to set up a CoMP cell for MS_2 and a MIMO cell for MS_1 can now take into account the amount of traffic that MS_2 and MS_1 want to communicate.

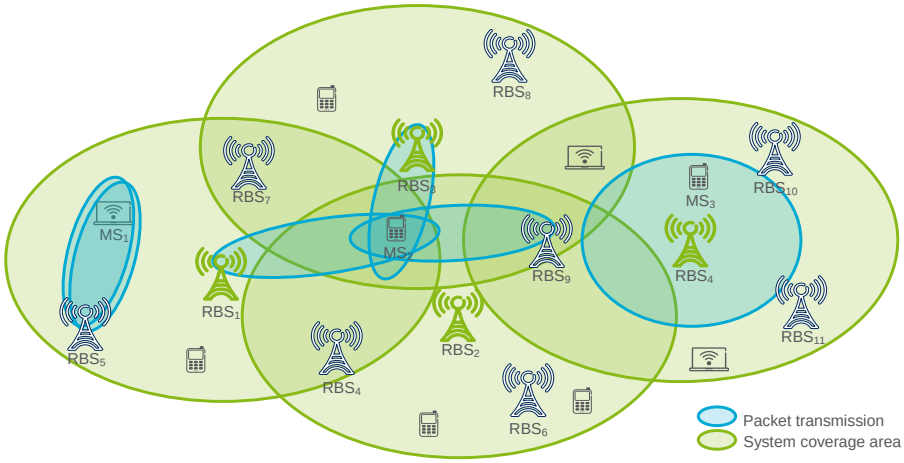

FIGURE 60. Example of system operation enabled by a logical separation of system broadcast channels and packed data transmissions.

By logically de-coupling system information from data transmissions we can thus enable BS sleep mode in an efficient way since not all nodes need to participate in the transmission of system information. We can also optimize the cells that we provide to the active users based on their current needs. This enables a system where the first challenge is effectively addressed by “soft cells” providing high packet data rates to active users only and

the second challenge is addressed by designing system overhead transmissions with maximum DTX in both time and space.

If we only consider energy consumption then there is today no strong reason not to re-use as much as possible from the LTE standard when designing a new energy optimized system. LTE is a state of the art system that makes use very good use of OFDM and MIMO technologies already. However in current cellular systems we spend a lot of energy of preparing the channel for optimum transmission conditions. We continuously transmit pilots and send closed loop feedback even when there are no packets communicated over the air interface. Before we can start sending packets a complicated procedure including e.g. assigning short identities to the users, establish radio access bearers, and set up security need to be accomplished. All this overhead enables the first packet in a stream to be transmitted with optimum settings. But when all the overhead energy is considered we must admit that this is not at all an efficient way to handle packet data, especially not if the data payload is moderate. This is an area where LTE need to evolve.

9.1.1. Distributing access information

There is no need to tie the random access procedure to a single cell before the MS has even contacted the network. Consequently, distribution of access information can be efficiently solved if we view it as a broadcast problem. In OFDM based systems, such as LTE, the natural solution to provide broadcast services is to make use of single frequency network (SFN) transmission techniques. SFN transmission of access information brings several advantages e.g. diversity gain, significantly reduced inter-cell interference, and better support for cell sleep. In LTE there is already support for defining SFN sub-frames and hence it would be possible to insert new broadcast signals inside these sub-frames. This would allow a phased introduction of the new system. As long as an operator need to support legacy UEs in an area the normal eNB-unique broadcast channels and signals are transmitted in parallel with the new non eNB-unique broadcast channels and signals.

To further reduce the amount of information that need to be broadcasted we divide the system information into “common system information” that is relevant for every node in the system; and “node specific information” that is relevant in a specific node only. The common system information and node specific information can be communicated to the MSs after initial system access and initial node access respectively (see FIGURE 61).

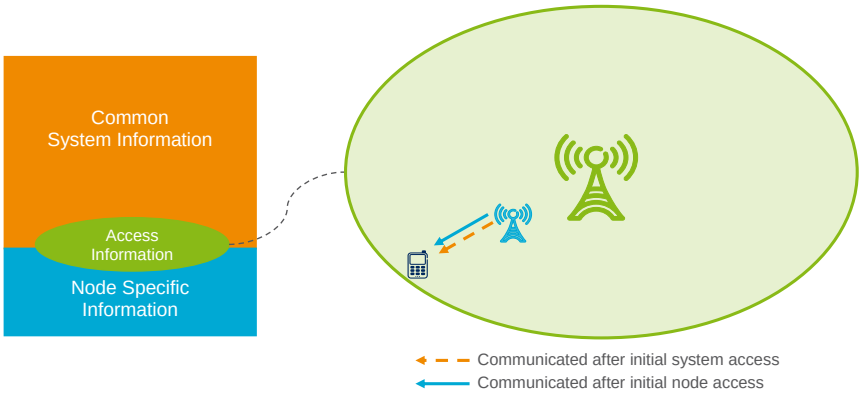

FIGURE 61. Only the small part of the system information related to initial access (denoted access information) need to be broadcasted.

9.1.2. Random Access and Paging

Since the random access is not cell or node specific in the described system, situations may arise where several network nodes answer the initial random access message transmitted from the UE. This calls for contention resolution also on the random access response message (i.e. the response from the network after the initial transmission of the random access preamble from the UE).

In case two random access responses collide and none of them can be decoded by the UE then the UE will need to start with a new random access attempt. For the following attempts it is important that the same error is not repeated over and over again. This can be resolved by designing a random access response contention resolution protocol. The random access procedure also needs to provide connectivity information concerning the mobile specific "soft cell" to the accessing user. Typical, this would include a physical identity of the serving cell and a short and unique identifier of the mobile within the serving cell.

A large BCH Area (BA) reduces the need for spending resources on transmission of system information. At the same time, a large BA may cause problems with paging. In order to contact an idle-mode MS the system need to send a paging message on a paging channel. When a BA has the size of a single cell, as in traditional systems, then we simply decide in which cells that a paging message shall be transmitted. But if the BA consists of several cooperating network nodes then we may not want to use all of them for transmitting a paging message. In FIGURE 62 we therefore introduce the term paging area that is defined as the coverage area of the network nodes that participate in transmission of a paging message. A paging area can typically be smaller than a BA. In a similar manner, we also introduce the term random access response area. In both cases, the assumption is that the network has decided which node or nodes to be included in the paging area and the random access response area, respectively. The left part of FIGURE 62 depicts the time-frequency grid of the system broadcast resource (solid resource elements represent data symbols and dashed resource elements represent demodulation reference symbols). The right part of FIGURE 62 depicts the mapping of system control plane channels (BCH, Paging, and random access response) to physical nodes

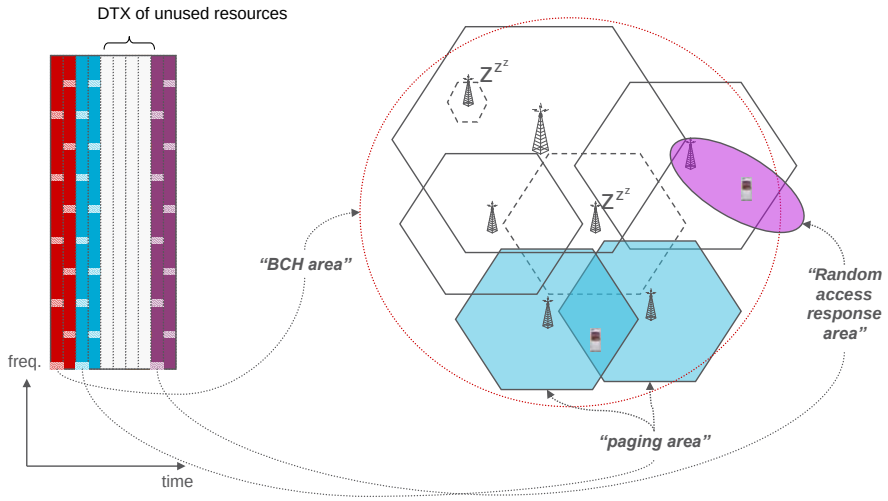

FIGURE 62. Example of how a paging message and a random access response message can be transmitted in an area smaller than the whole BCH area.

9.1.3. Mobility

Handover measurements are performed in a similar way in all present cellular systems. The UE measures on downlink pilot signals, transmitted by neighbouring BSs, and compares with the downlink pilot signal received from the serving BS this UE is currently connected to. Quantities measured are typically different means of signal strength, e.g. reference signal received power (RSRP) and signal quality, e.g. reference signal received quality (RSRQ).

Current mobility solutions are not designed for a network where the cells may be dynamically re-configured. In case a UE base the mobility decision on a downlink reference signal from a non-serving candidate cell then it is only possible for the UE to measure on a downlink beam that is not specifically targeting that UE. In case the non-serving candidate cell is capable of beam-forming the transmission towards the UE then it is not possible for the UE to in advance determine the quality of the signal after handover. For this reason we need a more advanced,

two-stage mobility procedure, which is depicted in FIGURE 63. We need to use first mobility mechanism to trigger the activation of second mobility mechanism. The first mechanism operates pretty much as in current systems, i.e. the UE searches for mobility pilots and reports to the serving node when a candidate is stronger than a reporting threshold. This triggers a second mobility procedure in which either uplink measurements or transmission of additional mobility reference signals are performed in the neighbouring nodes (see FIGURE 63). Instead of always transmitting all kinds of downlink pilot signals from every BS, it is more efficient to transmit those signals on a need basis. Thus, at any given time, the BS transmits none, a few, or all of these pilot signals.

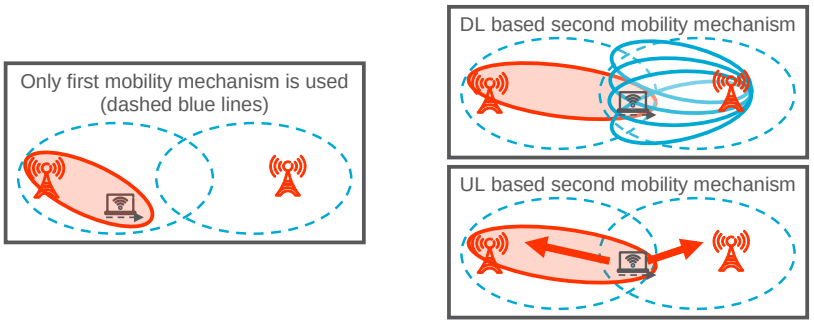

FIGURE 63. (left) First mobility mechanism has not yet triggered the second mobility mechanism; (right) second mobility mechanism is triggered.

9.2. MULTIHOP EXTENSION

During the past decades enormous research activities targeted ad-hoc networking, yet the widespread application of such networking techniques are not foreseen in the near future. However, utilizing various solutions from ad-hoc networks might be useful in future network architectures, targeting reduced energy usage. Ad-hoc protocol solutions targeting lower energy consumption were proposed abundantly in the literature, but these solutions target the energy saving for increasing UE battery lifetime, not for saving energy in the network side. Similarly, some literature is available for coverage extension purposes, again, in these cases network energy consumption was not considered. Moreover, these works do not consider Earth network solutions, which implicitly might require multihop extension for keeping coverage (e.g. cell turnoff in low load situation, coverage kept by means of multihop forwarding).

A particular example is the architecture where mobile devices are capable of relaying others' traffic towards/from the BS. The motivation of this is that by means of such multihop relaying, service can be provided to terminals dwelling in uncovered areas, or parts of the infrastructure might be turned off temporally (to save energy) and coverage could be still maintained. Due to the abundant number of mobiles dwelling over the area, multihop coverage or capacity extension is a viable possibility without the need of expensive deployment of infrastructure. 3GPP is also looking at the mobile relaying; however the foreseen [3GPPTS36.416] is not yet released.

There are lots of protocol, routing and control questions to be solved for such operation to be implemented, however, here only the basic capabilities (in terms of coverage extension) of multihop relaying are treated. Moreover, there are severe security threats to be solved and economic incentives to be applied, before such an operation can be utilized, but these are also out of the scope of this contribution.

For coverage extension it is assumed that there is a limited area (e.g. a settlement) covered by a number of BSs. However, there might be a few customers that are (maybe temporally) outside the coverage and new infrastructure is not worth deploying for their service. A similar scenario is when coverage is not contiguous, yet there might be customers in the area with no service (e.g. between settlements). The third case connects this investigation to other activities of WP3. Namely multihop extension can be used to maintain coverage in case

when several cells are switched off for energy saving purposes. In these cases however, due to the generally random placement and existence of terminals, the coverage extension caused by mobile relaying is also of probabilistic nature. It is worth noting that due to the problem of sharing radio capacity between relayed and ''normal'' traffic, multihop extension is feasible only in case of low traffic hours.

9.2.1. Coverage extension in single-cell macro system

First, a single omnidirectional cell was assumed and the average size of coverage extended by means of multihop relaying was evaluated by snapshot simulations, assuming even spatial distribution of customers. Terminal-terminal and BS-UE maximum link distances were calculated for suburban propagation and 2 Mbps achievable throughput as the edge of coverage, assuming 1800 MHz carrier frequency and 10MHz bandwidth. As single cell was assumed, only thermal noise was considered in the available throughput expression, which was expressed by the Shannon law.

We assume that coverage extension is directly translated into the decrement of the energy efficiency expressed in W/km^2. The reason behind is that we supposed low, sporadic traffic to be relayed by mobiles. This is assumed to be negligible increase in mobile's consumption, compared to what they would have consumed without relaying others' traffic. Moreover, we assume the total traffic to be so low that processing relayed traffic does negligibly rise in the power consumption of the BS as well. Therefore the ratio of covered area increase is the same ratio is EE metric W/km^2. However, as the targets of the project require the total power to be lowered, in cases where EE metric of W/km^2 is lowered due to the increase of the covered area (km^2), but total power consumption is not decreased, results are shown in terms of gain in the extended coverage area.

To get insight into the probabilistic nature of the extended coverage area, the pdf of EE increase (area increase) is plotted in the left of FIGURE 64, for different UE distributions and maximum number of 4 allowed relaying hops. The right hand side of FIGURE 64 shows the coverage extension percentage (compared to the original macrocell area) as function of UE density and allowed maximum number of hops. Here extended coverage was assumed as the area covered by 0.95 probability. It is apparent that significant coverage extension (up to 50%) is achievable, considering satisfactory user density and allowed hop numbers. As discussed above, this would directly represent 50% gain in EE metric expressed in W/km^2.

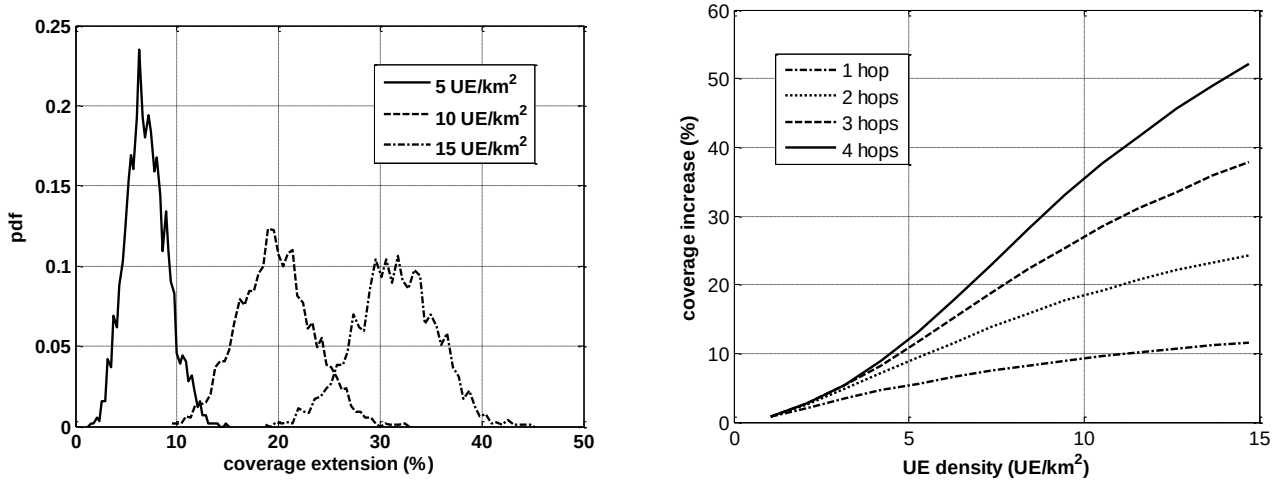

FIGURE 64. Coverage extension in single cell system.

9.2.2. Keeping coverage in multicell network

The next examination evaluates a 19 cell hexagonal layout and the possibility of keeping coverage when several cells are turned off. Terminal-terminal and base-station-terminal maximum link distances again were calculated for suburban propagation, but the multicell scenario required the interference to be taken into account as well.

Coverage is calculated for each parameter setup (UE density, number of allowed hops) as the area that is covered by multihop relaying with at least 0.95 probability. We set a 0.95 coverage criterion as well (at least this ratio of the area of the turned off cells should be covered by the said 0.95 probability). If this coverage criterion can be kept, this means that coverage is maintained by means of multihop relaying, even if parts of the infrastructure were turned off.

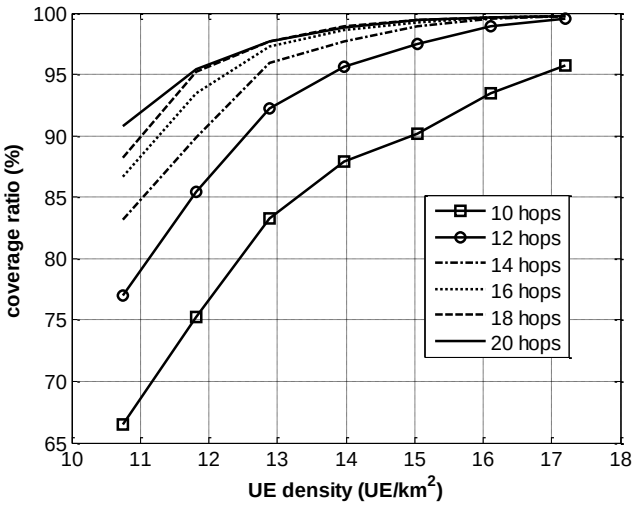

FIGURE 65. Coverage probability in multicell scenario.

In the scenario for which results are shown in FIGURE 65 six cells (the middle ring) out of 19 was switched off and the coverage ratio of the turned off cells' area was determined. Apparently the coverage criterion 95% can be achieved if user density is high enough and the number of allowed relaying hops is also high. In all the cases where the curves in the Figure cross the 95% coverage limit ratio, the 6 cells might be switched off and coverage is still kept. As in this case 6/19 of cells are switched off, this is the energy efficiency saving in this case, that is 31.5 % lowered power consumption in Watts (and as covered area did not change, this means 31.5% decrease of EE metric in W/km^2).

9.3. ACTIVE ANTENNAS IN COOPERATIVE SYSTEMS

The mobile operators are facing today several challenges like exponential growth of the traffic demand, request for increasingly higher bit rates services, operational complexity related to the coexistence of multiple RATs, rise of power consumption and reduced growth rate of the revenues. In order to meet these technical challenges and preserve the profitability of the operator's business, it is necessary to change the paradigm in the design and deployment of future RANs.

Concerning the growing traffic demand, mainly driven by Mobile Internet services and Smartphone diffusion, a possible approach is the deployment of HetNet. As for the provision of higher data rates the technical solution is to place the transmit antennas "closer" to the users. A further increase of the data rates per unit of used spectrum (and therefore a reduction of the cost per bit) can be achieved by implementing advanced digital signal processing techniques that exploit multiple antennas at the transmitter and at the receiver, such as MIMO. The user data rate increments promised by MIMO, and in particular by the spatial multiplexing, are possible only by guaranteeing very high SINRs to the users. This is particularly difficult to achieve in a HetNet, where transmission points at different power (e.g. macro/micro) coexist at the same frequency. The techniques for controlling the inter-cell interference, through the coordination of multiple geographically separated transmission points, known under the acronym of CoMP are therefore crucial for a successful application of MIMO.

All the aspects discussed above could be gathered together to introduce a new concept of RAN also known as C-RAN. C-RAN can be seen as an evolved distributed architecture, where multiple geographically separated nodes are connected to a common central controller. The C-RAN is commonly intended as a HetNet formed by a plurality of access points connected by fibre to a centralized pool of Baseband Units (BBUs) where common baseband processing takes place in a sort of "cloud" central management unit. The access points are typically in the form of RRHs that are small and easy to install on the existing urban infrastructure of the operator like cabinets, phone boots, lampposts, etc.

Recently the RRH units are also envisaged to be used in the C-RAN architecture as macro-sites, usually equipped with AASs. The acronym AAS refers to an antenna where each radiating element has its own RF transmitter and receiver, so that the phasing between the elements can be digitally controlled (see [EARTH-D4.1] and [EARTH-D4.2] for details on AAS).

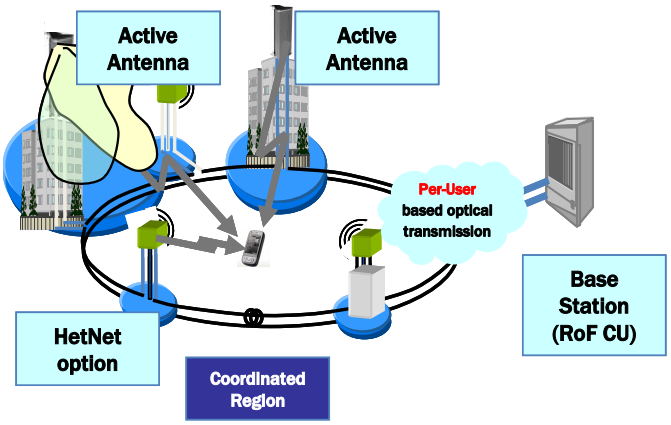

FIGURE 66. Layout for cloud RAN including AAS.

The layout enabling cloud RAN with AAS is schematically sketched in FIGURE 66 and is a means to energy consumption reduction as well due to better performance, reduced consumption in remote nodes; moreover it allows also costs reductions.

HetNet option in such a scenario is a first step in the network evolution towards the cloud RAN, as depicted in FIGURE 67. Performance assessment of HetNets (i.e. Macro and Micro eNBs) in a scenario aligned with 3GPP assumptions has been done, considering space-frequency block coding (SFBC) as transmission mode and 2 microcells for each macrocell in the scenario (located at 70% of the cell range).

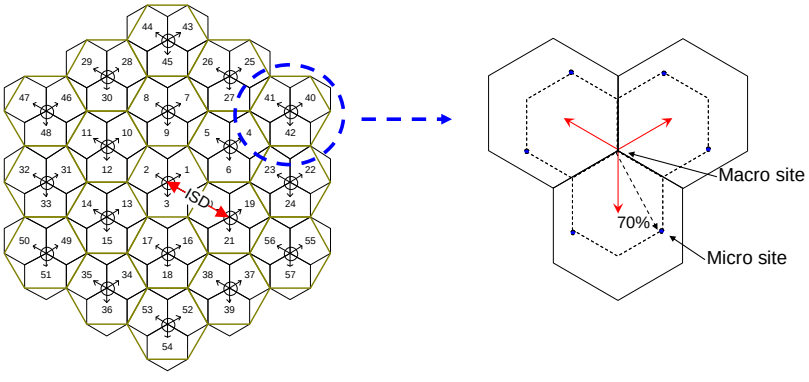

FIGURE 67. Scenario of the system model used for evaluation of HetNet.

The results of this simulation are reported in TABLE 10 in terms of SE improvements. A small improvement in the SINR distribution is translated into a big average throughput gain (~164%). In fact as the number of users is the

same in both scenarios, the introduction of more eNBs increases the amount of available radio resources in the scenario; in contrast a negligible effect is observed on cell edge users' performance.

TABLE 10. Results of HetNet scenario case.

	normalized user SE [bps/Hz]	
	average	cell edge
Macro only	0.128	0.029
Macro+Micro	0.333	0.028

The results reported here are to be considered only as a first and preliminary step to introduce architecture such as Cloud RAN as an interesting and promising enabler for energy saving. HetNet is generally considered as a part of the Cloud RAN concept, but more advantages are expected when it will be fully exploited and evaluated.

9.4. ENERGY-EFFICIENCY COMPARISON BETWEEN NETWORK CODING AND RETRANSMISSIONS

The conventional way to utilize NC is to maximize information flow in the network. On the data link layer, NC can be considered as an alternative to routing, and as such, a reliable solution to distributed packet delivery in decentralized future network architectures. As a new perspective, this study focuses on finding out whether the NC could help to reduce energy consumption. The considered system model assumes multicast transmission from a single source to multiple destinations over the erasure channel. The chosen performance metric counts the number of packets the source sends successfully to all destinations per energy spent. Random Linear Network Coding (RLNC) and automatic repeat request (ARQ) performances are compared with and without Forward Error Correction (FEC). FIGURE 68 depicts the multicast system model where packets $\{s_1, s_2, \ldots, s_K\}$ are transmitted from the source to D parallel destinations.

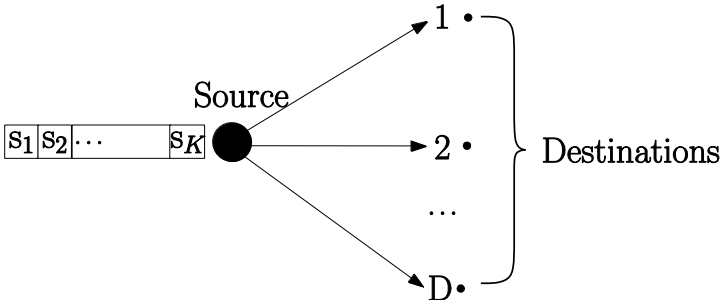

FIGURE 68. System model where a single source multicasts s_K packets to D destinations.

In the numerical results the source wishes to multicast a finite amount of data ($m \times K$ symbols) to a set of $D = 15$ destinations where $m = 256$ and $K = 8$. The channels between the source and each destination are assumed to be independent additive white Gaussian noise (AWGN) channels. Furthermore, 4-QAM modulation is used and noise power spectral density is set to $N_0 = -80$ dBm/Hz at all destinations.

In the absence of the FEC the energy consumption comparison is plotted as a function of the power per bit in FIGURE 69 (a). The results have been averaged over 100 iterations. It can be observed that there is a crossover point at -18.1 dBm that is also close to the minimum energy expenditure point at both schemes. For values less than that, i.e., in the highly unreliable link regime, the NC outperforms retransmission policy whereas for larger values the preference is shifted slightly to ARQ's benefit. The rationale for this kind of behaviour can be explained as follows. At low power per bit ratios packet erasures occur more frequently. In the case of ARQ retransmissions

to the destinations that failed to receive a packet take place one packet at a time and the rest of the destinations remain idle. For highly unreliable links the fraction of the idle destinations becomes large, which is energy inefficient. Contrary to that RLNC is by nature distributed approach and as such less sensitive to packet errors in individual links. At any time there is a chance that some of the destinations receive their useful information successfully although some of the transmissions fail. Thus, any transmission is potentially useful for all destinations.

FIGURE 69 (b) illustrates the energy consumption performance for RLNC and ARQ in the presence of FEC as a function of the number of the FEC codeword symbols. In this example the power per bit ratio is set to -21 dBm. The average time for the data to be delivered to all destinations is extracted from 10000 iterations in the case of ARQ and from 625 iterations in the case of RLNC. The simulation curves in FIGURE 69 (b) reveal that the energy needed to transmit $m \times K$ symbols decreases as the number of employed FEC symbols increases. Again, there is a point (28 FEC symbols) where the optimality of RLNC and ARQ is interchanged. At low numbers of FEC codeword symbols RLNC energy consumption is over 30% lower than that of ARQ strategy. At large numbers of FEC symbols the difference between RLNC and ARQ energy expenditure is marginal.

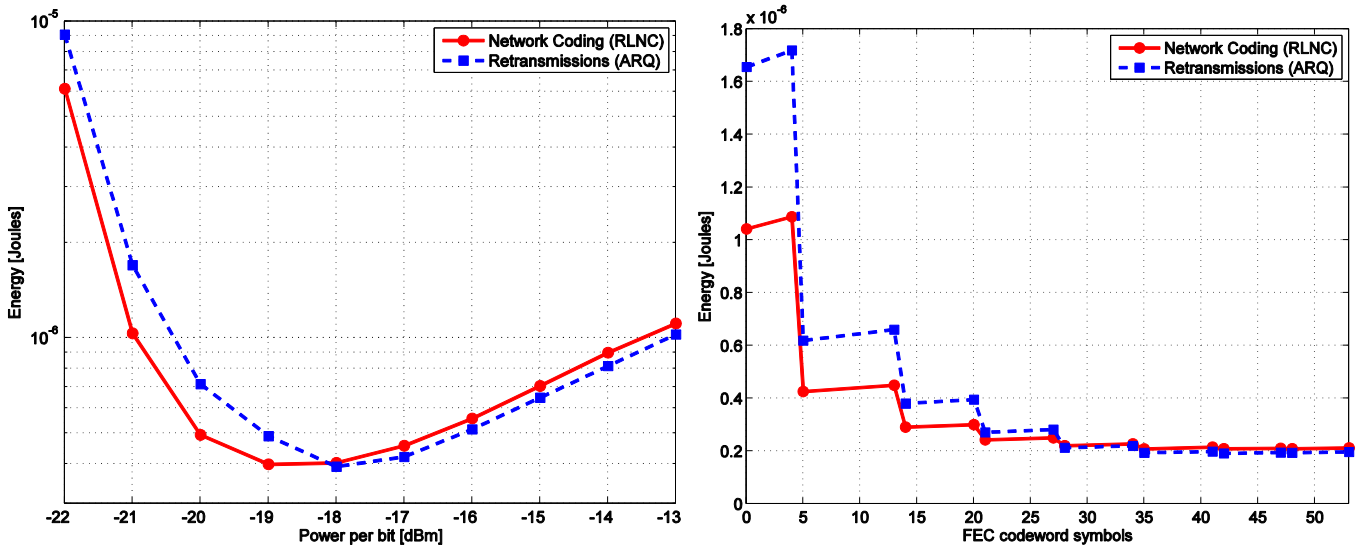

FIGURE 69. Energy consumption comparison of RLNC and ARQ (a) without FEC and (b) with FEC.

More details on this study can be found in [PaLaLa2011a] and [PaLaLa2011b].

10. CONCLUSIONS

This document contains the intermediate results on energy efficiency improvements provided by the different green network technologies selected as “Most Promising Tracks” in the EARTH deliverable [EARTH-D3.1]. These tracks include deployment strategies, network management concepts, RRM techniques and some proposal future architectures to be inherently designed to be energy efficient.

In traditional network planning the distance between BSs is adjusted to the maximum ISD that provides the requested system performance. However, each BS consumes power for basic operation and for signalling purposes. Thereby, a bad choice of the ISD can increase the power consumption by a factor of three. We found that in dense urban scenarios an ISD of 500m is optimum, while in urban scenarios 1400m is the best ISD in homogenous networks for the traffic level expected in the near future [EARTH-D2.3]. In heterogeneous deployments, it is beneficially place the small cells at the cell edge where the macro cell signal is most impacted by path loss and neighbour cell interference. In homogenous user distributions case 10% energy saving gain can be provided for high traffic scenarios above 150Mbps/km^2, meanwhile in case of hotspots even 20% energy saving can be achieved compared to a macro only deployment with more sectors or adding a second carrier.

Practical considerations call for investigating how to utilize operators’ existing legacy (GSM and 3G) deployments. Legacy systems will mainly provide the coverage and low-traffic demanding services in a multi-RAT scenario, while LTE will serve the increased capacity needs. Nevertheless, adopting more energy efficient RATs should be carefully balanced with the constraints coming from the forecast of capacity demand, terminal capabilities, coverage, emission limits, etc. The results showed site co-location could result in a decrease in power consumption up to around 5% due to better cooling efficiency depending on the balance between the different RAT types. It is also shown that network management reconfiguration actions can be pursued in case of changing traffic environment, resulting in up to 30% energy saving (see related results below, as well).

In addition to small cells, relays are also candidates to extend coverage and increase capacity. Nevertheless, gains strongly depend on several factors, especially on the offset power of the relays (see TABLE 2 and TABLE 3 for illustration of relay power model variants). In case of low offset power, relays nodes needs 5-10% less energy per bit than macro only deployments and two-hop scheme is better than the multicast cooperative scheme. From the transmission point of view several relaying techniques have been compared, and results showed that hybrid relaying DF/CF scheme can flexibly switch between two different forwarding schemes providing considerable gains compared to conventional non-hybrid solutions in large macro cells. When analyzing the possibility to use NC, numerical results showed that NC is not necessarily better than other forwarding schemes (like AF, DF or CF), but worth to consider as an alternative solution. In an in-building scenario, performance analysis revealed that relaying can increase the EE in comparison with P2P communication by either power saving or SE improvement.

The evolution of RANs introduced multiple antennas like MIMO, which provides further possibilities, e.g., for BS cooperation. The analysis proved that MIMO has a great potential for EE improvement over the Rayleigh fading channel in theory; in contrast, when a realistic PCM is considered, a MIMO system with two transmit antennas is not necessarily more energy efficient than a SISO system and utilizing more than two transmit antennas is likely to be energy inefficient.

Beyond the above described techniques focusing on densifying the network, coordination of BSs or cooperation between BSs are alternative solutions to cope with increased traffic by utilizing more the available bandwidth of the system. Analytical analysis of uplink cooperation schemes showed that saving energy per bit can be achieved only for cell edge users and cooperation of more than 3 BS did not improve the energy effort (J/Mbit) of the system compared to non-cooperative reception if realistic power models are taken into account. The analysis of coordinated transmission in the downlink showed that energy consumption of BSs can reduced by 15-25% energy per bit for a practical range of ISDs. Furthermore those gains are most pronounced in heavily loaded systems. During the above analyses we have recognized the importance of realistic backhaul power model for future work (see TABLE 4). The analysis of today’s most relevant backhaul technologies showed that the fraction of backhaul

energy that can be accounted towards each BS is not negligible, especially for small cells and PONs require the lowest power.

The daily variation of the traffic indicates that considerable amount of energy can be saved by dynamically reducing the number of active network elements to follow the actual traffic demands. Dynamic bandwidth management adaptively sets the maximum number of resource blocks used to schedule user data and the corresponding signalling. We have found that this technique provides approx. 25% energy saving and combines well with radio hardware improvements [EARTH-D4.2] providing more than 50% energy saving. Dynamic sectorisation of BSs is already applicable to currently operational RATs. In low traffic hours of interference limited urban networks, macro BSs can switch to fewer but larger sectors (using less radio units) without considerable impact on coverage or average user throughput. This technique provides 13-30% energy saving. Furthermore, in case of dense BS deployment, not only sectors, but complete BSs can be switched off in low traffic hours. In such cases, we have found that the idea of cell on/off in single layer networks provides approx. 14% energy saving. The great increase of traffic and MBB penetration calls HetNets that are in the focus of network modernization especially in densely populated urban environments. In these networks, a coverage layer serves conversational services and low data traffic (maybe provided by a legacy network), and a capacity layer serves high data traffic demands and large user throughput. Thereby the capacity layer is inherently overdimensioned providing room for on/off in HetNets and multi-RAT networks providing 25-40% energy saving and even more gain can be achieved in case of RRH (up to additional 7%).

Going further below the above timescales during the analysis of mobile systems, the goal of traditional RRM techniques should be rephrased to secure the minimal energy consumption when serving a given traffic demand with special focus on low traffic situations. The dynamics in scheduling can be exploited by putting the BS in sleep mode by utilizing MBSFN frames, where we can potentially disable both data and control signalling for empty periods. This technique requires 20-30% less energy per bit compared to the scenario without adapting the number of MBSFN frames. Cell DTX is another option to exploit sleep modes and together with power control (limited support in LTE) this technique can have a gain of as much as 45% with respect to the case when no power control and DTX is used especially in very low load scenarios and this gain decreases linearly with the traffic load of the system. By analyzing applications, we have found that the delay characteristics allows to reduce the transmit power by scheduling the data packets at the “best” time within the delay constraints of the QoS requirements. This approach requires up to 0-20% less energy per bits compared to the case without adaptive scheduling depending on the traffic load in the system. In low load situations, RRM can be extended to migrate users dynamically between RATs depending on the load of the multi-RAT system. By this VHO based technique up to 10% energy can be saved.

Looking further ahead in time and beyond today’s existing system standards and typical deployments, a promising conceptual idea is to logically separate the transmission of data and control information. Utilizing a user centric, soft cell concept the data transmission can be adapted to each user’s need and a large fraction of the nodes may be idle during long time periods significantly reducing the network energy consumption. Yet another promising conceptual idea is to create a distributed cloud RAN infrastructure where geographically separated central controllers are shared among the nodes. This concept is well suited for RRH solutions with AASs, e.g., in heterogeneous deployments providing substantial SE gains. Furthermore, in areas where no infrastructure has been deployed or some nodes are switched off to save energy, mobile multihop relaying may be used to fill up coverage holes and maintain a good service quality. In case of relatively high user density and large number of hops (> 15), it may be possible to switch off up to 30% of the nodes resulting in energy savings of the same magnitude. Beyond these ideas, NC is a possible technique to be used in future networks, e.g., as an alternative to the classical ARQ. The evaluations are performed in a multicast scenario and the results show that without any FEC NC outperforms ARQ in the low SNR regime.

Note that practically all of the above techniques combine well with most of the radio hardware improvements [EARTH-D4.2], which forms a solid basis for the integrated solutions that will be defined in the upcoming EARTH deliverable [EARTH-D6.2b] and EARTH-D6.3 later on.

11. REFERENCES

[3GPPTR36.814] 3GPP TR 36.814 V0.4.1 (2009-02), "Further Advancements for E-UTRA Physical Layer Aspects (Release 9)," Sept. 2009. Retrieved June 2, 2009. [Online]. Available: www.3gpp.org/ftp/Specs/

[3GPPTS23.203] 3GPP TS 23.203, "3rd Generation Partnership Project; Technical Specification Group Services and System Aspects; Policy and charging control architecture (Release 8)".

[3GPPTS36.104] 3GPP TS 36.104 V9.2.0 (2009-12): "Evolved Universal Terrestrial Radio Access (E-UTRA); Base Station (BS) radio transmission and reception (Release 9)", 3rd Generation Partnership Project; Technical Specification Group Radio Access Network.

[3GPPTS36.300] 3GPP TS 36.300 V9.8.0 (2011-09). [Online]. Available : http://www.3gpp.org/ftp/Specs/archive/36_series/36.300/36300-980.zip

[3GPPTS36.331] 3GPP TS 36.331 V8.6.0 (2009-06): "3rd Generation Partnership Project; Technical Specification Group Radio Access Network; Evolved Universal Terrestrial Radio Access (E-UTRA), Radio Resource Control (RRC); Protocol specification (Release 8)".

[3GPPTS36.416] 3GPP TS 36.416

[3GPPTS36.423] 3GPP TS 36.423 V10.2.0 (2011-06) Technical Specification Group Radio Access Network; Evolved Universal Terrestrial Radio Access Network (E-UTRAN); X2 application protocol (X2AP) (Release 10).

[3GPPTS423-890] 3GPP TS 423-890 Evolved Universal Terrestrial Radio Access Network (E-UTRAN); X2 application protocol (X2AP) (Release 8), 2011.

[AeaDai-Webs] [Online]. Available: http://www.aeasrl.it/ and http://www.daikin.com/csr/information/lecture/03_2.html web sites

[ArRiFe+2010] O. Arnold, F. Richter, G. Fettweis, and O. Blume, "Power Consumption Modeling of Different Base Station Types in Heterogeneous Cellular Networks," in Proc. ICT Future Network & Mobile Summit, Florence, Italy, Jun. 2010.

[Auer+2011] G. Auer et al., "How much Energy is needed to run a Wireless Network?," *IEEE Wireless Commun. Mag.*, vol. 18, no. 5, pp. 40–49, Oct. 2011.

[BaAySo+2009] J. Baliga, R. Ayre, W. V. Sorin, K. Hinton, R. S. Tucker, "Energy Consumption in Access Networks", in *Proc of OFC/NFOEC*, San Diego, USA, 2009.

[BelLas2009] E.V. Belmega and S. Lasaulce, "An information-theoretic look at MIMO energy-efficient communications," in *Proc. 4th ACM International Conference on Performance Evaluation Methodologies and Tools*, Oct. 2009.

[BiScCh+2011] T. Biermann, L. Scalia, C. Choi, H. Karl, W. Kellerer, "Backhaul Network Pre-Clustering in Cooperative Cellular Mobile Access Networks", in *Proc. of IEEE WoWMoM*, Lucca, Italy, Jun. 2011.

[BoyVan2004] S. Boyd and L. Vandenberghe, *Convex Optimization*. Cambridge, UK: Cambridge Univ. Press, 2004.

[CalGre2010] E. Calvanese Strinati and P. Greco, "Green resource allocation for OFDMA wireless cellular networks," in *Proc. IEEE PIMRC'10*, Istanbul, Turkey, Sep. 2010, pp. 2775 –2780.

[ChiSiv1998] F. Chiussi and V. Sivaraman, "Achieving high utilization in guaranteed services networks using early-deadline-first scheduling," in *Proc. IWQOS'98*, May 1998.

[CuGoBa2004] S. Cui, A. J. Goldsmith, and A. Bahai, "Energy-Efficiency of MIMO and Cooperative MIMO Techniques in Sensor Networks," *IEEE J. Sel. Areas Commun.*, vol. 22, no. 6, pp. 1089-1098, Aug. 2004.

[DasVis2006] S. Das and H. Viswanathan, "Interference mitigation through interference avoidance," in *Proc. ACSSC'06*, Pacific Grove, California, Oct. 2006, pp. 1815 –1819.

[EARTH_Leaflet] Earth project Summary leaflet. [Online]. Available: **https://www.ict-earth.eu/**

[EARTH-D2.2] A. Ambrosy et al., "D2.2: Definition and Parameterization of Reference Systems and Scenarios," *INFSO-ICT-247733 EARTH (Energy Aware Radio and NeTwork TecHnologies)*, Tech. Rep., Jun. 2010. [Online]. Available: **https://bscw.ict-earth.eu/pub/bscw.cgi/d31481/EARTH_WP2_D2.2.pdf**

[EARTH-D2.3] G. Auer et al., "D2.3: Energy Efficiency Analysis of the Reference Systems, Areas of Improvements and Target Breakdown," *INFSO-ICT-247733 EARTH (Energy Aware Radio and NeTwork TecHnologies)*, Tech. Rep., Nov. 2010. [Online]. Available: **https://bscw.ict-earth.eu/pub/bscw.cgi/d31515/EARTH_WP2_D2.3.pdf**

[EARTH-D2.4] M. A. Imran et al., "D2.4: Most suitable efficiency metrics and utility functions," *INFSO-ICT-247733 EARTH (Energy Aware Radio and NeTwork TecHnologies)*, Tech. Rep., Dec. 2011.

[EARTH-D3.1] O. Blume et al., "D3.1: Energy Most Promising Tracks of Green Network Technologies," *INFSO-ICT-247733 EARTH (Energy Aware Radio and NeTwork TecHnologies)*, Tech. Rep., Dec. 2010. [Online]. Available: **https://bscw.ict-earth.eu/pub/bscw.cgi/d31509/EARTH_WP3_D3.1.pdf**

[EARTH-D4.1] T. Bohn et al., "Most Promising Tracks of Green Radio Technologies," *INFSO-ICT-247733 EARTH (Energy Aware Radio and NeTwork TecHnologies)*, Tech. Rep., Dec. 2010. [Online]. Available: **https://bscw.ict-earth.eu/pub/bscw.cgi/d29584/EARTH_WP4_D4.1.pdf**

[EARTH-D4.2] D. Ferling et al., "D4.2: Green radio technologies," *INFSO-ICT-247733 EARTH (Energy Aware Radio and NeTwork TecHnologies)*, Tech. Rep., Dec. 2011.

[EARTH-D6.2b] M. A. Imran et al., "D6.2b: Draft Integrated Solutions," *INFSO-ICT-247733 EARTH (Energy Aware Radio and NeTwork TecHnologies)*, Tech. Rep., Dec. 2011.

[Ericsson2005] Ericsonn, "Inter-cell interference handling for e-utra," 3GPP TSG-RAN WG1 42, Tech. Rep., Sep. 2005.

[FeMaFe2010] A. Fehske, P. Marsch, and G. Fettweis, "Bit per Joule Efficiency of Cooperating Base Stations in Cellular Networks," in *Proc. IEEE Globecom workshops (GC workshops)*, Miami, USA, Dec. 2010.

[GlLaLe2008] A. Gladisch, C. Lange, R. Leppla, "Power efficiency of optical versus electronic access networks", in Proc. of *ECOC*, Brussels, Belgium, 2008.

[HélmTa2011a] F. Héliot, M. A. Imran, and R. Tafazolli, "Energy Efficiency Analysis of Idealized Coordinated Multi-Point Communication System," in *Proc. IEEE VTC-Spring*, Budapest, Hungary, May 2011.

[HélmTa2011b] F. Héliot, M. A. Imran, and R. Tafazolli, "On the Energy Efficiency Gain of MIMO Communication under Various Power Consumption Models," in *Proc. of ICT Future Network & Mobile Summit*, Warsaw, Poland, Jun. 2011.

[HélmTa2011c] F. Héliot, M. A. Imran, and R. Tafazolli, "Energy Efficiency Analysis of In-Building MIMO AF Communication," in *Proc. of IWCMC*, Istanbul, Turkey, Jul. 2011.

[HélmTa2011d] F. Héliot, O. Onireti, and M. A. Imran, "An Accurate Closed-Form Approximation of the Energy Efficiency-Spectral Efficiency Trade-Off over the MIMO Rayleigh Fading Channel," in *Proc. of IEEE ICC'11, 4th International Workshop on Green Communications*, Kyoto, Japan, Jun. 2011.

[HélmTa2012a] F. Héliot, M. A. Imran, and R. Tafazolli, "On the Energy Efficiency-Spectral Efficiency Trade-Off over the MIMO Rayleigh Fading Channel," to appear in *IEEE trans. Commun.*, 2012.

[HélmTa2012b] F. Héliot, M. A. Imran, and R. Tafazolli, "A tight Closed-form Approximation of the SISO Efficiency-Spectral Efficiency Trade-Off," submitted to *ICT Future Network & Mobile Summit*, Berlin, Germany, Jun. 2012.

[HélmTa2012c] F. Héliot, M. A. Imran, and R. Tafazolli, "Energy-Efficiency based Resource Allocation for the Scalar Broadcast Channel," submitted to *IEEE WCNC*, Paris, France, Apr. 2012.

[HevGod2011] L. Hévizi and I. Gódor, "Power saving in mobile networks by dynamic base station sectorization", in *Proc. IEEE PIMRC'11, W-GREEN workshop*, Toronto, Canada, Sep. 2011.

[HoAuHa2011] H. Holtkamp, G. Auer, and H. Haas, "On Minimizing Base Station Power Consumption," in *Proc. IEEE VTC-Fall*, San-Francisco, USA, Sep. 2011.

[HolAlo2004] H. Holm and M.-S. Alouini, "Sum and difference of two squared correlated Nakagami variates in connection with the McKay distribution," *IEEE Trans. on Commun.*, vol. 52, no. 8, pp. 1367–1376, Aug. 2004.

[HuLi2006] R. Hu and J. Li, "Practical compress-forward in user cooperation: Wyner-Ziv cooperation," in *Proc. ISIT*, Seattle, USA, Jul. 2006, pp. 489-493.

[HuSuSh2010] P. Hu, C. W. Sung, and K. W. Shum, "Joint Channel-Network Coding for the Gaussian Two-Way Two-Relay Networks," *EURASIP Journal on Wireless Communications and Networking*, vol. 2010, pp. 1-13, Mar. 2010.

[KimChu2008] S. Kim and J. Chun, "Network Coding with Linear MIMO Pre-equalizer using modulo In Two-way channel," in *Proc. IEEE WCNC*, Las Vegas, USA, Mar. 2008, pp. 517–521.

[Laiho+2002] J. Laiho et al., "Radio Network Planning and Optimisation for UMTS", Wiley, 2002.

[LanGla2009] C. Lange, A. Gladisch, "On the Energy Consumption of FTTH Access Networks", in Proc. of *OSA/OFC*, San Diego, USA, 2009.

[LanWor2000] J. N. Laneman and G. W. Wornell, "Energy-Efficient Antenna Sharing and Relaying for Wireless Networks," in *Proc. IEEE WCNC*, Chicago, USA, Oct. 2000.

[LiChLi+2006] Z. Liu, S. Cheng, A. Liveris, and Z. Xiong, "Slepian-Wolf coded nested lattice quantization for Wyner-Ziv coding: high-rate performance analysis and code design," *IEEE Trans. Inform. Theory*, vol. 52, no. 10, pp. 4358-4379, Oct. 2006.

[MiHiLi2010] G. Miao, N. Himayat, and G. Y. Li, "Energy-Efficient Link Adaptation in Frequency-Selective Channels," *IEEE Trans. Commun.*, vol. 58, no. 2, pp. 545–554, Feb. 2010.

[NeierH1989] K. S. Neier-Hellstern, "The analysis of a queue arising in overflow models," *IEEE Trans. on Commun.*, vol. 37, no. 4, pp. 367-372, 1989.

[NRC_US2010] Workshop Tabletop Poster, HOV-to-HOT Lanes Workshop, National Road Pricing Conference, June 2-4, 2010, Houston, Texas.

[OFCOM-web] OFCOM website. [Online]. Available: **http://www.ofcom.org.uk**

[OnHélm2011a] O. Onireti, F. Héliot, and M. A. Imran, "Closed-form Approximation for the Trade-Off between Energy Efficiency and Spectral Efficiency in the Uplink of Cellular Network," in *Proc. European Wireless Conference*, Vienna, Austria, Apr. 2011.

[OnHélm2011b] O. Onireti, F. Héliot, and M. A. Imran, "Trade-off between Energy Efficiency and Spectral Efficiency in the Uplink of a Linear Cellular System with Uniformly Distributed User Terminals," in *Proc. IEEE PIMRC'11, W-GREEN workshop*, Toronto, Canada, Sep. 2011.

[OnHélm2012] O. Onireti, F. Héliot, and M. A. Imran, "On the Energy Efficiency-Spectral Efficiency Trade-Off in the Uplink of CoMP System," to appear in *IEEE trans. Wireless Commun.*, 2012.

[PaLaLa2011a] A. Pantelidou, K. Lähetkangas, and M. Latva-aho, "An energy-efficiency comparison of RLNC and ARQ in the presence of FEC," in *Proc. IEEE VTC-Spring*, Budapest, Hungary, May 2011.

[PaLaLa2011b] A. Pantelidou, K. Lähetkangas, and M. Latva-aho, "Energy-efficient multicasting over the erasure channel," in *Proc. IEEE ICC'11*, Kyoto, Japan, Jun. 2011.

[PerezR2007] J. Pérez-Romero, "Operator's RAT Selection Policies Based on the Fittingness Factor Concept", in *Proc. of 16th IST Mobile and Wireless Communications Summit*, Budapest, Hungary, Jun. 2007.

[RicFet2012] F. Richter and G. Fettweis, "Base Station Placement Based on Force Fields," submitted to *IEEE VTC-Spring*, Yokohama, Japan, May 2012.

[ROCKET-4D2] C. Antonopoulos et al., "4D2 – Multi-cell Coordination Techniques for OFDMA Multi-hop CellularNetworks," *ICT-215282 STP ROCKET (Reconfigurable OFDMA-based Cooperative NetworKs Enabled by Agile SpecTrum Use)*, Tech. Rep., Dec. 2009. [Online]. Available: **http://www.ict-rocket.eu/documents/Deliverables/ROCKET_4D2UPCj.pdf**

[Sandvine2010] "Mobile internet phenomena report," Sandvine, Technical Report, 2010, [Online]. Available: **http://www.sandvine.com/downloads/documents/2010%20Global%20Internet%20Phenomena%20Report.pdf**

[SarKam2012] M. Sarkiss and M. Kamoun, "Energy Efficiency Analysis under Limited Backhaul Capacity," submitted to *ComNet'2012*.

[Section 6.2 of TS 36.104] "Evolved Universal Terrestrial Radio Access (E-UTRA); Base Station (BS) radio transmission and reception (Release 8)," Technical specification 3GPP TS 36.104 V8.12.0, Jun. 2011.

[SeMoCi2006] K. Seong, M. Mohseni, and J. Cioffi, "Optimal resource allocation for OFDMA downlink systems," in *Proc. IEEE ISIT*, Seattle, USA, Jul. 2006, pp. 1394 –1398.

[SerCor2007a] A. Serrador and L. M. Correia, "A Cost Function for Heterogeneous Networks Performance Evaluation Based on Different Perspectives", in *Proc. of 16th IST Mobile and Wireless Communications Summit*, Budapest, Hungary, Jul. 2007.

[SerCor2007b] A. Serrador and L. M. Correia, "Policies For a Cost Function For Heterogeneous Networks Performance Evaluation", in *Proc. IEEE PIMRC'07*, Athens, Greece, Sep. 2007.

[SinDat2004] L. N. Singh and G. R. Dattatreya, "A novel approach to parameter estimation in Markov-modulated Poisson processes," in *Proc. IEEE ETC*, Richardson, USA, Oct. 2004.

[SkLiDa2010] B. Skubic, , S. Dahlfort, "Power Efficiency of Next-Generation Optical Access Architectures", in *Proc. of OSA/OFC/NFOEC*, Los Angeles, USA, 2010.

[StLeHe+2002] D. Staehle, K. Leibnitz, K. Heck, B. Schroder, A. Weller and P. Tran-Gia, "Approximating the other cell interference distribution in inhomogeneous UMTS networks", in *Proc. IEEE VTC-Spring*, Birmingham, USA, may 2002.

[StSiBa+2009] I. Stanojev, O. Simeone, Y. Bar-Ness, and D. Kim, "Energy efficiency of non-collaborative and collaborative hybrid-ARQ protocols," *IEEE Trans. Wireless Commun.*, vol. 8, no. 1, pp. 326-335, Jan. 2009.

[Telata1999] E. Telatar, "Capacity of Multi-antenna Gaussian Channels," *European Transactions on Telecommunications*, vol. 10, no. 6, pp. 585–595, Nov. 1999.

[TorFaz2010] I. Törős and P. Fazekas, "Automatic Base Station Deployment Algorithm in Next Generation Cellular Networks," in *Proc. 5th AccessNets*, Budapest, Hungary, Nov. 2010.

[TorFaz2011a] I. Törős and P. Fazekas, "An energy efficient cellular mobile network planning algorithm," in Proc. *IEEE VTC2011-Spring,* Budapest, Hungary, May 2011.

[TorFaz2011b] I. Törős and P. Fazekas, "Planning and network management for energy efficiency in wireless systems," in *Proc. Future Network and Mobile Summit*, Warsaw, Poland, Jun. 2011.

[VidGod2011] A. Vidács and I. Gódor, "Power Saving Potential in Heterogeneous Cellular Mobile Network", in *Proc. IEEE PIMRC'11, W-GREEN Workshop*, Toronto, Canada, Sep. 2011.

[WINNER II] "D2 D1.1.2 V1.2 WINNER II Channel Models," IST-4-02-7756 WINNER II, Tech. Rep., Sep. 2007.

[WiSaGi1994] J. H. Winters, J. Salz, and R. D. Gitlin, "The Impact of Antenna Diversity on the Capacity of Wireless Communication Systems," *IEEE Trans. on Commun.*, vol. 42, no. 2, pp. 1740–1751, Feb. 1994.

[WynZiv976] A. Wyner and J. Ziv, "The Rate-distortion Function for Source Coding with Side Information at the Decoder," *IEEE Trans. Inform. Theory*, vol. 22, pp. 1–10, Jan. 1976.

[XuHua2010] S. Xu and Y. Hua, "Source-Relay Optimization for a Two-way MIMO Relay System," in *Proc. IEEE ICASSP*, Dallas, TX, USA, Mar. 2010, pp. 3038–3041.

[YaLeCh2007] H. J. Yang, K. Lee, and J. Chun, "Zero-forcing based two-phase relaying," in *Proc. IEEE ICC*, Glasgow, UK, Jun. 2007, pp. 5224–5228.

[ZhLiLa2006] S. Zhang, S. C. Liew, and P. P. Lam, "Hot Topic: Physical-Layer Network Coding," in *Proc. ACM Mobicom*, Los Angeles, CA, USA, Sept. 2006, pp. 358-365.